UNIVERSITÄTSKLINIKUM HAMBURG-EPPENDORF

Zentrum für Experimentelle Medizin

Institut für Computational Neuroscience

Direktor: Prof. Dr. Claus C. Hilgetag

Characteristic Topology of Brain Networks: Emergence through plasticity and computational aspects

Dissertation

zur Erlangung des Doktorgrades PhD

an der Medizinischen Fakultät der Universität Hamburg

vorgelegt von

Fabrizio Damicelli

aus Cordoba (Argentinien)

Hamburg 2021

Angenommen von der
Medizinischen Fakultät der Universität Hamburg am: 23.03.2021

Veröffentlicht mit Genehmigung der
Medizinischen Fakultät der Universität Hamburg.

Prüfungsausschuss, der Vorsitzende: Prof. Dr. Claus C. Hilgetag

Prüfungsausschuss, zweiter Gutachter: Prof. Dr. Thomas Oertner

Table of Contents

Chapter 1

Introduction

1.1 A networks perspective of the brain

One of the currently most exciting scientific challenges is to understand how the brain works. The consequences of cracking that problem are simply countless, ranging from explaining fundamental aspects of human existence, such as consciousnes, all the way through a myriad of other applications, such as human-machine interface for prosthetics and developing the next generation of artificial intelligence (Marcus 2020).

Needless to say, understanding the brain is an intrinsically difficult problem. The brain has many different layers of complexity and, as a consequence, the study of its structure and function can be approached from many different perspectives, both in experimental and theoretical terms (Kandel et al. 2000).

The work presented in this thesis looks at the brain through the lens of *networks*. That means, it lays within the interdisciplinary field of *network neuroscience*, a mixture between the more general fields *network science* and *neuroscience* (Bassett & Sporns 2017). This approach entails the important commitment to the notion that abstracting away some details of the system and representing the brain as a network of interacting elements provides us with a useful description that serves as an underlying explanation to observed phenomena at higher scales. For example, better understanding of the connectivity patterns between different brain regions

could help explaining the consequences of specific brain lesions (Bassett et al. 2018; Heuvel & Sporns 2019).

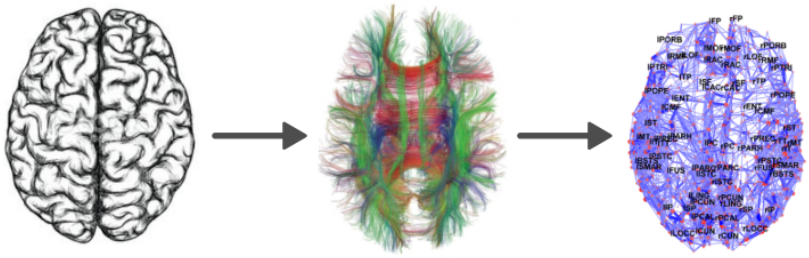

Figure 1.1: The brain as a network. Example of brain network extraction for human brains. By means of modern experimental techniques, such as diffusion tensor MRI, the connectivity between different brain areas can be inferred (Middle). Such connectivity information is then used to derive a network representation of the brain (Right), where each brain area (derived from a parcelation) is a node, and the axonal tracts between them the edges of the network. Adapted from (Hagmann et al. 2008).

So the core idea behind this network approach in neuroscience is to generate an abstract model representation of the brain (or parts of it) as a set of elements (*nodes*) connected to each other via links (*edges*) constituting a *network*.[1] This network is then the object of study that provides with the possibility of addressing questions about brain organization and functional mechanisms, both experimentally and theoretically.

1.2 Why networks?

The pervasiveness of networked systems in nature and the remarkable usefulness of networks for modeling complex systems, have led to the blooming of the *network science* field in the last ~25 years, although the initial applications of graph theory are certainly older. Since networks have a special focus on the interactions between elements of a system, they constitute a natural representation of many

[1] In this context, an equivalent term to refer to a network is a *graph*. Those two terms are interchangeably used in this thesis and they refer to the same object: a set of links connecting nodes.

complex systems, such as the brain, capturing crucial relationships between their components. Network science is a highly interdisciplinary mixture of researchers, using and developing tools to analyze a huge variety of systems, at first sight not necessarily related, but whose abstraction as networks helps deriving more general principles (Newman 2006).

Networks are especially useful models of the brain for a number of reasons. At an abstract level of complex systems in general, two principal characteristics enabling complex emergent behaviour are the presence of numerous elements and the non-linear nature of the *interactions* between them (Chialvo 2010). In the brain, millions of neurons "talk to each other" through non-linear mechanisms (e.g., spikes and action potentials) via billions of synapses (Roth & Dicke 2005). Those facts make the brain the complex biological network *par excellence*. In contrast to other complex biological systems that also can be *represented* as networks, such as gene interactions networks, we can make an even stronger claim about the brain: *The brain is literally a network.*[2]

Thus, network approaches have recently become central in neuroscience, offering a novel description level and a set of tools to approach old and new open questions in the field. But networks can represent very different things, even within the neuroscience context. For the sake of clarity, and unless otherwise explicitly stated: all the brain networks I will refer to represent *physical connections* between neural elements. Thus, these are called *structural brain networks* (in contrast to functional networks). For example, the network nodes might be meant to model individual neurons or brain regions, while the links (edges) could represent individual axons or bundles of them, respectively. In other words, they can refer to different spatial scales. I will generically refer to them as *brain networks*.

[2] A fact which, by the way, settled one of the hottest scientific debates in the history of neuroscience between Ramón y Cajal and Golgi (De Carlos & Borrell 2007).

1.3 Studying brain networks with graph theory

1.3.1 Basic concepts

Even thought representing the brain as a network already implies some simplifications, the complexity of that network representation still implies that even simple questions can become challenging. For example, given an individual brain (or its network representation), we could ask ourselves: How centralized is the organization of that network? That is a fundamentally qualitative question, but, in order to test it with statistical validity, we need to translate that qualitative notion into a quantitative one. A set of mathematical concepts coming from *graph theory* allows us to do exactly that by providing us with precise metrics that function as a language to state those qualitative questions in more mathematical terms (Sporns et al. 2004).
Graph theoretical metrics are typically estimated by means of computational methods and they provide us with concrete quantities that give us a handle on different qualitative properties of the network.

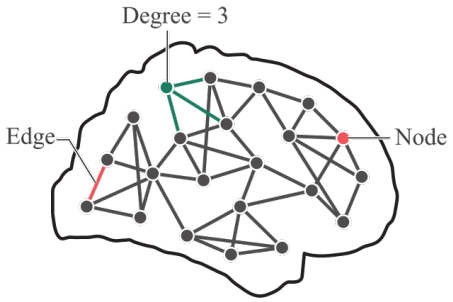

Figure 1.2: The brain as a network. Schematic representation of a brain represented as a graph, pointing to the most fundamental components of the network: nodes and edges as well as a basic metric - the node degree. Reproduced from (Sporns & Betzel 2016).

A network is composed of *nodes* and *edges* (or *links*). Thus its minimal description is the set of its links, represented as pairs (i, j), indicating a connection from node i to node j. The most basic properties of a network are therefore the number of nodes, N, and the total number of links, L. The number of links of a single node i is called the *node degree* and denoted as k_i.

Unweighted networks (also referred as *binary networks*) have links that can only either exists or not. In contrast to that, the links of a network can have a weight, so defining a *weighted network*, where each link has a particular strength. If the links are allowed to have a directionality, the network is said to be *directed*. In such case, the pairs $(i, j), (j, i)$ refer to different links, one going from i to j and another from j to i. The opposite case is with *undirected* networks, where the pairs $(i, j), (j, i)$ actually refer to the same one link, which has no directionality.
It is important to notice that this connectivity information only specifies the wiring diagram ("who is connected to whom"). This is known as the *topology* and does not give any information about the actual, geometrical embedding of the network (known as *topography*). Thus, the topological properties of a network refer to the characteristics of the wiring diagram, independently of how those nodes and links could be embedded in the physical space.

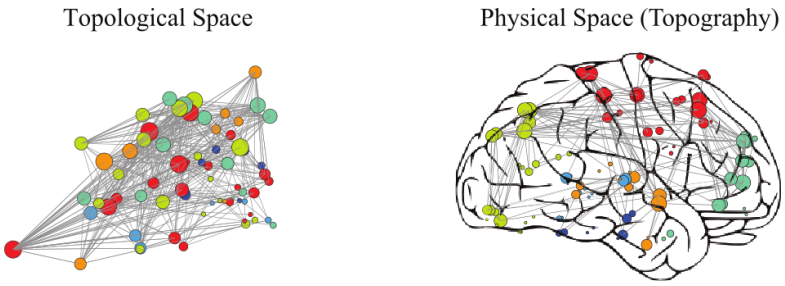

Figure 1.3: Topology vs. Topography. Left: A network with purely topological information. This two-dimensional layout of the network was generated by grouping nodes in the plane according to their connections, regardless of the physical distance between them. Right: The same network as in the left side of the figure, but spatially embedded according to the real physical positions of the nodes in the brain. Adapted from (Bullmore & Bassett 2011).

Going back to the hypothetical question about how centralized a brain network might be, by means of graph theoretical tools, we could compute a specific metric called *betweenness centrality* for each brain region, and then study the distribution of values across all the nodes. A highly skewed distribution would speak for a network with a centralized organization. In that way, the network approach allows us to translate a qualitative question ("how centralized is the organization of a given brain?") into a quantitative one ("which function describes

the distribution of centrality values?") that gives us precision and the potential advantage of leveraging statistical tools to test our hypothesis.
In sum, graph theory provides us with a tool that allows us to state qualitative questions about brain organization as quantitative ones in terms of topological metrics which can be addressed more precisely.

1.3.2 Scales of network analysis

As mentioned above, in order to quantitatively describe a network, different topological properties can be defined and computed. These are called *network metrics* and the recent rapid development of network science in general, and network neuroscience in particular, has led to the development of a large number of them to describe the connectivity patterns of complex brain networks. Before defining specific metrics and details about their relevance, it should be mentioned that each network metric can capture connectivity properties at a *different scale*, ranging from *global* to *local*, i.e. whole network to individual nodes perspective, respectively.

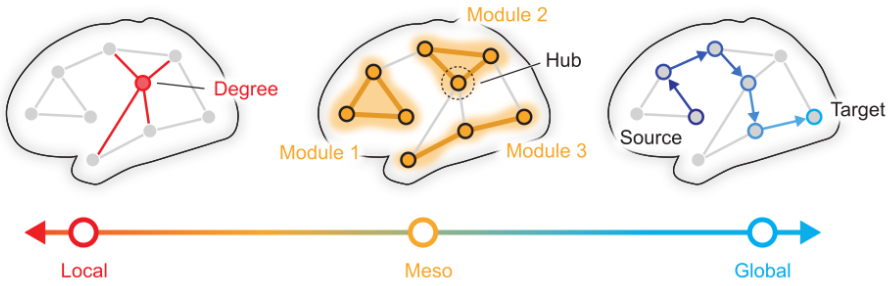

Figure 1.4: Scales of network analysis. Analysis of brain networks can be carried out at the local and global scales, which focus on properties of individual network elements (nodes and edges) or the network as a whole, respectively. Situated between these extremes is a meso-scale that focuses on sub-networks, for example, clusters of nodes. Adapted from (R. F. Betzel 2020).

Global metrics describe general organization patterns of the network that determine emergent macro-properties, for example, how efficiently information can spread across the network. On the other side of the spectrum, local metrics describe

individual nodes, thus useful when comparing the role of different elements of the network with each other, such as the importance of brain regions in terms of number of connections. Those are the two extremes of the spectrum, but at a meso-scale between them there are other properties, such as the presence of modules, that provide relevant information as well. These scales are not always really mutually exclusive and there can be overlapping of scales and granularity which contributes to the complexity of the network organization (R. Betzel 2020).
Now we can revise the specifics of topological properties of brain networks, focusing on the intuition behind the most important ones, which will pave the way to understand the conceptual core of this thesis.

1.4 Features of brain networks

First of all, why is the topology of brain networks important in the first place? A short high level answer is that topological features of complex networks have a direct impact on the dynamical processes that take place on the network.
Dynamical properties at all scales, such as network resilience and self-sustained activity patterns, are highly dependent on the underlying topological features of the network (Albert et al. 2000; Kaiser & Hilgetag 2010). The reason being that the topology of a network is the substrate upon which the dynamical processes unfold and thus constrains and, to some extent, determines brain function (Arenas et al. 2006; Zhou et al. 2006; Müller-Linow et al. 2008; Mišić & Sporns 2016; Messé et al. 2018).
Thus, understanding the topological organization of brain networks becomes a fundamental perspective to understanding brain function, both in healthy and pathological conditions (Bassett & Sporns 2017; Heuvel & Sporns 2019).
Brain networks exhibit a number of typical connectivity patterns. Those connectivity patterns are ubiquitously found across species and they can often be captured by network metrics (Sporns et al. 2004).
Generally speaking, the most prominent feature of brain networks is the non-random organization of their connectivity, a fact that is observable at different

spatial scales (Sporns 2011). That means, random graphs[3], with nodes connecting to each other with an independent uniform probability, are an inappropriate description of the topology of brain networks. At the same time, brain connectivity is far from being a regular network, where each node is connected to a characteristic number of other nodes around it. Brain networks sit somewhere in between these two extremes, a fact that is also important in terms of the wiring economy of brain connectivity, as explained in Fig. 1.5.

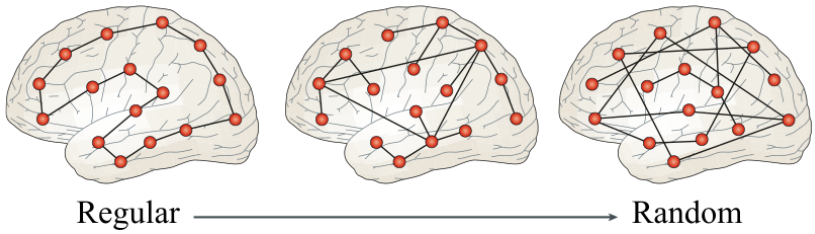

Figure 1.5: Non-random organization of brain networks. (Left) Regular connectivity pattern with minimal wiring cost. This topology has poor global integration of information. Such integrative processing would be maximized by a random topology (Right). However, random topology comes at a high wiring cost due to long-distance connections. Brain networks sit between these two extreme cases with clusters of connections between spatially neighbouring nodes which tend to minimize wiring cost. But brain networks also include high-cost components, such as long-distance connector hubs in different modules and different anatomical regions. Adapted from (Bullmore & Sporns 2012).

This "regular-random"-axis of connectivity organization is only one of the many possibilities to take into account. Revising in detail all the reported topological features of brain networks is beyond the scope of this introduction. Instead, I will focus here on what are believed to be the most fundamental aspects of the topological organization of brain networks, which are also the most pertinent ones in the context of the work carried out in this thesis.

1.4.1 Brain networks are modular

A modular organization refers to the existence of groups of nodes that are more interconnected between them than with other nodes of the network. These

[3]Also known as Erdős–Rényi (ER) graph after the authors first characterizing this random graph generative model (Erdős & Rényi 1959).

groups are known as *communities* or *modules*. Such segregation of the connectivity is a fundamental organizational principle found in real brain networks and it indeed implies a number of interesting functional properties as well (Sporns & Betzel 2016).

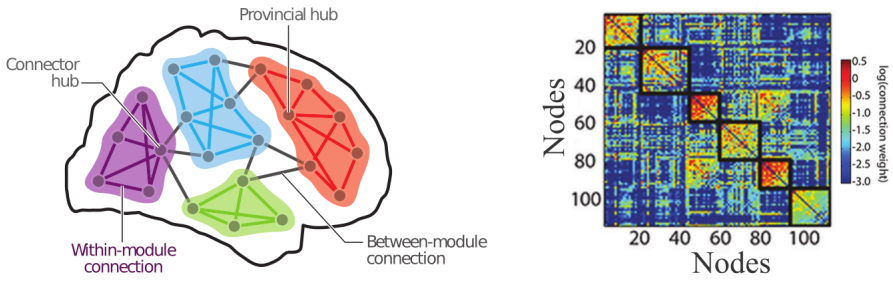

Figure 1.6: Modular organization of brain networks. Left: Schematic representation of the modular organization of brain networks. Modules consisting of brain regions with many connections between them and sparser connectivity to the rest of the network. Adapted from (Sporns & Betzel 2016). Right: Mouse connectivity matrix derived from tract-tracing experiments. The connectivity matrix was reordered in order to facilitate the visualization of modules. The blocks along the main diagonal show the modular structure of this brain network. Adapted from (Bassett & Bullmore 2017).

Modularity was among the first topological features of complex networks to be associated with a systematic impact on dynamical network processes. Random walks are trapped in modules (Rosvall & Bergstrom 2008), the synchronization of coupled oscillators over time maps out the modular organization of a graph (Arenas et al. 2006) and co-activation patterns of excitable dynamics tend to reflect the graph's modular organization (Zhou et al. 2006; Müller-Linow et al. 2008; Messé et al. 2018).

Modularity in the brain is thought to be important for information processing, the balance between segregation and integration as well as system evolvability in the long temporal scale (Sporns & Betzel 2016). More concretely, the modular organization of brain networks forms the substrate of functional specialization, e.g., sensory systems (Hilgetag et al. 2000), contributes to the generation and maintenance of dynamical regimes, e.g. criticality (Wang & Zhou 2012), and supports the development of executive functions (Baum et al. 2017). Moreover, it has been demonstrated that modularity contributes to a number of other relevant network

features, such as buffering effects of random fluctuations (Sporns & Betzel 2016) and promoting metastability (Wildie & Shanahan 2012). In sum, modularity is a key component of structural brain networks with important functional consequences.

1.4.2 Brain networks have heterogeneous degree distributions

The degree distribution reflects how links are distributed amongst the nodes of the network. In its simplest definition, the degree distribution is the count of occurrences of each node degree k, typically aggregated into a histogram or a probability distribution $P(k)$. The global shape of this distribution allows us to infer properties of the network.
Brain networks usually have *heterogeneous degree distributions*. Colloquially, this implies that some few nodes in the network accumulate many links, while a vast majority of nodes have fewer connections. Those highly connected nodes are often referred to as *hubs*[4], which are a fundamental feature of brain networks, as explained in more detail in the following section.

The relevance of heterogeneous degree distributions in brain networks comprises multiple aspects, as it constrains the dynamical processes that take place on the network. More specifically, the ability of different nodes to receive and send information in the network is intimately related to their importance in terms of number of connections, thus, in turn affecting communication processes in the brain (Avena-Koenigsberger et al. 2018). Also, some of these hubs in the brain, together with the presence of modules, shape brain networks into a "small-world" network organization. Concretely, hubs act as a counterpart to modules, integrating information across different systems (modules), thus aiding the multisensory processing and integration across the network (Zamora-López et al. 2009). Moreover, the consequences of network perturbations depend heavily on the underlying

[4]This definition of a hub purely based on its degree is at the core of a metric called *degree centrality*, which is a normalized form. Other definitions of "hubness" exist in the literature, but here I will stick to the degree-based notion of hub.

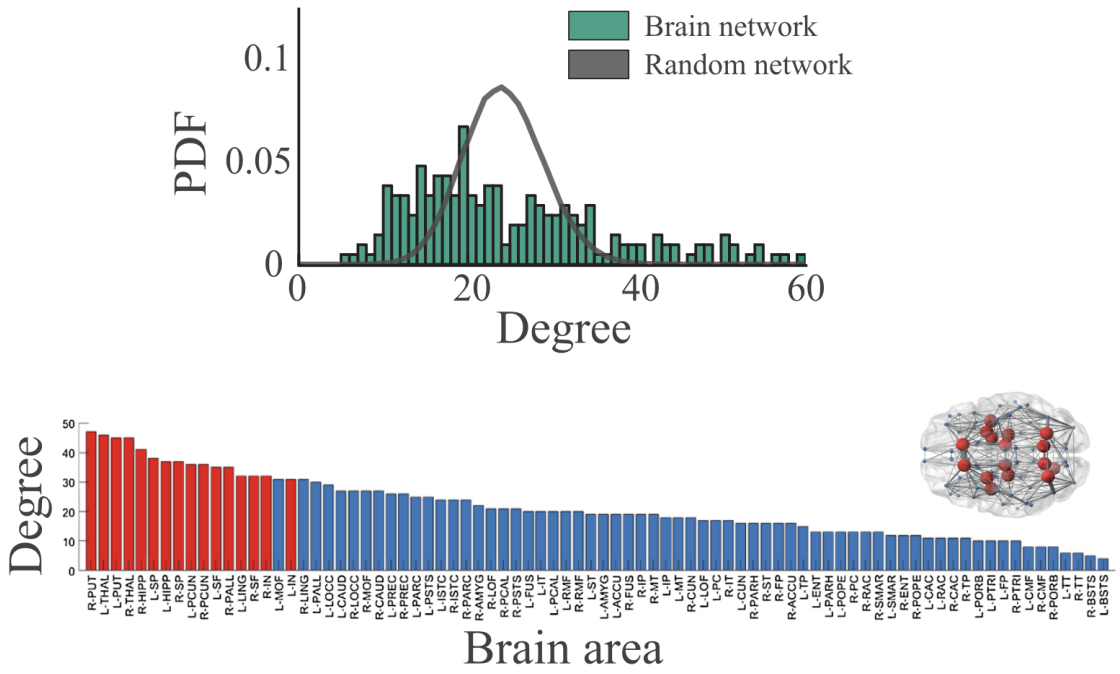

Figure 1.7: Typical heterogeneous degree distributions of brain networks. Left: Mouse connectome's degree distribution (blue) compared to standard graph generative models. Adapted from (Oh et al. 2014). Right: Example of structural hubs of the adult human brain. The bar chart shows the degree for each node (area). Nodes with degree one standard deviation above the mean are identified as "hubs" (red). Adapted from (Oldham & Fornito 2019).

connectivity patterns (Albert et al. 2000). In consequence, having a heterogeneous degree distribution determines a very different susceptibility and resilience of the nodes of the network (and the network in general). For example, a brain lesion on a more central node could affect the function of the network much more drastically than a lesion on a less central region.

1.4.3 Modules and hubs: Primitives of brain connectivity

We have so far looked at only a few dimensions along which we can place brain networks according to their topology, namely the *random/regular*, *non-modular/modular*, *homogeneous/heterogeneous degree distribution*. But there are other potential axes to be considered and we can rather think about network properties as a multi-dimensional space of features, also known as *topological morphospace* (Avena-Koenigsberger et al. 2015), where brain networks can be embedded and be compared simultaneously with regard to several topological properties. When we look at brain networks from this multi-dimensional perspective, we are faced with another problem, with practical and theoretical implications: Network metrics can often be "entangled." That is, network metrics are often correlated or show complex interdependencies, in some cases, even theoretically impossible to tear apart (Bounova & Weck 2012).

In consequence, the contribution of a particular network property to an observed effect can be really misleading, since the metric could simply be a confound factor, a trivial consequence of other metrics co-varying with it. For example, a network that has modular structure will typically also show a high clustering level (i.e. "cliquishness" of local neighborhoods), but the opposite is not necessarily true, and highly clustered networks can have low modularity (Meunier et al. 2010). This is also important from a conceptual standpoint, for the conclusions to be drawn about the properties and processes of formation of brain networks can be substantially different if those network metrics interdependencies are (not) taken into account. In more abstract terms, the problem is to tear apart essential or *primitive* topological properties from the *epiphenomenal* ones. These byproducts are also known as *spandrels* in evolutionary biology (Gould et al. 1979).

This raises strong concerns about common approaches in network neuroscience, where often several network metrics are simultaneously reported (e.g., comparing experimental conditions) without taking into account circularities resulting from how the metrics are related (Rubinov 2016). Therefore, the core question is: *What are the basic topological building blocks of brain networks?* This is so far a rather under-explored aspect in the literature, but there is evidence pointing to *modules* and *hubs* as basic hallmarks of brain connectivity. That is, it is hypothesized that networks having simultaneously modules and hubs as structural constraints would be bound to induce other structural byproducts (Rubinov 2016). In simpler words, complex topological features, such as rich club organization[5], can be byproducts ("spandrels") of modules and hubs. From a functional point of view, this hypothesis is also related to the fact that modules and hubs represent the canonical forms of segregation and integration of information, respectively. That is, modules tend to represent systems (e.g., sensory), while hubs are association areas integrating systems (Sporns 2013).

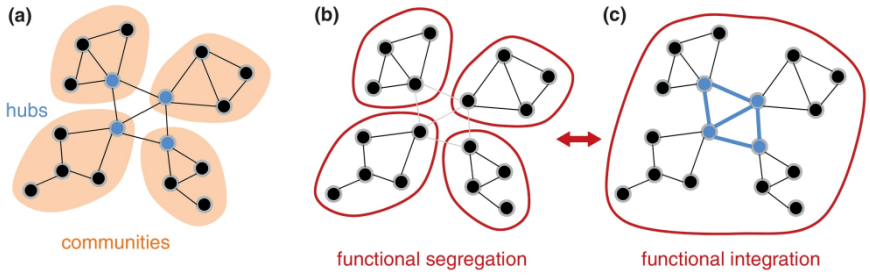

Figure 1.8: Modules and hubs, segregation and integration. (a) Schematic diagram showing a set of nodes and edges arranged into a network comprised four network communities (orange) interconnected by highly connected and highly central network hubs (blue). Since these hubs are at the same time very interconnected between themselves, they are said to form a "rich club." (b) Functional segregation indicated by strong functional coupling within communities (red) with little or no functional coupling across communities. (c) Functional integration indicated by globally strong functional coupling, including strong information flow across network hubs. Adapted from (Sporns 2013).

In sum, modules and hubs are in a way essential building blocks, primitive

[5]A network is said to have a rich club organization if the most influencial nodes are also more densely connected amongst them than expected by chance, thus forming a "rich club." See Methods for details.

components of brain connectivity.

1.4.4 Brain networks are plastic

A distinctive property of brain networks is their dynamical nature: Links of the network can change in time, where new connections may appear and initially established ones may be removed, so modifying network connectivity (Abbott & Nelson 2000). In other words, brain networks are *plastic*, which adds a whole new layer of complexity to the system.
In particular, the two most prominent factors contributing to such dynamical nature are ontogeny and neuronal plasticity. These factors also interact with each other in complex ways and it is often difficult to determine their individual contributions to the global connectivity pattern.
Nevertheless, ontogeny and plasticity can sometimes act at rather different spatio-temporal scales. For example, activity-dependant synaptic plasticity might play an important role in fine tuning the connectivity within brain regions, but less so in determining if a given brain area connects to its contra-lateral counterpart, which is more likely determined by developmental processes.
As mentioned before, the topology of a network shapes the dynamical processes unfolding on that network, i.e. the neural dynamics. If we now also consider that such activity patterns may at the same time cause topological changes, e.g., through Hebbian plasticity, a loop of interactions emerges, in which we have intertwined dynamics *on* networks and dynamics *of* networks.

This interplay between plasticity mechanisms and topological evolution is one of the fundamental aspects of the work presented in this thesis. In particular, the first part of it, dedicated to understand the emergence of brain connectivity patterns.

1.5 Emergence of brain connectivity patterns

The first core question addressed in this thesis is: *How do brain connectivity patterns emerge?* This is challenging because of the diversity of factors and

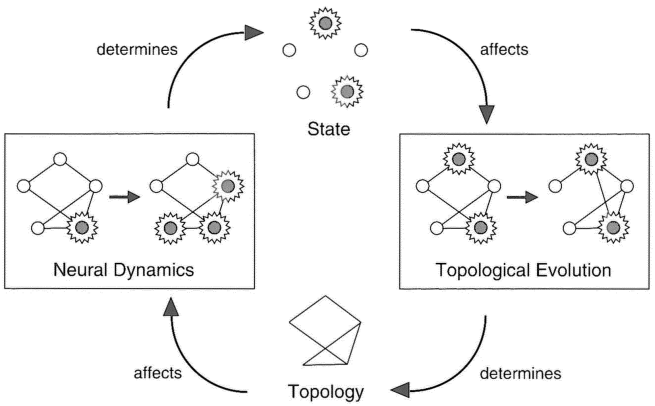

Figure 1.9: Dynamics on networks and dynamics of networks. Network dynamics and topological evolution are tightly related. This schematic diagram illustrates the interplay between neural dynamics and the temporal evolution of the connection topology. More generally, this constitutes an example of an adaptive co-evolutionary network. Figure from (Sporns 2010).

mechanisms that play a role in shaping brain networks.

To begin with, developmental processes are important determinants of the global architecture of brain networks. Complex patterns of cell division, migration and differentiation, constrained by the spatial embedding of the brain, result in a global organization of brain networks that is more or less typical for a given species (Goulas et al. 2019). So which general principles govern those developmental patterns?

Early ideas about brain wiring economy have been traditionally very influential (Cajal & others 1995; Bullmore & Sporns 2012; Rubinov et al. 2015). The core rationale behind them boils down to the fact that the interplay between spatial embedding and metabolic cost of generating and maintaining connections in the brain define a notion of *wiring cost*. The theoretical argument is that brain connectivity patterns that are more optimal in term of such cost would represent an evolutionary advantage.

But there are two crucial points to be explicitly pointed out: First, wiring economy principles and developmental processes only partially explain the connectivity experimental data observed in adult brains. Early analyses of connectivity datasets have proven the insufficiency of wiring cost to explain connectivity data (Kaiser

& Hilgetag 2006) and evidence from more recent work with state of the art, high resolution data also supports those ideas (Rubinov 2016). So this means that there is a need for considering other contributing factors beyond wiring cost that shape the topology of brain networks. Following that, recent studies have also included network topology descriptors (e.g., homophily[6]) in these statistical models of brain connectivity (Betzel et al. 2016). Although that is a step forward in summarizing brain connectivity patterns, there is still one aspect missing, which brings us to the second point: Wiring cost and homophily ideas are not mechanistic explanations but statistical descriptions of the observed data (Betzel et al. 2016). That is, they do not state biologically plausible causal events that guide the formation of the observed connectivity patterns in a given individual brain. Thus, mechanistic models of brain connectivity formation are also a fundamental missing piece of the puzzle explaining the emergence of brain networks.

Beyond the above mentioned statistical descriptions of brain connectivity, computational modeling studies of the developing brain have shown that a few assumptions about the spatio-temporal unfolding of developmental processes (e.g., cell migration waves) can promote the emergence of some topological properties of brain networks (Kaiser & Hilgetag 2007; Bauer & Kaiser 2017; Goulas et al. 2019). Although these modeling studies do not completely explain the experimental data, they are important in showing how some scaffold properties, a skeleton of network features arise, which could later be amplified or refined by activity-dependant plasticity.

Beyond developmental processes, another natural way for brain networks to change their connectivity pattern is neuronal plasticity, which indeed takes place across the whole lifetime of an individuum, supporting basic functions such as learning and memory. For example, neuronal plasticity enables the formation of *engrams*, that is, ensembles of neurons that constitute the cellular basis of and support the formation and consolidation of memories in the brain (Semon 1921). In general, a robust corpus of evidence situates these plastic changes at the core of current the-

[6]Homophily principle: Experimental observation that two brain regions with similar connectivity profiles, i.e. they strongly connect to many common other brain regions, are likely to be themselves strongly connected.

ories of learning and memory in general (Abbott & Nelson 2000). Given the well accepted role of synaptic plasticity in brain development and activity-dependent adaptation, some modeling studies have focused on changes driven by local plasticity mechanisms. A considerable proportion of this work aims at explaining empirically observed distributions of physiological parameters at the cellular scale, such as synaptic weights (Effenberger et al. 2015), and only a few studies have paid attention to topological aspects, such as the proportion of local motifs (Stone & Tesche 2013). Some other modeling studies showed emergence of modular network structure and attempted to provide an underlying mechanism based on the reinforcement of paths between highly correlated nodes (Jarman et al. 2017). Yet, the problem of a topological gradient, along which network changes should occur during the rewiring process in order to promote the emergence of network properties, was not explicitly investigated. I will return to this point in more detail in the following chapters as I explain our studies in depth.
In sum, current explanations of the formation of brain connectivity patterns still lack mechanistic models, in particular for connectivity properties determined by processes other than embryological development. Neuronal plasticity plays a crucial role supporting brain function and from a networks perspective, we can expect these plastic changes to have multiple effects on the topology of brain networks, such as generating new topological features, refining or amplifying pre-existent ones, which is tightly related to our research goals of the studies presented here.

1.6 Brain network topology and computation

I have so far emphasized how several real brain topological properties have dynamical consequences, sometimes with potential advantages at the functional level, e.g., supporting segregation and integration of information (Hilgetag et al. 2000; Sporns et al. 2000). Nevertheless, it is worth noticing the fact that some topological properties are beneficial in abstract theoretical terms, but it is not very informative about how networks with those properties would perform on *solving concrete tasks*. That is, the relationship between computation ability on concrete tasks and the connectivity patterns of brain is largely unknown and that is a cru-

cial point, as brains are supposed to solve tasks in the real world.

This is also relevant for Artificial Neural Networks (ANNs), since many recent improvements of ANNs rely on novel network architectures, which play a fundamental role in task performance. In other words, such connectivity patterns encode useful structure about the outer world (i.e. the data) and/or they let the networks learn better (i.e. find patterns in the data). Nevertheless, *ANNs exhibit architectures that are not grounded on empirical insights from real brains network topology.* For example, ANNs do not follow ubiquitous organization principles of BNNs, such as their modular structure, and BNNs are also much sparser than ANNs (Sporns 2011; Hassabis et al. 2017).

Given that Biological Neural Networks (BNNs) present complex, non-random connectivity patterns, it is hypothesized that this "built-in" structure could be one key factor supporting their computation capabilities. In consequence, a focus on BNNs' topology has started to gain traction in recent ANNs research. For instance, building feedforward networks based on graph generative models, e.g., Watts-Strogatz and Barabási–Albert models, showing competitive performances compared to optimized state-of-the-art architectures (Xie et al. 2019). In a complementary vein, feedforward networks may spontaneously form non-random topologies during training (Filan et al. 2020).

In sum, current evidence supports the notion that non-random topologies can lead to desired performance of ANNs. However, studies thus far have only focused on network topology models that have almost no similarities (or only abstract ones) to BNNs unravelled by experimental connectomics.

Hence, it is to date unknown if and to what extent the *actual, empirically discerned* topology of BNNs can lead to beneficial properties of ANNs, such as better performance or shorter training, which leads to the second core question addressed in this thesis: *Does real brain connectivity have an effect on the performance of brain networks on concrete tasks?*

1.7 Research goals

In the first part of this thesis, I will present a series of studies addressing the general question: *How do topological properties of brain networks emerge?* More precisely: **Which plasticity mechanisms could contribute to the emergence of characteristic topological features of brain connectivity?**
As already explained in this introduction, **modules** and **heterogeneous degree distributions** are believed to be the most fundamental hallmark topological properties of brain networks. Thus, our work focused on trying to explain the emergence of those two specific topological properties.
The second part of the work here presented is devoted to the question:
Which effect does the connectivity of brain networks have on their performance on concrete tasks? We addressed that by means of a hybrid approach that combined Biological Neural Networks (BNNs) and Artificial Neural Networks (ANNs), where we tested the performance of ANNs built from connectomes of human and non-human primate species, in an effort to bridge the gap between BNNs and ANNs.
Having a general overview about the background and goals, I will address on each chapter the specifics and the most relevant details of our studies and related previous work.

Chapter 2

Methods

2.1 Networks and Metrics

Networks were represented by its *adjacency matrix* A, where the element $a_{ij} = 1$ if there is a link between node i and j, otherwise $a_{ij} = 0$. In the case of a weighted network, we represented the connectivity with a matrix W, where w_{ij} is a continuous value representing the strength (weight) of the connection between node i and j.

The most basic properties of a network are the number of nodes N, and the total number of links L.

The number of links of a single node i is called the *node degree* and denoted as k_i.

The mean degree λ of a network is the average value of k across all nodes:

$$\lambda = \frac{1}{N} \sum_{i=1}^{N} k_i$$

The density d of a network is the fraction of links present out of all the potentially existent, thus varies from 0 to 1, or 0% to 100%, if expressed as a percentage.

2.1.1 Degree distribution

The degree distribution $P(k)$ is defined as:

$$P(k) = \frac{N_k}{N}$$

where N_k is the number of nodes having degree k and N is the network size as above defined. That is the normalized count of occurrences of each degree k and it reflects how links are distributed amongst nodes in the network. This count is typically aggregated as a histogram or as the probability function that describe the occurrences of all the present node degrees in the network in given bins/intervals.

2.1.2 Modularity

The intuition of a modular organization is the idea that certain groups of nodes (called modules) have more links to the nodes within the group than to the rest of the network.[1] To quantify this property, we will consider the so called Q value (Newman 2006). If we divide a network into disjoint groups of nodes, the Q value quantifies "how good" that partition is. The higher the Q value of a partition, the better segregated from each other are the modules.
More formally, the Q value is defined as a value in the range $[-1/2, 1]$ that measures the density of links inside communities compared to links between communities. Modularity is defined as:

$$Q = \frac{1}{2m} \sum_{ij} \left[A_{ij} - \frac{k_i k_j}{2m} \right] \delta(c_i, c_j)$$

where:
- A_{ij} represents the edge weight between nodes i and j; - k_i and k_j are the sum of the weights of the edges attached to nodes i and j, respectively; - m is the sum of all of the edge weights in the graph; - c_i and c_j are the communities of the nodes; and - δ is the Kronecker delta function: $\delta(x, y) = 1$ if $x = y$, 0 otherwise.

[1] To be more precise, this is the *assortative* definition of modularity, which is not the only one, but certainly the one used in this thesis.

2.1.3 Module detection

Algorithm that results in the assignment of nodes to mutually exclusive groups, i.e., modules. The outcome may be deterministic or stochastic, depending on the specific algorithm. We used the Louvain method to extract communities (Blondel et al. 2008), an efficient algorithm based on the modularity optimization. Once each node is assigned to a module, we call that the *module partition*, which can be represented by an affiliation vector, where the entry value at the position i represents the label of the community assignment of the node i.

2.1.4 Homophily

Homophily refers here to the experimental observation that the more similar the connectivity profiles of two neurons/areas, the stronger the connection between them (on average) (Goulas et al. 2015).

2.1.5 Average path length

It is a measure of how well connected is the network, on average. The *shortest path length* between two nodes i and j is the minimum number of hops that are necessary to get from i to j traversing the links of the network. Averaging that value for all pairs of nodes renders the *average path length*. Formally:
Consider an unweighted directed graph G with the set of vertices V. Let $d(v_1, v_2)$, where $v_1, v_2 \in V$ denote the shortest distance between v_1 and v_2. Assume that $d(v_1, v_2) = 0$ if v_2 cannot be reached from v_1. Then, the average path length l_G is:

$$l_G = \frac{1}{N \cdot (N-1)} \cdot \sum_{i \neq j} d(v_i, v_j)$$

where N is the number of vertices in G.
Low values of the average path length speak for a network whose connectivity is such that nodes are, on average, easy to reach (i.e., few hops are necessary to travel between two arbitrary nodes). Brain networks tend to have significantly low average path lengths (compared to null models) and that is believed to be crutial

since this implies the *possibility* that the information flows very efficiently across the brain.

2.1.6 Clustering

For a given node i, the clustering coefficient is the proportion of neighbors of i that are also connected to each other. By averaging the clustering coefficient across all nodes we obtain the *mean clustering coefficient*, which in reflects the general tendency to form local clusters in the network.
Clustering expresses the "cliquishness" of local neighborhoods, or the extent to which connected nodes share common neighbors. In simple words, it responds to the question "how many of my friends are also themselves friends?" The average clustering coefficient across all nodes reflects the general tendency to form local clusters in the network. Brain networks typically exhibit high clustering, partly as a consequence of the spatial embedding (neurons/areas closer to each other tend to be more strongly connected) and, more generally, related to a property known as *homophily*.

2.1.7 Small-world index

The small world property describes a combination of average path length and clustering, such that a high small-world index (greater than 1) indicates that the network is simultaneously highly clustered and has a low average path length (compared to a regular graph of same number of nodes and links).
In its classical formulation, the small-worldness of a network can quantified by a small-world index S, calculated by comparing clustering and path length of a given network to an equivalent random network with same degree on average (Humphries 2008):

$$S = \frac{C/C_r}{L/L_r}$$

if $S > 1$ ($C \gg C_r$ and $L \approx L_r$), the network is considered small-world.

2.1.8 Rich club organization

This property describes the tendency of some high degree nodes to be (statistically speaking) prefferentially connected to *also* high degree nodes (Shi Zhou & Mondragon 2004). Thus those *rich* nodes with many links form a tight subnetwork (*club*) that can be highly influential and have more direct access to each other. For example, there is evidence pointing to the existence of such rich club organization in the mammalian brain. It is hypothetized that this rich club areas have an integrative function across brain systems.

2.1.9 Topological Overlap (TO)

TO represents the neighborhoods' similarity of a pair of nodes by counting their number of common neighbors (Ravasz et al. 2002). Considering the connectivity represented as the adjacency matrix A:

$$to_{ij} = \frac{\sum_k a_{ik}a_{kj} + a_{ij}}{\min(\sum_k a_{ik}, \sum_k a_{kj}) + 1 - a_{ij}}$$

The origin of the TO concept stems from applications of set theory to network analysis, which became established as a relevant approach for quantifying the similarity of nodes in terms of their common network neighborhoods (Bass et al. 2013). TO is closely related to the matching index an adaptation of the Jaccard index to neighborhoods of nodes in a graph (Hilgetag 1999; Hilgetag et al. 2000; Hilgetag et al. 2002; Sporns 2003). Higher-order variants of this quantity have also been discussed in the literature (Li & Horvath 2006).

2.1.10 Network analysis tools

Synthetic graph realizations, basic graph properties (clustering, path length, small-world), community detection, matrix reordering and graph layouts were performed using the Python packages: Brain Connectivity Toolbox (Rubinov & Sporns 2010) (Python version 0.5.0; github.com/aestrivex/bctpy), NetworkX (Hagberg et al. 2008), igraph (Csardi et al. 2006) and Netwulf (Aslak & Maier

2019).

2.2 Excitable SER model

The SER model is a three-state cellular automaton model of excitable dynamics, where nodes can be in one of three possible states: Susceptible, Excited or Refractory, thus SER. In spite of its simplicity, the model has proven to be useful for understanding basic mechanisms of activity propagation as well as the influence of network topology on functional correlations.
The SER model operates in discrete time and employs the following synchronous update rules, a node in the state:

- S $\rightarrow$ E, if at least one neighbour is excited; or with probability f (spontaneous activation);
- E $\rightarrow$ R;
- R $\rightarrow$ S, with probability p (recovery).

In the deterministic SER scenario, $f = 0$ and $p = 1$.
In the stochastic SER scenario, $f > 0$ and/or $p < 1$.
The details about the initialization and time windows of the activity will be specified for each specific case.

2.2.1 Co-activations functional connectivity (FC)

To analyse the pattern of excitations in the SER model, we computed the number of joint excitations for all possible pairs of nodes during activity time window. The outcome matrix is the so-called co-activation matrix, a representation of the functional connectivity FC of the nodes:

$$c_{ij} = \sum_t \mathbb{1}_E(x_i^t)\mathbb{1}_E(x_j^t),$$

where $x_i^t \in \{S, E, R\}$ is the state of node i at time t, and $\mathbb{1}_E$ the indicator function

of state E.
FC was then normalized to scale values between 0 and 1:

$$fc_{ij} = \frac{c_{ij}}{\min(c_{ii}, c_{jj})}$$

2.2.2 Sequential activation

We also define for the SER model the sequential activation matrix S. That means, each entry s_{ij} represents the count of number of times that the activation of node i preceded the activation of the node j during an activity time window. So we can think of it as a delayed co-activation as defined above; formally:

$$s_{ij} = \sum_t \mathbb{1}_E(x_i^t)\mathbb{1}_E(x_j^{t+1}),$$

where $x_i^t \in \{S, E, R\}$ is the state of node i at time t, and $\mathbb{1}_E$ the indicator function of state E.

2.3 Minimal plasticity model with deterministic excitable dynamics

2.3.1 Networks

Simulations were performed using synthetic directed random graphs with 100 nodes and a density varying between 20% and 60%, and scale-free and modular graphs of ~20% density.

2.3.2 Network activity

We used the SER excitable model to model dynamics on the network (see Methods). For each network type (random, modular or scale-free), we simulated 15 runs of 12500 time steps, comprising 500 rewiring steps (see below). For each

run, at the very beginning of the simulation (before the first rewiring step), the initial conditions were generated with 1% of randomly chosen active nodes and the remaining nodes assigned either to refractory (R) or susceptible (S) state with equal probability.

2.3.3 Plasticity rule

The plasticity rule is Hebbian in the sense that is based on activity correlations (more strictly, co-activations) of the nodes, which in turn influence the probability of maintaining connections between nodes connected.
The network was allowed to evolve throughout the simulation by applying after every 25 time steps the following rewiring rule:

1. Functional Connectivity (FC) matrix was computed (as explaind in Methods section);
2. FC was transformed to a retention probability (P) by the following rule:

$$p_{ij} = P_{min} + \frac{P_{max} - P_{min}}{FC_{max} - FC_{min}} \times (fc_{ij} - FC_{min})$$

   where $P_{min} = 0.8$ and $P_{max} = 1$ in all cases, unless differently stated;
3. Links were maintained (or not) according to this retention probability;
4. The same number of pruned links was reintroduced into the network without delay in a randomly uniform fashion, conserving the original density.

Step (2) assigns high retention probability to pairs of nodes with high co-activation values. Thus, the rule generally promotes the pruning of links between nodes with weaker co-activation values, although the random reinsertion of pruned links (step 4) may reintroduce some links just pruned, whose nodes have low co-activation values. In this way, the plasticity rule aims to capture the possible binary modification (pruning) of weaker synapses as a result of neuronal plasticity, beyond the potential strength modulation of synaptic weights, in order to study how such local topological changes may affect the global network organisation.
For each run, a new graph was instantiated and new initial conditions were set, the

plasticity rule was applied in total 500 times (rewiring steps), every 25 time steps of dynamic simulation, resulting in total to simulations lasting 12500 (25x500) time steps. Statistical assessment was performed by exploring averages across 15 runs.

2.3.4 Statistical assessments

To investigate the effect of the plasticity rule on network topology, modularity and degree distribution of the networks were computed.
The relationship between network structure and activity was explored by the marginal (Pearson) correlation coefficient between the structural connectivity matrix (SC) and the co-activation matrix (or functional connectivity; FC). These measures were computed after each rewiring step of the network simulation (see below).
Additionally, the consecutive similarity of the structural connectivity of networks along the rewiring process was investigated. The coefficient of correlation was used to quantify the overall similarity of connectivity, and mutual information to quantify the similarity between the modular partitions of SC matrices.

2.4 Topological Reinforcement plasticity model

2.4.1 Networks

We considered synthetic undirected networks without self-connections of size $N = 100$ nodes and average connectivity $\lambda = 10$ (equivalently, a density of 0.1). Initial networks were generated according to the classical Erdős-Rényi model (Erdős & Rényi 1959). We explored the robustness of the plasticity rule across various network realizations and multiple runs (using the same initial network). We generated 100 synthetic random initial graphs and performed 500 runs for each of them. In order to study the scaling properties of our model, we also evaluated graphs with different densities (λ, average number of links per node, ranging between 6 and 20 by step of 2) and size (N, varying between 60 and 500 by step of 40).

2.4.2 Topological reinforcement

Topological reinforcement was based on the topological overlap measure (see Methods). TO represents the neighborhoods' similarity of a pair of nodes by counting their number of common neighbors (Ravasz et al. 2002).
At each rewiring step, the rule connects a randomly selected node that is neither disconnected nor fully connected with a non-neighbor with the highest TO, while pruning another link with uniform probability, hence preserving graph density. For computational efficiency, the rewiring was applied by inserting simultaneously one link on $\frac{N}{2}$ random different nodes at each step, and pruning the same number of links at random, so that $2\frac{N}{2} = N$ links were reallocated at each rewiring step, with statistically equivalent results as when only two links (one insertion, one pruning) per step were modified. In order to compare the results across different graph sizes and densities, we computed the length of each run, r, by fixing the average number of rewiring per link, K, so that $r = \frac{\lambda NK}{2N/2} = \lambda K$. For all the presented results $K = 3$, which ensures that the networks remain connected (see Fig. 7.3 for details).

2.4.3 Network activity

We used a three-state cellular automaton model of excitable dynamics, the SER model (see Methods).
In the deterministic SER scenario, for each network and initial condition setting, the activity time windows consisted of 5000 runs of 30 time steps each and FC was averaged over runs. The initial conditions were randomly generated, covering the full space of possible proportions of states. In the stochastic SER scenario, for each parameter setting (f, p), the activity time window consisted of one run of 50000 time steps. The initial conditions were randomly generated with a proportion of 0.1 nodes excited, while the remaining nodes were equipartitioned into susceptible and refractory states. To analyse the pattern of excitations in the SER model the Functional Connectivity (FC) matrix as computed as explained above in the Methods section.

2.4.4 Implementation with Hebbian plasticity rule

When transposing the topological reinforcement into a biological context, using a plausible model of brain dynamics, it turns out that the rule corresponds to the well known Hebbian rule, where we substituted FC for TO. In other words, the rewiring events occurred with the exact same algorithm, but based on the FC derived from the activity during the given time window. So we used the SER model for activity simulation during a time window after which FC was derived and the rewiring was applied: a random node was selected and connected to a non-neighbor node with maximum FC, while a link was selected randomly with uniform probability and pruned. Once rewired, we iterated through the same steps until the end of the simulation. As for the topological reinforcement and for computational efficiency, the rewiring was applied simultaneously on $\frac{N}{2}$ different nodes at each step. In order to keep the final networks comparable, the total number of rewiring steps was the same for both plasticity modalities, as defined above. According to the SER scenario, stochastic or deterministic, we evaluated the model for different parameter constellations or initial conditions, respectively. For one initial graph, we studied each possible combination of parameter constellation/initial condition by performing 150 simulation runs and the final graph measures were averaged across runs.

2.4.5 Module agreement and "proto-modules"

From a given initial network, multiple simulation runs (500) were performed and the community detection algorithm was applied on each final graph to find a partition of the nodes into communities. Then, an agreement matrix P was computed across all final partitions, where p_{ij} quantifies the frequency with which nodes i and j belonged to the same community across partitions. Finally, the community detection algorithm was applied 100 times on P, yielding a representative set of final partitions of the nodes into non-overlapping communities given an initial graph (Fig. 3.9). In order to probe the structure of each initial graph and find potential 'proto-modules,' we applied the community detection on the initial graph. Due to the weak signal of random graphs, the stochasticity and associated

degeneracy of classical community detection algorithms, a consensus clustering was employed to generate stable solutions. For each random initial graph, the community detection algorithm was applied 500 times, then a agreement matrix was computed, named P_{init}, and finally the community detection algorithm was applied 100 times on this agreement matrix yielding a representative set of (stable) partitions of the initial graph (Fig. 3.9).
Similarity between networks and agreements was assessed by means of the Pearson correlation between their connectivity matrices. Overlap between partitions was probed based on the normalized mutual information between the communities (Meilă 2007).

2.4.6 Statistical assessments

In order to assess the significance of the results, null network models were generated. When comparing networks in terms of similarity (by Pearson correlation), a null model was generated by randomly rewiring a given graph (once per link), while preserving the degree distribution (Maslov & Sneppen 2002). Two null models where used when comparing networks in terms of partition overlap. For comparison of individual runs (initial vs. final structures or initial vs. final agreements), we simply used a rewired initial graph as explained above instead of the actual one that was used as initial condition for the run. As null model for the comparison of agreement matrices, a null agreement P_{null} was constructed by first shuffling the individual partitions (i.e., conserving the number of modules and their sizes, but randomly altering the nodes affiliation) and then computing the agreement across them. Thus, such a null model generates the expected distribution of agreement values that would occur purely by chance for a given number of nodes and modules of given sizes.

2.5 Sequential Reinforcement plasticity model

2.5.1 Networks

We considered synthetic undirected networks without self-connections of size $N = 1000$ nodes and average connectivity $\lambda = 10$. Initial networks were generated according to the classical Erdős-Rényi model (Erdős & Rényi 1959).
We explored the robustness of the plasticity rule across various network realizations and multiple runs (using the same initial network).

2.5.2 Network activity

We used a three-state cellular automaton model of excitable dynamics, the SER model in its stochastic formulation, with parameters $f = 0.005$, $p = 0.3$ (see Methods). The activity time window consisted of one run of 5000 time steps. The initial conditions were randomly generated with a proportion of 0.1 nodes excited, while the remaining nodes were equipartitioned into susceptible and refractory states.

2.5.3 Sequential Reinforcement

The Sequential Reinforcement rule was based on the sequential activation of nodes as defined for the SER model (see Methods). At each rewiring step, first the SER model activity was simulated during a time window after which the sequential activation was computed and normalized to the range [.1, 1]. Then the rewiring was applied: a random node (not yet fully connected) was selected and connected to a non-neighbor node with maximum sequential activation, while a link was selected randomly with uniform probability and pruned, hence preserving graph density. For computational efficiency, the rewiring was applied by inserting simultaneously one link on $\frac{N}{10}$ random different nodes at each step, and pruning the same number of links at random, so that $\frac{N}{10}$ links were reallocated at each rewiring step, with statistically equivalent results as when only one link per step was modified.
Each simulation run consisted of 500 rewiring steps.

For visualization purposes, the results presented in the main text correspond to sub-sampled simulation runs, where every fifth step is displayed (although the rewiring occurred at every step as explained above).

2.5.4 Statistical assessments

The skewness of the degree distribution was evaluated with the Fisher-Pearson coefficient. For normally distributed data, the skewness is about zero. The rank correlation between the sequential activation and the degree of the non-neighbors of a node was evaluated with the Spearman's correlation coefficient. The similarity between degree distributions was computed by means of the Pearson's correlation coefficient

2.6 Bio Echo State Networks

2.6.1 Echo State Networks (ESN)

Echo State Networks (ESNs) are one kind of recurrent neural networks (RNNs) belonging to the broader family of reservoir computing models, typically used to process temporal data (Lukoševičius & Jaeger 2009). The ESN model consists of an input, a reservoir and an output layer. The input layer feeds the input(s) signal(s) into a recurrent neural network with fixed weights, i.e., the reservoir. The function of the reservoir is to non-linearly map the input signal onto a higher dimensional space by means of the internal states of the reservoir. Formally, the input vector $\mathbf{x}(t) \in \mathbb{R}^{N_x}$ is fed into the reservoir through an input matrix $W_{in} \in \mathbb{R}^{N_r \times N_x}$, where N_r and N_x indicate the number of reservoir and input neurons, respectively. Optionally, the input can be scaled by a factor $\epsilon \in \mathbb{R}$ (*input scaling*) before been fed into the network. The discrete dynamics of the leaky neurons in the reservoir are represented by the state vector $\mathbf{r}(t) \in \mathbb{R}^{N_r}$ and governed by the following equations:

$$\mathbf{r}'(t) = f(W_{in}\mathbf{x}(t) + W\mathbf{r}(t-1) + \mathbf{b})$$

$$\mathbf{r}(t) = \alpha \mathbf{r}'(t) + (1-\alpha) W \mathbf{r}(t-1)$$

Where $W \in \mathbb{R}^{N_r \times N_r}$ is the connectivity matrix between reservoir neurons, $\mathbf{b} \in \mathbb{R}^{N_r}$ is the bias vector, f the nonlinear activation function.
For all the presented results $f = tanh$, the hyperbolic tangent function which bounds the values of $\mathbf{r}$ to the interval $[-1, 1]$. With $\alpha = 1$, there is no leakage, which we found to perform better so we fixed them for all presented results. Thus, the equation can be re-written as follows:

$$\mathbf{r}(t) = tanh(W_{in}\mathbf{x}(t)\epsilon + W\mathbf{r}(t-1) + \mathbf{b})$$

The output readout vector $\mathbf{y}(t) \in \mathbb{R}^{N_y}$ is obtained as follows:

$$\mathbf{y}(t) = g(W_{out}[\mathbf{x}(t); \mathbf{r}(t)])$$

Where g is the output activation function and $[.;.]$ indicates the vertical vector concatenation and $W_{out} \in \mathbb{R}^{N_y \times (N_x + N_r)}$ is the readout weights matrix. For all results presented g was either rectified linear unit ($ReLU$) or the identity function. Training the model means finding the weights of W_{out}. Linear regression was used to solve $W_{out} = Z^+ Y$, where Z^+ is the pseudoinverse of $Z = [\mathbf{x}(t); \mathbf{r}(t)]$, i.e., the vertically concatenated inputs and reservoir states for all time steps.
We initialized the incoming weights in W_{in} with random uniformly distributed values between $[-1, 1]$. Further considerations about weights initialization as well as sparsity of the reservoir are detailed in the section . The activity of the reservoir neurons is initialized with $\mathbf{r}(t) = 0$. That produces an initial transient of spurious activity which has nothing to do with the inputs and is therefore useless for learning the relationship to the outputs. We discard that initial transient of 100 time steps in all cases, both for training and for testing.
All presented results with ESNs training where obtained using the Python package

echoes, publicly available (Damicelli 2019).

2.6.2 ESN hyperparameters tuning

The typically most influential hyperparameters in ESNs are reservoir size N_r, spectral radius of the reservoir ρ, input scaling factor ϵ and the leakage rate α (Lukoševičius 2012). In our scheme, the reservoir connectivity W is determined by the real connectome, thus determining a fixed N_r. So the hyperparameters explored where: spectral radius of the reservoir connectivity matrix $\rho = \{0.91, 0.93, ..., 0.99\}$, input scaling $\epsilon = \{10^{-9}, 10^{-8}, ..., 10^{0}\}$, leakage rate $\alpha = \{0.6, 0.8, 1\}$ and bias $b = \{0, 1\}$. A train/validation/test split of the data was performed. For each hyperparameters constellation, the model was trained on the train set and based on the validation score we chose and for the sake of comparison between different conditions, we fixed a common, not necessarily optimal but generally well-performing, set of hyper-parameters: spectral radius $\rho = 0.99$, input scaling $\epsilon = 10^{-5}$, leakage rate $\alpha = 1$, bias $b = 1$. Since the output values Memory Sequence Task are bounded to be greater than 0, we used ReLU as activation out function. Given that such boundary does not exist for the outputs of the Memory Capacity Task, we simply used the Identity as activation out function.
The data for train/validation was split as follows:
Sequence Recall Task: 800 trials for training and 200 for test for each hyperparameters/task difficulty/reservoir generation constellation.
Memory Capacity Task: 4000 time steps for training and 1000 for test for each hyperparameters/task difficulty/reservoir generation constellation (see Supporting Information). For each constellation, we tested 10 independent runs with newly instantiated networks.
After fixing the best hyperparameters, newly instantiated networks were generated and evaluated on the test set not yet seen by any model. The presented results in the main text are the test performances.

2.6.3 Mapping and upscaling connectomes with *bio2art*

We refer to a *connectome* as the map of all the connections obtained from a single brain (Sporns et al. 2005). We used the following publicly available datasets: Macaque monkey (Markov et al. 2012), Marmoset monkey (Majka et al. 2016) and Human (Betzel & Bassett 2018).

For the sake of clarity, let us disect the connectivity into two components: topology and weights. The topology refers to the wiring diagram (i.e., who connects to whom), regardless of the strength of the connection (assuming non-binary connectivity). So if we think of the connectivity in terms of its representations as a connectivity matrix, the topology refers here to the binary mask that indicates which positions of the matrix have values different from zero. The weights describe the precise strength of those connections between neurons. This differentiation is not necessarily completely consistent with common uses in the literature, but serves the purpose of explaining the work presented here. As our goal is to evaluate the role of the topology of real brains, i.e., the mentioned wiring diagram. We propose a scheme to map real connectomes onto reservoirs of ESNs, with topology corresponding to real brains, but weights drawn from a uniform distribution of values between [-1, 1], as in classical ESN approaches (Lukoševičius & Jaeger 2009). Classical ESNs reservoir have weights randomly from a symmetric probability distribution, typically Uniform or Gaussian, and place them at random between neurons, thus generating random graph from the perspective of the topology as well. Another common practice is to use a relatively sparse network, e.g., common choices are pairwise probability of connection $p < 0.1$ or a low fixed mean degree, e.g., $k = 10$). So for the sake of comparison and testing the effect of topology in the performance of ESNs, we the following surrogate connectivity variations as null models (see Fig. 3.20 for a visual comparison):

- ***Bio (rank)*:** Preserves the empirical topology, i.e., wiring diagram or "who connects to whom". Weights are placed such that the rank order of them is the same as the empirical, i.e., strong weights in the empirical connectome will correspong to higher positive weights in the *Bio (rank)* condition, and viceversa.

- ***Bio (no-rank)*:** Preserves the empirical topology, i.e., wiring diagram or "who connects to whom". Weights are placed randomly, so no rank order is preserved.
- ***Random (density)*:** Wiring diagram is completely random, but allowing only as many connections as to match the density of connections of the empirical connectome. The density is defined as the fraction of present connections out of all the possible ones. Weights are placed randomly.
- ***Random (k)*:** Wiring diagram is completely random, but allowing only a fixed number of connections per neuron, i.e., a mean degree $k = 10$. Weights are placed randomly.
- ***Random (full)*:** Wiring diagram is completely random and all neurons connect to all other neurons, i.e., the density of connections is 1. Weights are placed randomly.

The *bio2art* functionality builds artifical recurrent neural networks by using the topology dictated by empirical neural networks and by extrapolating from the empirical data to scale up the artifical neural networks.
We explored here a range of network size scaling factors between 1 and 30x by step of 1.
bio2art offers the possibility to control the within and between area connectivity as well.
There are currently no empirical comprehensive data for neuron-to-neuron connectivity within each brain region. However, existing empirical data suggest that within-region connectivity strength constitutes approximately 80% of the extrinsic between-region connectivity strength (Markov et al. 2012). Therefore, the intrinsic, within-region connectivity in our work followed this rule. It should be noted that the number of connections that a neuron can form within neurons of the same region is controlled by a parameter dictating the percentage of connections that a neuron will form, out of the total number of connections that can be formed. Here we set this parameter to 1, that is, all connections between neurons within a region are formed.
The exact details of the implementation can be found here http://www.github.c

om/AlGoulas/bio2art, together with a freely available Python toolbox to apply the tools used here.

2.6.4 Tasks

Memory Capacity (MC) Task. In this memory paradigm, a random input sequence of numbers $X(t)$ is presented to the network through an input neuron. The network is supposed to independently learn delayed versions of the input, thus there are several outputs (Jaeger 2001). Each output Y_τ predicts a delayed version of the input $X(t)$ by τ time steps, i.e., $Y_\tau(t) = X(t-\tau)$. The values of the input signal $\mathbf{X}$ were randomly drawn from a uniform distribution, i.e., $X(t) \sim Uniform(-0.5, 0.5)$. The networks were trained with 4000 time steps and tested on the subsequent 1000. Each output is trained independently and the performance, the so called *Memory Capacity (MC)*, is calculated as the cumulative score (squared Pearson correlation coefficient ρ) across all outputs (i.e., all time lags) as follows:

$$MC = \sum_{\tau} \rho^2(y_\tau, \hat{y}_\tau)$$

Sequence Recall Task. In this task the network is presented with two inputs, $X_1(t)$, $X_2(t)$, a sequence of random numbers to memorize and a cue input, respectively. The cue input signals whether to fixate (output equal to zero) or recall. After the recall signal, the network is supposed to output the memorized sequence in the L steps previous to recall signal, where the pattern length L is a parameter regulating the task difficulty (see Fig. 2.1). One trial of the task consists of one fixation period and the subsequent recall period. The values of the input signal $X_1(t)$ were randomly drawn from a uniform distribution, i.e., $X_1(t) \sim Uniform(0, 1)$. The performance was evaluated with the R^2 score only during the recall steps because the fixation phase was much easier for the model to get right and would have inflated the performance. Each BioESN was trained with 800 trials and tested on 200 trials. For each pattern length L in {5, 6, 7, ..., 25}, 100 different networks with newly instantiated weights were tested.

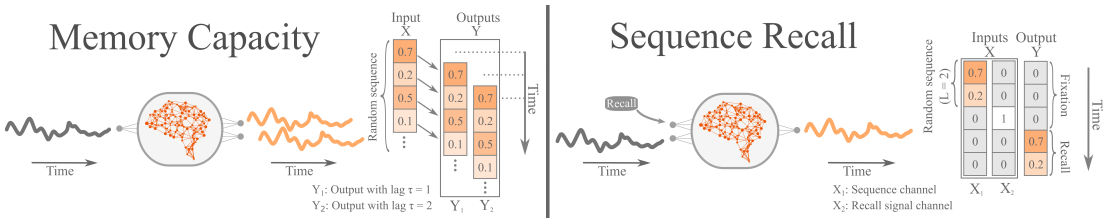

Figure 2.1: Cognitive tasks Schematic representation of the tasks and the input/output data structure for each of the cognitive tasks used to evaluate the performance of the BioESNs. Left: Memory capacity (MC) task, where the network receives a stream of random values as single input X and has several independent outputs Y (for simplicity, the example shows only two. Each output is memorized by an independent output neuron of the network and is supposed to recall the input at a specific time lag τ. The BioESNs were trained with 4000 time steps and tested on the subsequent 1000. Right: One trial of the sequence recall task. The network receives inputs X_1, X_2 coming from a random sequence and a recall signal channel, respectively. There is only one output neuron, which after the recall signal channel indicates it (i.e., $X_2 = 1$) is supposed to reproduce the input received in the previous L steps, i.e., the pattern length parameter determining the difficulty of the task (for simplicity, in the scheme $L = 2$). The BioESNs were trained with 800 trials and tested on 200 trials. The score was computed considering only the recall phase in order to avoid inflation of the metric, given that the fixation periods were much easier to get right.

Chapter 3

Results

3.1 Modules from plasticity model with deterministic dynamics

3.1.1 Brief background and specific goal

In spite of many new insights on brain connectivity in recent years, the origin of such characteristic structural organization remains unclear. Previous work has shown that some of these connectivity patterns may emerge spontaneously, as indicated by studies of functional connectivity in vitro (i.e., cultured tissues) (Schroeter et al. 2015; Bettencourt et al. 2007), and may be associated with long-term memory consolidation (Wheeler et al. 2013). Beyond these descriptive observations, however, a mechanistic understanding of the self-organized emergence and maintenance of brain networks remains elusive.

Typical modelling work on Hebbian plasticity is based on the modification of connection strengths between neural units as a result of network activity (Markram et al. 2012). This is in line with classical experiments of inducing Long Term Potentiation (LTP) or Long Term Depression (LTD) of neuronal connections (Bi & Poo 1998). However, recent empirical work that showed evidence supporting a causal relationship between LTD induction and the probability of removal or maintenance of individual dendritic spines, resulting in higher removal of depressed synapses

(Wiegert & Oertner 2013). This finding indicates that plasticity may act on network connectivity in a binary fashion, in addition to changes of synaptic strength, directly affecting neural network topology. Inspired by those experimental results, in the study presented in this chapter, we formulated a minimalistic plasticity model. The plasticity rule is Hebbian in the sense that is based on activity correlations (more strictly, co-activations) of the nodes, which in turn influence the probability of maintaining connections between nodes connected.
The goal of this study was to explore the effects of a local Hebbian plasticity rule on the global network topology using a minimalistic network model with excitable nodes and discrete deterministic dynamics. In spite of its simplicity, the model has proven to be useful for understanding basic mechanisms of activity propagation as well as the influence of network topology on functional correlations (Garcia et al. 2012; Messé et al. 2015). For more details on the SER model and the plasticity rule, see Methods section.

This section has been published in (Damicelli et al. 2017).

3.1.2 Emergence of modular network topology

Despite the relative simplicity of the dynamical model and the plasticity rule, random networks evolved in a systematic way into a modular structure (see Fig. 3.1). The modularity (Q) increased quasi linearly until it reached a plateau after few steps around which small fluctuations occurred. The resulting modular structure is shown in Fig. 3.1 a. where three distinct modules emerged. Interestingly, this reorganization produced by the plasticity rule did not influence the degree distribution of the network, that is, the final network had the same out/in degree distributions as the initial random structure (Fig. 3.1 c.). The correlation between structural and functional connectivity (SC-FC) followed a similar trend as Q, showing that the structural reorganization also had functional consequences (Fig. 3.1 d.).

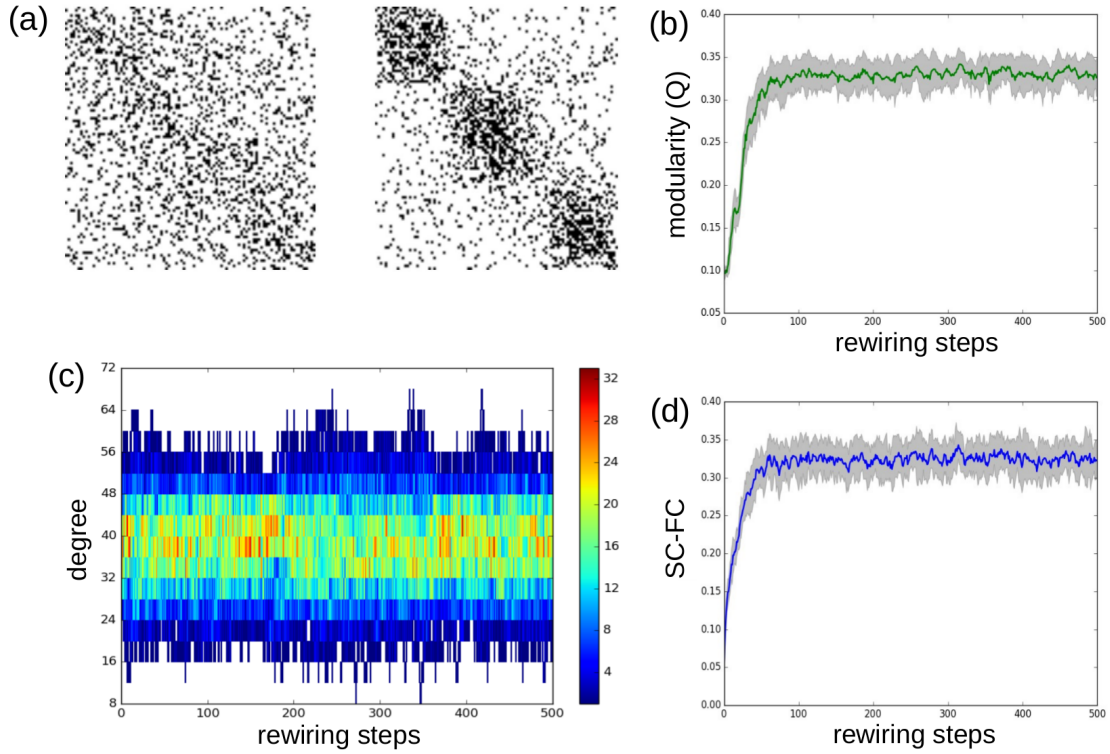

Figure 3.1: Emergence of modular structure. (a) Example of an initial random structural connectivity network with a density of 20% (before rewiring, left), and the structural connectivity network resulting from the plasticity rule (right). Networks were reordered to highlight the modular structure. (b) Modularity (Q value) as a function of the number of rewiring steps. Coloured line and grey area represent the mean and standard deviation across 15 simulations, respectively. (c) Illustration of the evolution of the total degree (sum of in- and out- degrees) distribution as a function of the number of rewiring steps in one run. Frequency of occurrence is colour-coded. (d) Relationship between structural and functional connectivity (linear correlation) as a function of the number of rewiring steps, with mean and standard deviation across runs.

3.1.3 SC turnover and modular composition

Next we assessed the pace at which the structural connectivity pattern was modified by the plasticity rule along the simulation. A gradual and continuous reorganization took place along the whole simulation, even after a modular structure was present. The correlation between successive SC matrices in time decayed fast, and after approximately 50 rewiring events it approximated zero (Fig. 3.2 a.). This held true for every segment of the simulation, even after the modular structure was already present. Regarding the modular structure, the modular pattern appeared to be the same independently of the specific segment of the simulation considered. The modular partitions also differentiated relatively fast, showing a dynamic equilibrium in the structural organization, conserving the modular organization in general, but varying the composition of the modules (Fig. 3.2 b.). This finding indicates a dynamic equilibrium in the structural organization with a permanent turnover, where the network after a relative small number of rewiring events is completely different (with the precise number of events depending on the retention probability parameters). Despite of preserving the modular structure, the composition of the modules varied in time.

3.1.4 Robustness of findings to density variations

Given the predominant effect of density on the topological characteristics of networks, the robustness of the rewiring rule was explored over a range of densities. As is apparent in Fig. 3.3 a., for all densities studied, modularity was induced by the plasticity rule and the network was reorganized showing three modules. Modularity and SC-FC correlation measures also showed the same pattern as for the sparser network (Fig. 3.3 (b, c)).

3.1.5 Dependence of findings on parameter variations

We evaluated the dependence of the findings on the plasticity rule parameters, that is, the link retaining probabilities (P_{min}, P_{max}). The range of evaluated values for the retaining probability was chosen following the experimental results

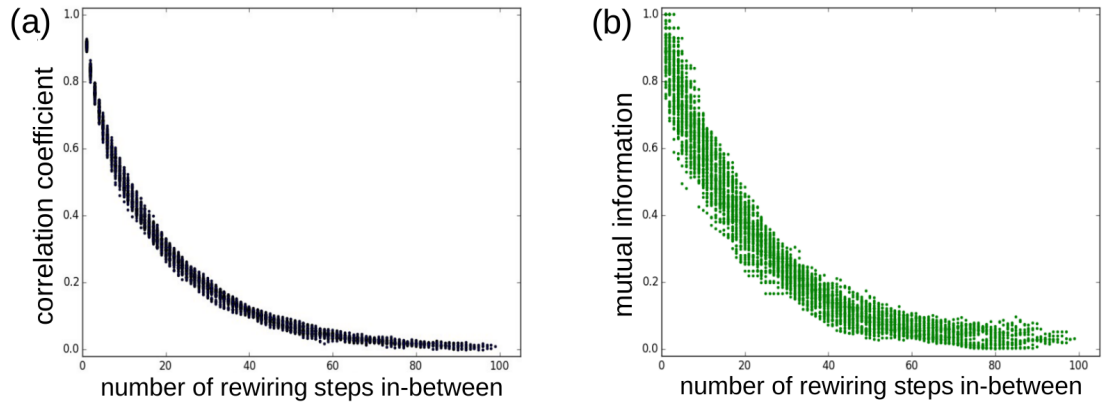

Figure 3.2: Fluctuations of network composition in time. (a) Decay of network similarity. Linear correlations were computed between each adjacency matrix and all adjacency matrices at all subsequent time points until the end of the simulation. The plot shows the Pearson linear correlation coefficient as a function of the separation in time (number of rewiring events in-between) between all considered matrices. (b) Decay of partition pattern. To evaluate how long a given partition was maintained in time, the partition distance was computed between each adjacency matrix and all adjacency matrices at all subsequent time points until the end of the simulation. The plot shows the partition distance measures as a function of the separation in time (number of rewiring events in-between) between the considered matrices. The first 100 rewiring events were excluded, in order to begin the comparison when the modular structure was already present. The decay curves did not change after 100 rewiring steps in-between, therefore that is the maximum distance plotted.

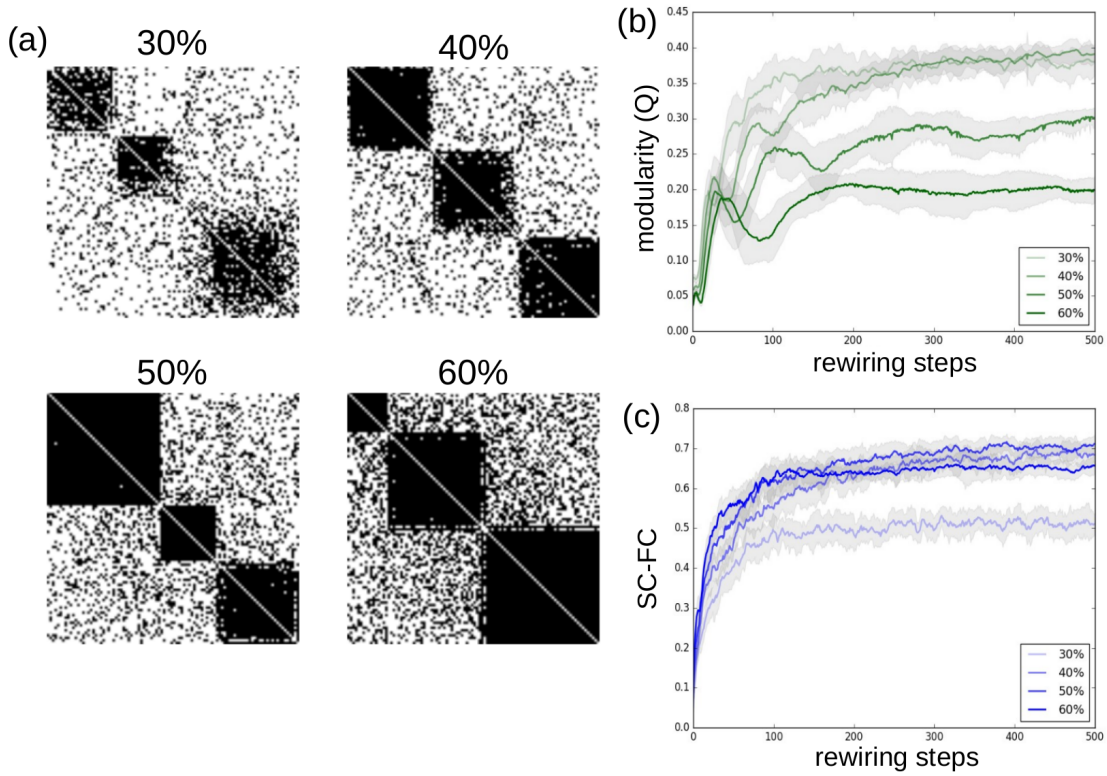

Figure 3.3: Effect of graph density. (a) Structural connectivity network resulting from the plasticity rule for different network densities. Matrices were reordered to highlight modular structure. (b, c) Emergence of modularity and SC-FC correlation was also observed for higher densities.

in (Wiegert & Oertner 2013), where only 30% of the depressed dendritic spines persisted in the long term (i.e., one week after LTD), while the remainder was pruned. The emergence of modularity and SC-FC correlation can be appreciated in Fig. 3.4, which shows the mean of final values across simulations. This could be observed for a large subset of parameter values, especially when the retaining probability was close to one for the highest co-activation, and when the difference between the maximum and the minimum retaining probability was large. The coincidence between modularity and SC-FC emergence can also be appreciated.

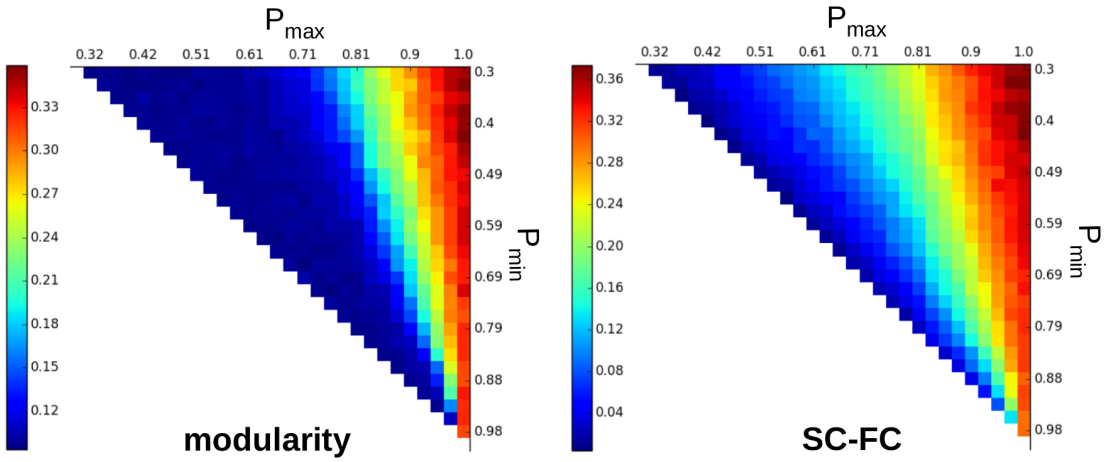

Figure 3.4: Dependence of modularity and SC-FC correlation on the plasticity rule parameters. Lower and upper bound ranges (for P_{min} and P_{max} , respectively) correspond to the retaining probability values used to rewire the adjacency matrix according to the co-activation matrix. Left: Modularity at the end of the simulation as a function of the bound parameters. Right: SC-FC correlation. For each parameters constellation the average across 15 simulations is shown.

3.1.6 Simulations starting from structured networks

A valid question at this point is whether the plasticity rule might somehow amplify a pre-existent modular structure (e.g., small cores of densely connected nodes embedded in the random network that work as seeds from which the large modules are built) or if it can be accounted for by other factors (such as synchronization properties of the dynamic model). In order to address this question,

we carried out simulations starting from two prototypical structured networks, instead of randomly connected ones, namely a flat random modular graph and a Barabási-Albert graph (N=100, m=12, density=0.21) (Barabási & Albert 1999) (Fig. 3.5). Interestingly, the plasticity rule was able to disassemble this initial structure in both cases, and a new modular network was generated where the typical three modules emerged. The degree distribution also converged in both cases to a Gaussian distribution. At this point it is worth noting that the final structure of the network did not correspond to the initial co-activation map either (data not shown), although the model dynamics appeared to be sufficient for the plasticity to generate the modules.

In sum, the explored plasticity rule generated a global reorganization of the network into a modular structure, which also led to an increase in correlation between structural and functional connectivity. The dynamics of the deterministic SER model seemed to dominate the outcome of the model (i.e., final network connectivity), independently of the initial network connectivity and to generating a fixed number of final modules, which then turns out to be a limitation trying to understand the relation between structure and function on the network.

This section has been published in (Damicelli et al. 2017).

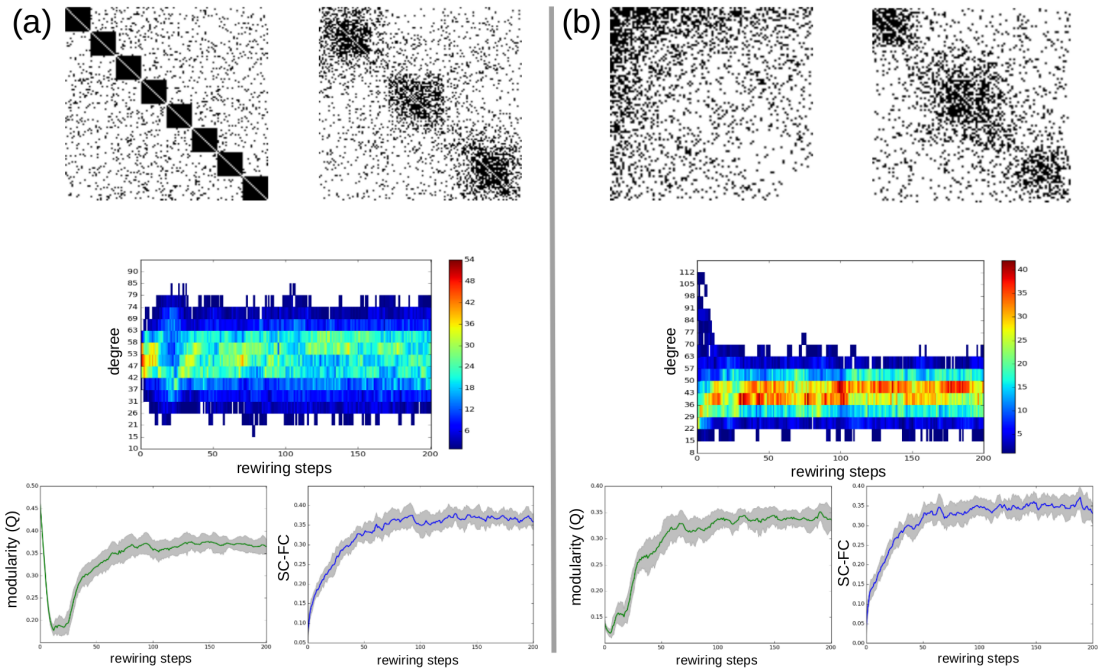

Figure 3.5: Plastic reorganization of structured network. (a) An initially multi-modular network (left) was used as initial graph. The simulation ran applying the plasticity rule, and at the end of the simulation (right) the matrix was reordered to highlight the modular structure. The results show that the plasticity rule destroyed the initial connectivity pattern and promoted the reorganization of the network into three modules. The heat map in the middle row shows the total degree distribution in time. Lower plots show Modularity and SC-FC as a function of time. (b) The same for a Barabási-Albert network (left) as initial graph. The transition from a long- tailed distribution to a Gaussian distribution can be observed. After 200 rewiring steps no qualitative changes were observed, thus only the evolution until 200 rewiring steps is plotted, so that the transition between the initial and the final degree distribution is observable.

3.2 Modules emergence through Topological Reinforcement

3.2.1 Brief background and specific goal

The general principles leading to the emergence of brain modules remain elusive, both in terms of the necessary topological changes for generating them, as well as with respect to a plausible biological realization of such changes.
In this chapter, I present a model that constitutes a plausible underlying mechanism leading to the formation of modules. The model bridges the gap between pure generative models[1] (e.g., "homophily-driven models") and activity-based models (e.g., Hebbian-like plasticity models), whose binding element lays at the topological level.
Concretely, we present the topological reinforcement (TR) rule, a rewiring mechanism based on the topological overlap (TO) (Ravasz et al. 2002). For each pair of nodes, the TO metric quatifies the number of direct common neighbors between them. The higher similarity, the higher value of TO (for more details on TO and the precise definition, see the Methods section).
Prompted by the exploration of network motifs (that is, few-node sub-graphs which are often statistically enriched in real networks, see (Milo et al. 2002; Milo et al. 2004)) the interplay of different topological scales in a graph has become an object of intense research. In particular, several studies have shown that global network properties, such as hierarchical organization (Vazquez et al. 2004) or modularity (Fretter et al. 2012), can systematically affect the composition of networks in terms of local topology or network motifs, see also (Reichardt et al. 2011). Intriguingly, that line of research inspires the complementary possibility: a systematic iterative selection on local network structures may conversely install, or at least enhance, certain global network properties. This is the conceptual approach we set out to explore here, where our topological reinforcement rule iteratively enhances the lo-

[1] In this context, "generative model" refers to a statistical model that is able to create data by assuming underlying probability distributions of the independent variables and then fitting the parameters of such distributions based on the observed dependent variable. See (Betzel & Bassett 2017) for a more extensive discussion.

cal topological overlap.
As a further step, we explore a plausible dynamical implementation of the topological reinforcement. We used an excitable network model, the SER model, in which the discrete activity of network nodes is described by susceptible, excited and refractory states, representing a stylized neuron or neural population (see Methods for details). In this case, the plasticity acts in a Hebbian-like fashion based on the functional connectivity (FC) derived from co-activation patterns of network nodes. In short, starting from initial random configurations, we evolved networks according to the topological reinforcement rule. Topological reinforcement was based on the TO between nodes of a network. At each rewiring step, a randomly selected node was connected to a non-neighbor with the highest TO, while pruning another link with random uniform probability, in order to preserve network density.

This section has been published in (Damicelli et al. 2019).

3.2.2 Random networks evolve towards modular, small-world organization

The topological reinforcement rule reliably evolved synthetic random networks toward high modularity (Fig. 3.6). Moreover, due to increased clustering, the final networks had a small-world organization (Fig. 3.7). The results were robust across multiple runs and multiple initial network realizations (Supp. Fig. 7.1). We also explored the effect of network size and density on the TR rule (Fig. 3.6). The results were consistent, showing similar scaling curves across conditions, which speaks for the robustness of TR in generating modular networks.

The scaling pattern of final number of modules could be roughly approximated based on the average network degree. The rationale is that the number of modules is intuitively proportional to the number of nodes while inversely proportional to the average size of neighborhoods containing nearest and next to nearest neighbors. As we do not have an analytical expression for the sizes of such neighborhoods, we assume that it is proportional to λ^{1+a}, where a is some exponent with $a < 1$. The exponent one accounts for nearest neighbors and a for the double counting of nodes when going to next-to-nearest neighbors. We observe a good

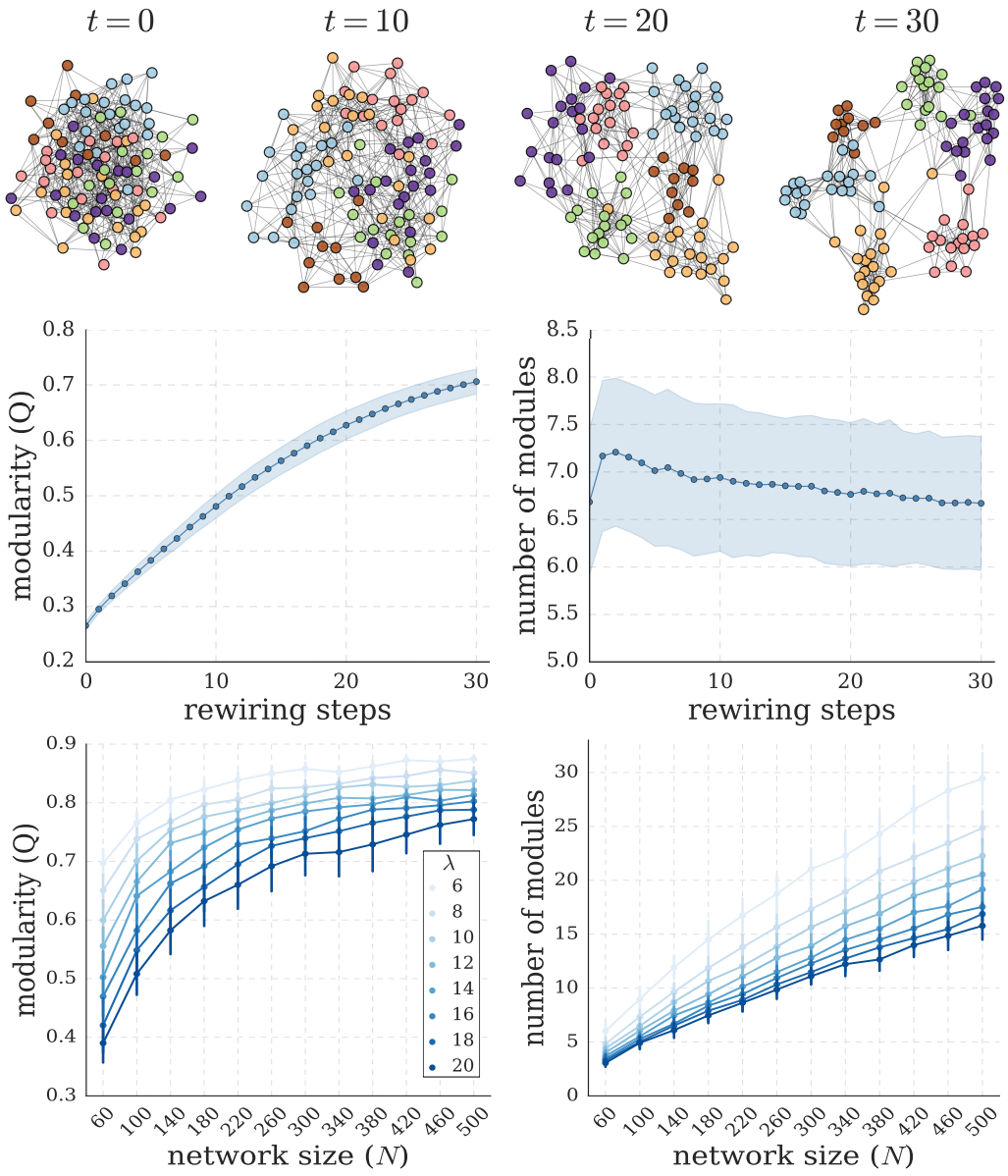

Figure 3.6: Emergence of modular network organization from topological reinforcement. (Top) Example of network evolution resulting from topological reinforcement, starting from a random network. Layouts are generated according to the Fruchterman-Reingold force-directed algorithm. Nodes are consistently coloured according to the final modular structure. At each rewiring step (t), a total of $\frac{N}{2}$ nodes were affected, reallocating a total of N links (two per node). (Middle) Evolution of the modularity (Q) and number of modules as a function of the number of rewiring steps (mean and standard deviation across 500 simulation runs). (Bottom) Final modularity (left) and number of modules detected (right) for different network sizes (N) and densities (λ, average number of links per node) (mean and standard deviation across 50 independent graph realizations).

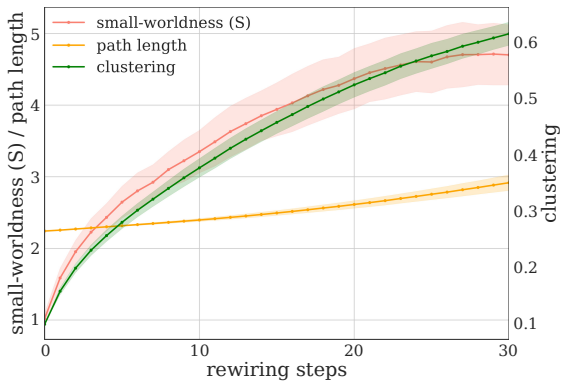

Figure 3.7: Evolution of the mean clustering coefficient, characteristic path length and small-world index (S). Results are expressed as mean and standard deviation across 500 simulation runs as a function of the number of rewiring steps.

(though not perfect) agreement with the numerical results for $a \approx \frac{1}{4}$ (see Fig. 3.8).

3.2.3 Final network organization reflects initial network structure

The topological reinforcement rule appeared to amplify weak 'proto-modules' already present in the initial random graph. The similarities between the initial and final network structures were investigated in terms of Pearson correlation and partitions overlap between networks; see Methods section and Fig. 3.9 for details.

Statistical analysis across multiple runs showed a significant similarity and partition overlap between the final graphs and the initial one (Fig. 3.10 A). Moreover, the results also showed a consistent pattern of final modular organization (Fig. 3.10 B). The module agreement of final networks across multiple runs (P) displayed pairs of nodes with high probability (beyond chance) to end up in the same module. Fig. 3.10 B shows the mean intra-module density of the initial random graph according to different partitions. The distribution of the mean intra-module density according to the modules detected in the agreement P coincides fairly well with the mean intra-module density of the partitions detected on the graph itself. In contrast, intra-module density from partitions coming from a null

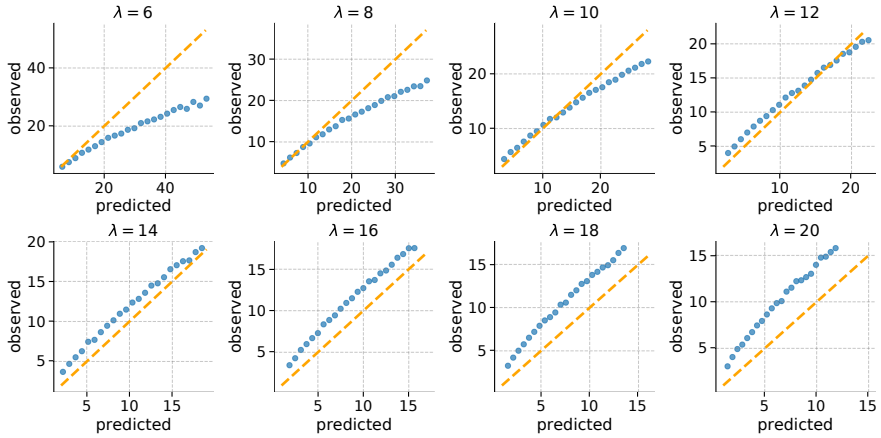

Figure 3.8: Prediction of final number of modules. The scatter plots show the average number of observed modules across simulations versus its predicted values, estimated based on the average degree. Each panel represents an average network degree (6 to 20 by step of 2), and for each panel, each blue point corresponds to a network size (60 to 500 by step of 40). The orange dashed line shows the identity.

model is centered around 0.1, that is, the graph density (i.e., probing density of randomly chosen groups of nodes). In the random graphs used as initial condition, no variations in link density are expected (since, by definition, connection probability is uniform for all pairs of nodes). Importantly, that is the case *on average across graph realizations*, but, due to stochastic variations and finite-size effect, individual graphs might contain groups of nodes with slightly higher density of edges than expected. We refer to these groups as 'proto-modules.' In order to highlight these modules, a module detection algorithm was applied multiple times on the initial graph and a module agreement matrix was built (P_{init}). The correspondence between the initial and final network structures is also evident comparing the final agreement P with its analogous on the initial graph P_{init} (Fig. 3.10 C). The similarity (as measured by correlation) between both agreements is high. Additionally, we generated a set of partitions from P and another set of partitions from P_{init}, and quantified the overlap between all possible pairs of partitions P_{init}-P. We observed a significant overlap between the partitions from P_{init} and those from P. Furthermore, the results were robust across multiple initial network realizations (Supp. Fig. 7.1).

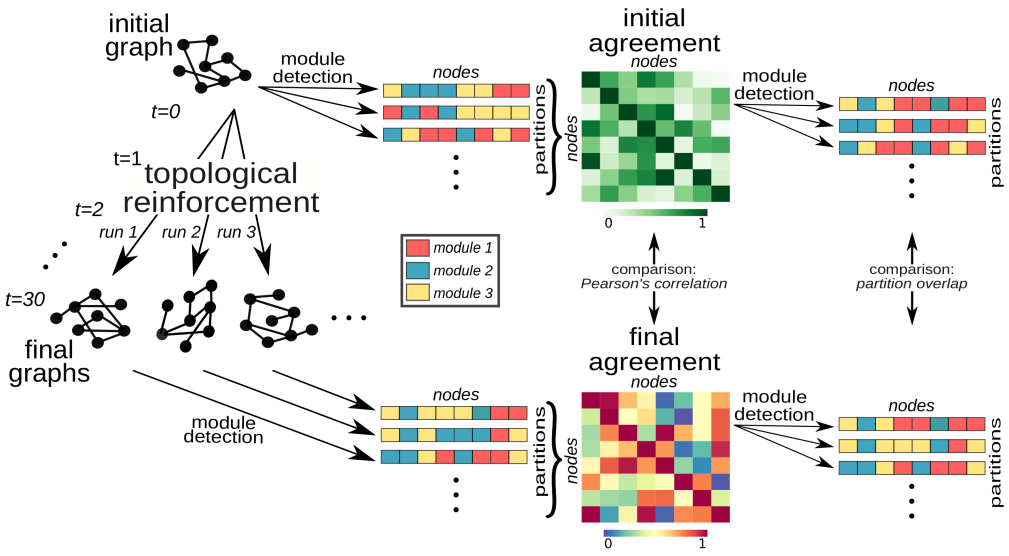

Figure 3.9: Modules agreement and 'proto-modules.' Schematic example for a graph with $N = 8$ nodes and 30 rewiring steps of the procedure for probing the existence of 'proto-modules' in the initial graph and the relationship between initial and final network structure. Each simulation run starting from the same initial graph is represented by a grey color. A schematic representation of the affiliation vectors can be viewed under module partitions. *Each element of the vector represents a node and its color indicates the module that it was assigned to. The probability that two nodes end up in the same module across partitions is represented by the* agreement *matrix, in other words, a consensus across module partitions. The agreement matrices where compared both in terms of their values (Pearson's correlation) and their modular composition (partition overlap). See Methods for details.*

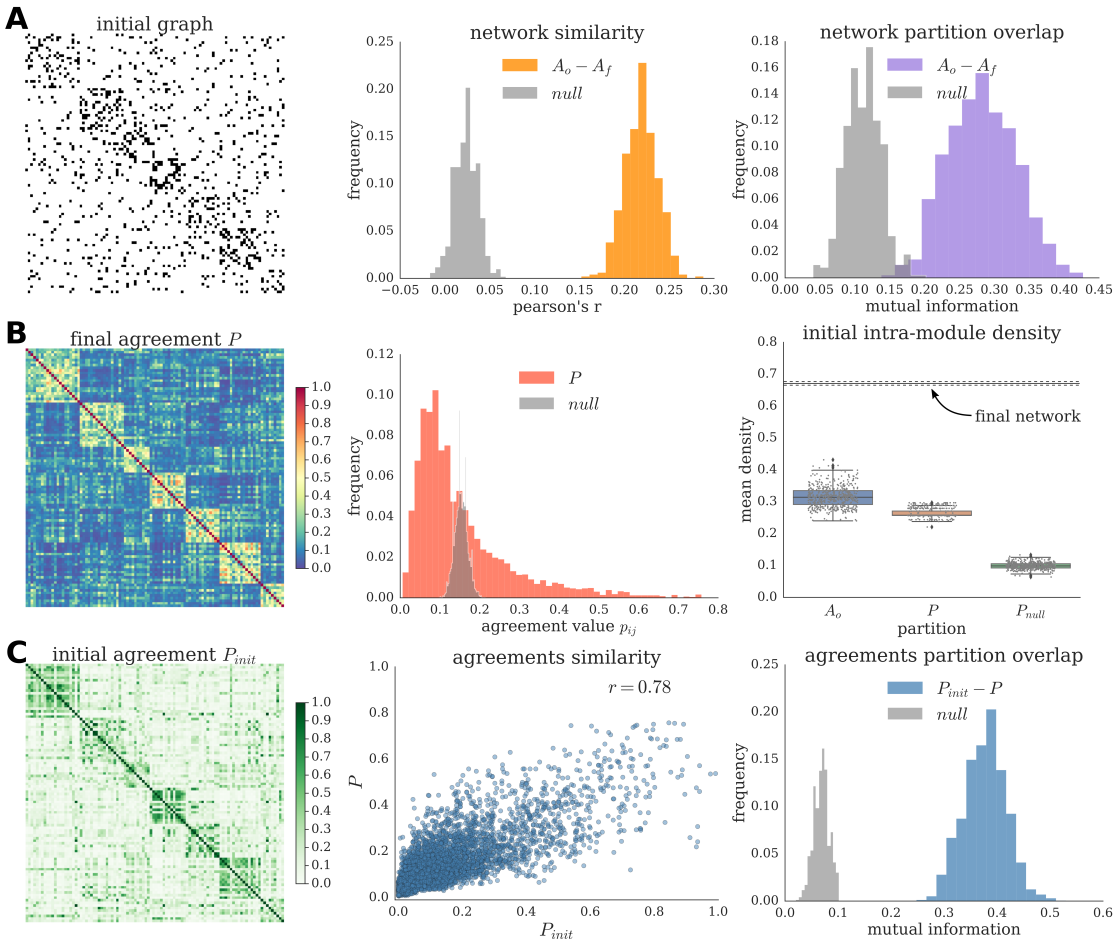

Figure 3.10: Relationship between initial and final network structures. (A) Initial adjacency matrix (left) reordered according to the modular partition of the agreement P. Similarity (middle) and partition overlap (right) between all pairs of initial and final networks, and the corresponding null distributions. (B) Agreement matrix across multiple runs (P, left) reordered according to its modular partition. Histogram of the P values and of the corresponding null model (middle). Distributions of the intra-modular density of the initial network (right). Average intra-module density of the initial network according to different types of module partitions. The procedure was repeated 500 times for each type of partition. As a reference, the mean intra-module density of the final network modules are also plotted (average and standard deviation). (C) Initial agreement matrix (P_{init}, left) reordered according to the modular partition of P. Similarity (middle) and partition overlap (right) between P_{init} and P and the corresponding null distribution.

3.2.4 Implementation of topological reinforcement with Hebbian plasticity rule

In the brain, the topological reinforcement may be implemented through various plausible activity-based models. We explored one such model, in which the activity of network nodes was described by discrete susceptible, excited and refractory states, the SER model, representing a stylized neuron or neural population. TR when transposed into biological context simply corresponds to the so-called Hebbian rule, where we substituted FC for TO, see Methods section for details. In order to explore the FC-based rule and its relation to TR, we exploited an interesting feature of the SER model: for a given graph topology, the relationship between TO and FC varies according to the parameters of the model. More specifically, the SER model allows both deterministic and stochastic formulations, depending on the definition of the state transition probabilities. In the deterministic case, only initial the proportions (e, s, r) of nodes in each state may vary, since the transition probabilities are fixed ($f = 0$ and $p = 1$). While in the stochastic case, different parameter constellations may me achieved by varying such state transition probabilities (for more details, refer to Methods and (Messé et al. 2018)).

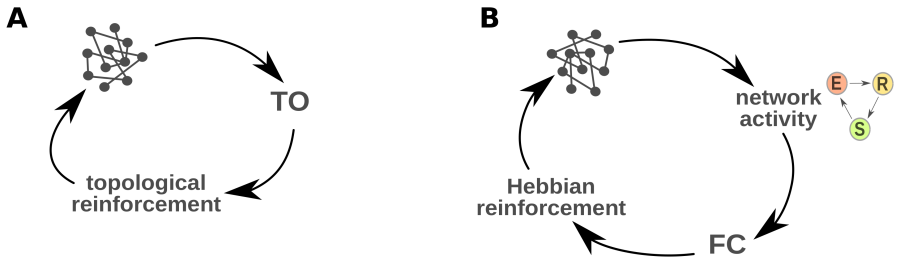

Figure 3.11: Rewiring rules comparison. We applied two different model scenarios. The first one, based solely on the topology, and we applied the topological reinforcement (TR) rule, which is based on the Topological Overlap (TO). While the second considered activity on the nodes (SER model), and the rewiring occurred in a Hebbian fashion, i.e., based on functional connectivity (FC) between nodes and reinforcing connections between highly correlated nodes. The following schemes show the core loops of both schemes for comparison. Each iteration of a loop is equivalently denoted as a rewiring step. See Methods for more details. (A) Topological reinforcement. (B) Biological implementation - Hebbian rule.

After exhaustive evaluation of the possible constellations for each case, we found: first, that the FC-based rule was also able to generate a modular network structure. Importantly, a sufficiently high similarity (as measured by correlation) between TO and FC within the initial configuration was a necessary condition for modularity emergence, as illustrated by the sharp transition from the non-modular to the modular regime (Fig. 3.12); second, the results produced by the FC-based plasticity were consistent with the ones from TR, both in terms of final network configurations and their module partitions (Fig. 3.13). Fundamentally, this indicates that, provided the correlation between TO and FC is high enough, the Hebbian rule acts indirectly as topological reinforcement.

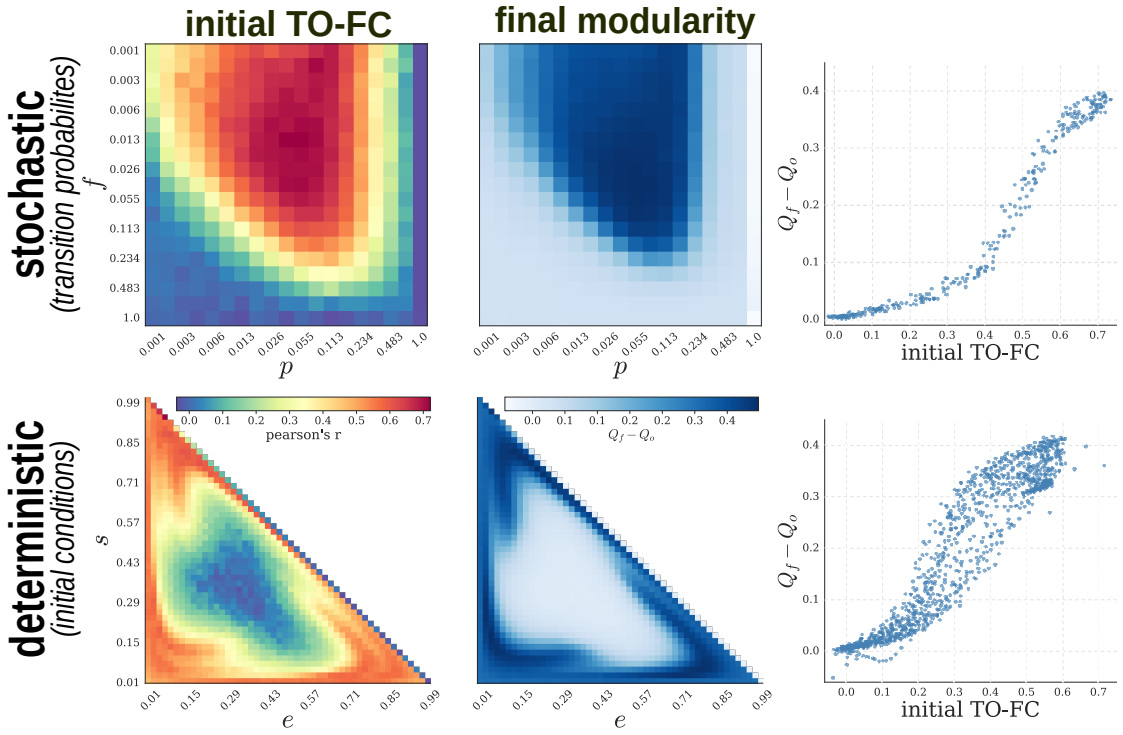

Figure 3.12: Biological implementation of the topological reinforcement. Parameter space exploration of the stochastic (top) and deterministic (bottom) SER model. Similarity (measured by correlation) between TO and FC in the initial graph (left), final modularity (middle) expressed as the difference between the mean final modularity value and the modularity of the initial random graph (across multiple (500) community detection). (Right) Scatter plot of the relationship between both quantities. Note logarithmic scale for the stochastic case.

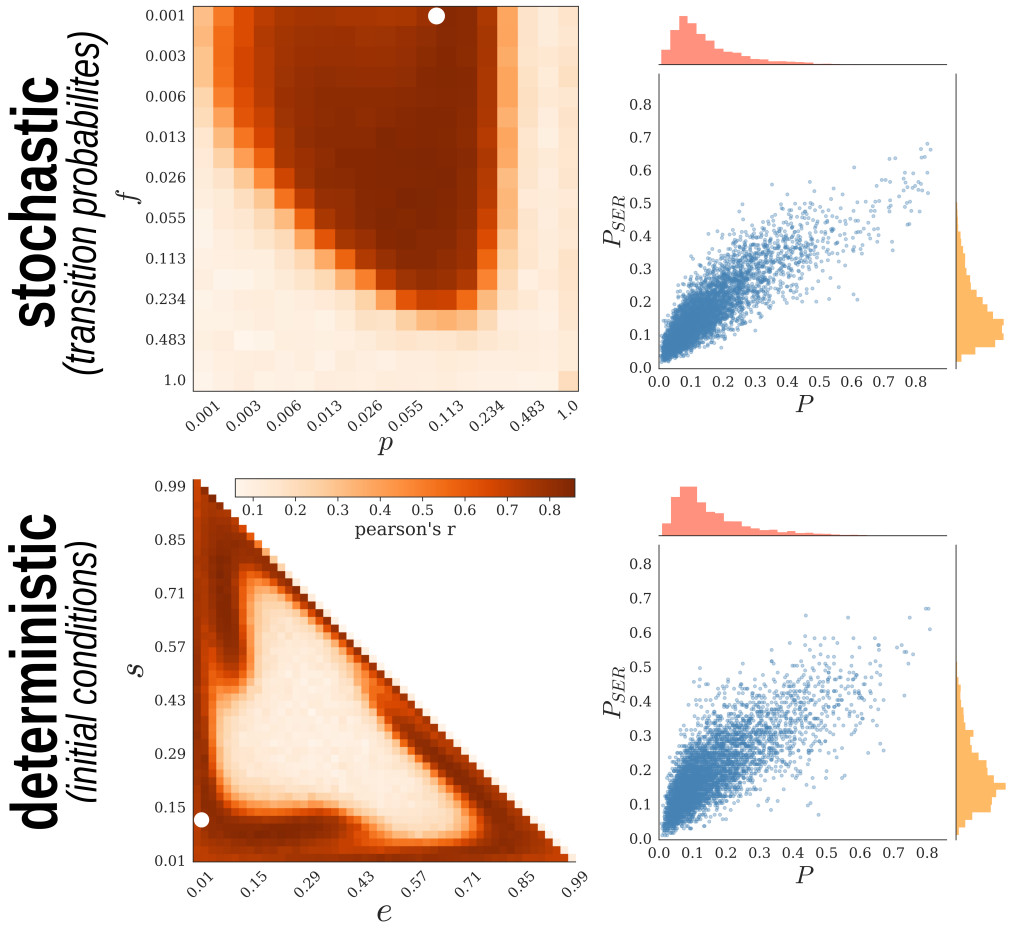

Figure 3.13: Correspondence between the topological reinforcement and the Hebbian rule. Similarity between P from the topological reinforcement and from the Hebbian rule using the stochastic (top) and deterministic (bottom) SER models. Pearson's correlation coefficient was computed to summarize the similarity between both rules across the parameter spaces. Scatter plots represent the relationship for a selected setting (white dots in the heat-maps).

The results confirm a correspondence between the two plasticity modalities, which speaks in favour of the dynamical implementation representing a biologically plausible mechanism through which topological reinforcement may take place in real systems, thus supporting its role as a contributor to the emergence of modular brain networks.

3.3 Heterogeneous degree distribution through Sequential Reinforcement

3.3.1 Brief background and specific goal

As exposed in the Introduction, heterogeneous degree distributions with their characteristic hubs are a fundamental property of brain networks. Thus, explaining the emergence of such property is key to understand the formation of connectivity patterns in the brain. That was the focus of the work presented in this section.

Previous literature on modeling the emergence of heterogeneous degree distributions is largely dominated by a particularly family of generative models, namely the so-called "preferential attachment" and different variations of it (Barabási & Albert 1999; Golosovsky 2018). In spite of some interesting properties of this type of model, such as its analytical tractability, it is often difficult to map it onto biological systems, such as brain networks. For example, most formulations of the preferential attachment model imply growth of a network (addition of nodes and links) and do not take into account the potentially changing connectivity, such as in brain networks affected by neuronal plasticity.

Regarding brain connectivity in particular, a few modeling studies have paid attention to topological changes resulting from plasticity rules. Those studies are mainly aimed at describing network properties at the micro-level though, such as the distributions of sub-network motifs and weights (Stone & Tesche 2013; Effenberger et al. 2015). Thus it remains unknown if global properties, such as the degree distribution, could be shaped by more simple principles, such as spatio-temporal constraints of brain development (Goulas et al. 2019) and/or plasticity mechanisms.

We approached the problem from the perspective of plasticity mechanisms and formulated if a simple model, based on the sequential activations of neural units. We also used the previously presented minimalistic SER model (see Methods) to represent the activity of neurons and implement a rule-based rewiring framework to study how a network evolved in time. The model encouraged the formation

of connections between nodes whose activity was such that the activations of a node was correlated with the future activations of a second other node. Part of the inspiration to formulate the model came from previous work studying patterns of spreading activity on excitable networks with different underlying topologies (Müller-Linow et al. 2008). In particular, hubs functioned as activity propagators generating radial excitation waves starting from them. More recent work along those lines has shown self-organized patterns of activity, where hubs shaped the directionality of activity waves in non-trivial ways (Moretti & Hütt 2020). In a complementary vein, our model explored the consequences of a plasticity rule that promoted links that would reinforce that pattern of activity propagation away from higher degree nodes. The model was somehow also loosely related to the biological principle of Spiking Time Dependant Synaptic Plasticity (STDP) in the general notion that it promoted creation of links when the activations of a node were predictive of activations of another node (Caporale & Dan 2008).

3.3.2 Emergence of heterogeneous degree distributions

The Sequential Reinforcement model entails a plasticity rule based on the dynamics of the nodes. After an epoch of network activity, the rule connects a node i to a non-neighbor node j for which the activations of i were most predictive of the activations of j. In other words, the node i was connected to a non-neighbor that maximized the sequential activation of $i \rightarrow j$, thus *Sequential Reinforcement* (see Methods for details).

We found that the Sequential Reinforcement led to the remodeling of an initially random network (with a binomial degree distribution) into a network with a long-tailed degree distribution. This finding was consistent across independent runs (Fig. 3.14).

A potential explanation for this finding could be the fact that the sequential activation of a node i to its non neighbors is to some extent correlated with the degree of those non-neighbors, thus turning the sequential activation metric into a proxy variable (Fig. 3.15).

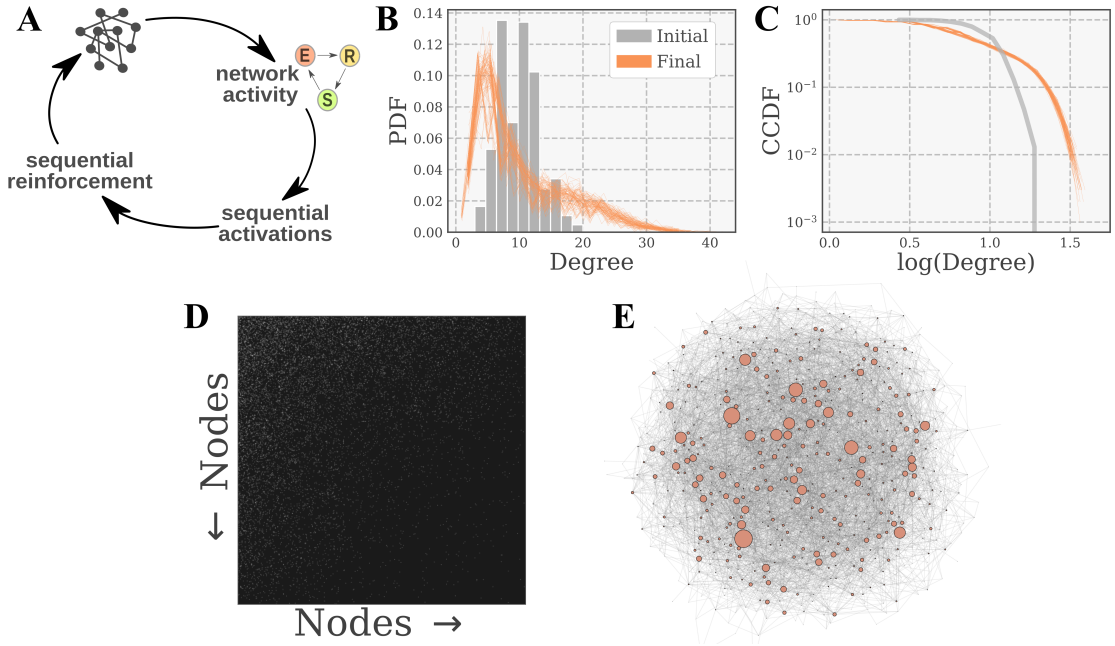

Figure 3.14: Sequential Reinforcement leads to heterogeneous degree distribution. (A) Schematic representation of the Sequential Reinforcement plasticity rule. Each iteration of a loop is equivalently denoted as a rewiring step (see Methods for more details). (B) Initial and final degree distribution of the network nodes resulting from the plasticity model, represented as the probability densities (PDF). The initial degree distribution (grey) is also plotted for comparison. The plot shows results of 100 independent simulations starting with the same initial graph. Each trace corresponds to one simulation. Data are shown in a linear-linear scale. (C) The same data as in (B) but represented as the complementary cumulative density function (CCDF) and in a log-log scale. (D) Adjacency matrix of the final network, node presence represented by white points. Nodes were sorted by degree in decreasing order (as indicated by the arrows). (E) Final network layout, with node sizes proportional to node degree.

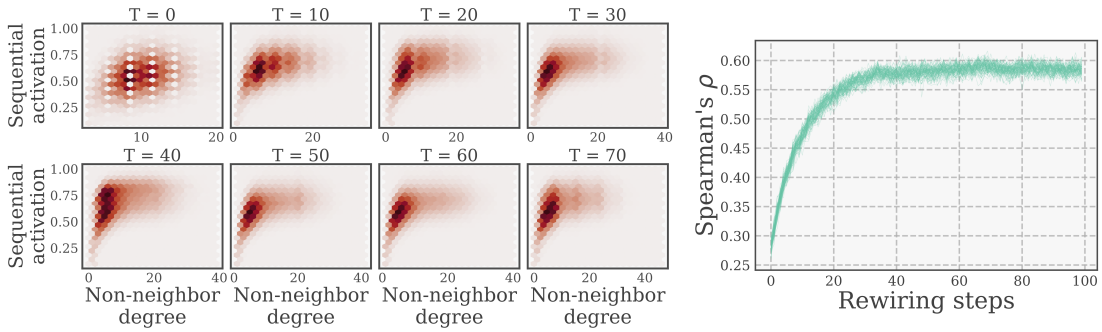

Figure 3.15: Non-neighbors sequential activation vs. degree. Left: Normalized sequential activation of a node i to its non-neighbors. At rewiring step, a node i is connected to the non-neighbor with maximum sequential activation. Thus each non-neighbor constitutes a "candidate" to gain a link to node i. The plot shows the relationship between the degree of those candidates and the sequential activation. The plot shows aggregated results from 10 independent simulation runs. Sequential activation is normalized as for the rewiring rule (see Methods). Right: Summary of the relationship depicted in the diagrams on the left but for the whole simulation run. The plot shows results of 10 independent simulations starting with the same initial graph. Each trace corresponds to one simulation. The plots show a sub-sampled version of the simulations (every fifth step is shown).

3.3.3 Stability of the final degree distribution

Interestingly, the model showed a stable asymptotic behaviour. After an initial period of strong remodeling, the degree distribution stabilized with a heterogeneous degree distribution (Fig. 3.16). In spite of the ongoing rewiring and the stochastic events playing a role in the time evolution of the network, the networks evolving under Sequential Reinforcement rule showed a convergence to a self-regulated state, in which the larger hubs reached a ceiling in the number of connections. This upper bound in the maximum size of the hubs as well as the unfolding of the degree distribution remodeling was also consistent across independent simulation runs.

3.3.4 Predictability of the final degree distribution

As a follow-up question we investigated the predictability of the final degree distribution. That is, to which extent the initial node degrees could determine the

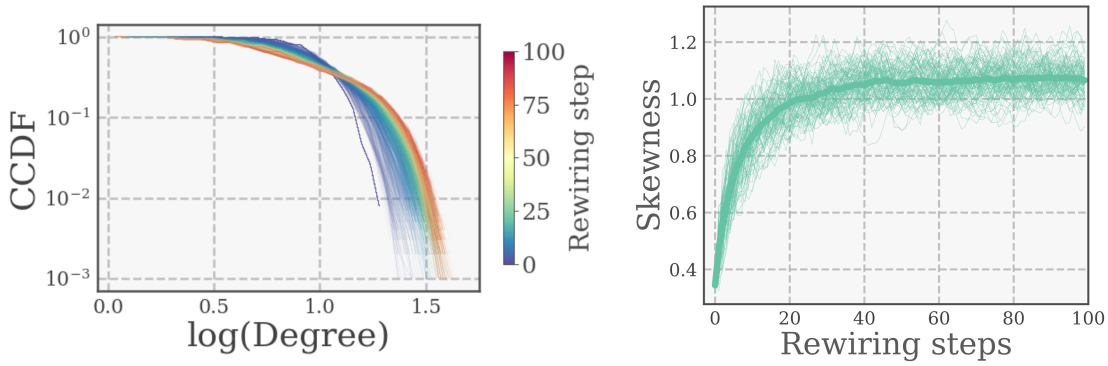

Figure 3.16: Evolution of the degree distribution along the simulation. Left: The evolution of the degree sequence along one complete simulation is shown, with rewiring steps color coded (colorbar). The plot shows results from 100 runs. Each trace corresponds to the degree distribution of a run at a given time step. Right: Evolution of the skewness along the simulation. The plot shows results from 100 runs. Each trace corresponds to a run. The thick line depicts the mean across runs. The plots show a sub-sampled version of the simulations (every fifth step is shown).

final outcome. To answer that, we tracked the evolution of the degree distribution in time, comparing it to the initial degree distribution. We found a mild correlation between the initial and the final degree distribution. In Fig. 3.17 (A) it is possible to visualize the trace of the high-degree nodes back in time along the simulation. For a more quantitative demonstration of that, in Fig. 3.17 (B, C) we observe the decay in the correlation of the degree distribution to the initial step is slow enough that right after the period of initial strong remodeling (~200 rewiring steps) the degree distribution still had a moderate correlation to the initial one. The consistency across independent simulation runs was also evident in this analysis.

3.3.5 Stability of the node degree ranking structure

Besides the global shape of the final degree distribution being stable as a whole and to some extent related to the initial state, a more detailed question is how the complete ranking of degrees evolves in time. In other words, after ordering the nodes into groups according to their degrees, we asked how stable the composition of such ranking groups in time was. For illustration purposes, let us think of the following example: Assume that nodes i and j have degrees

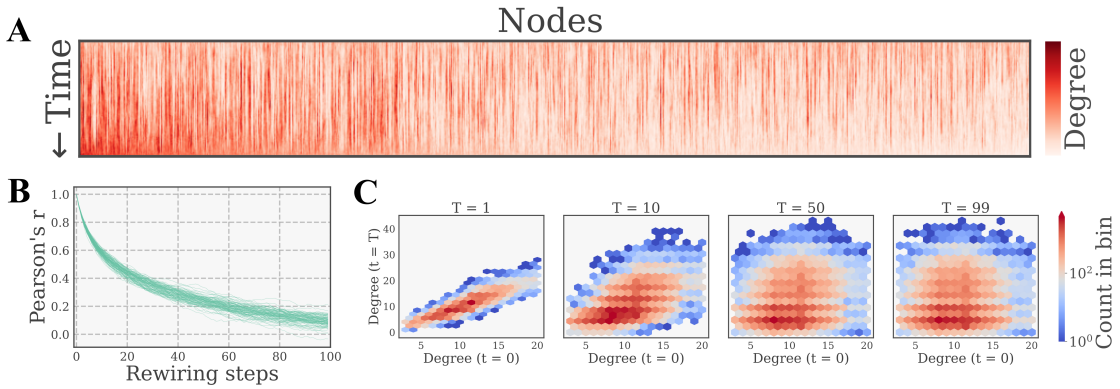

Figure 3.17: Predictability of the final degree distribution. (A) Two dimensional representation of the degree distribution along a simulation run. In order to visually trace back the origin of the hubs, the nodes where sorted from left to right in decreasing order according to their degree at the end of the simulation, (B) Similarity of the initial degree distribution. At each rewiring step T, the correlation between the degree sequence at time $t = 0$ and the degree sequence at time $t = T$ was compared by means of the Pearson's correlation coefficient. Each trace corresponds to one simulation run (100 in total). The plot shows a sub-sampled version of the simulations (every fifth step is shown). (C) More detailed visualization of the relation summarized in (B) for specific time points (1, 10, 50, 99). Each subplot aggregates results of the 100 independent simulation runs starting with the same initial graph.

$k_i = 10$ and $k_j = 20$ at time step t. If the plasticity rule acted in such a way that those degrees perfectly swapped to $k_i = 20$ and $k_j = 10$ at time $t + 1$, then the global degree distribution would remain unchanged, but the ranking composition would change. To tackle that situation, we studied the temporal unfolding of this hierarchy of nodes degrees by quantifying the overlap in the composition of degree ranking in successive time points. For example, considering the hundred nodes with highest degree at time t, we counted how many of those nodes were still in the first hundred positions of the ranking at time $t+1$ and denoted that as the "nodes overlap." The same analysis was repeated for the following degree ranking groups, i.e., in the second, third, etc. hundred highest positions. We found a clear pattern that was fairly stable in time: The highest and the lowest degree ranking groups were the most stable in time (group 1 and 10, respectively), while the intermediate ranking positions were more unstable. This can be observed in Fig. 3.18, where the above explained overlap of nodes in time of each degree ranking group is plotted along the simulation run. Interestingly, the highest degree nodes were the most stable across the whole simulation run. We show this quantitatively in Fig. 3.18 B, where the variance across simulation runs is shown for each group along the run and the group 1 shows the lowest variance.

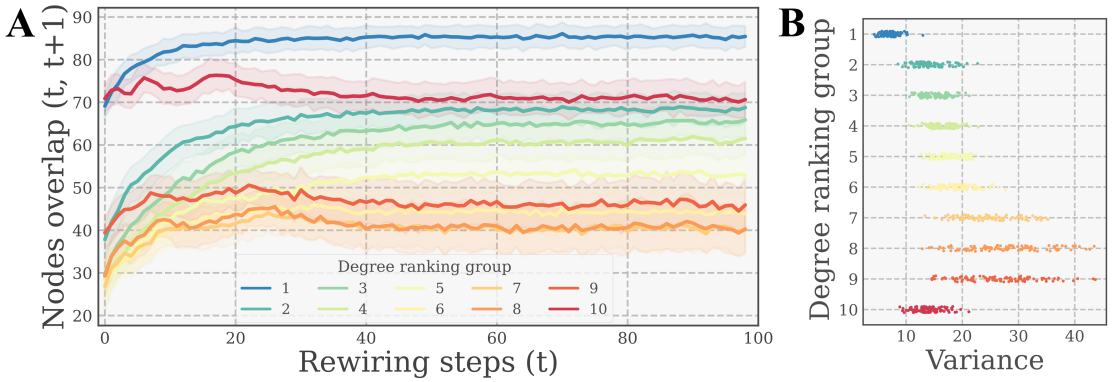

Figure 3.18: Stability of the degree distribution along the simulation. (A) At a time step t, the nodes were ranked by their degree and such ranking was split into ten groups, i.e., given a network with 1000 nodes, the ranking groups were 1-100, 101-200, etc. The same was repeated for time step $t+1$ and, for each ranking group, the number of nodes belonging to the same group in consecutive time steps was counted, denoted as nodes overlap $(t, t+1)$. The same was repeated for 100 simulation runs. The plot shows the mean and standard deviation across runs. (B) For each degree ranking group, the across-runs variance along the whole run is shown. Each point corresponds to the variance across simulation runs for a given time step. The plots correspond to a sub-sampled version of the simulations (every fifth step is shown).

3.4 Bio Echo State Networks

3.4.1 Brief background and specific goals

Computational implications of brain connectivity have so far mainly been probed for general functional properties, e. g. ability to sustain activity, but has not yet been tested on concrete tasks. Certain connectivity properties of brain networks imply dynamical consequences that can be theoretically beneficial for information processing in the brain. Nevertheless, it is highly non-trivial to relate such theoretical, somehow abstract results to the performance of brain networks *solving concrete tasks*. In other words, it is unknown if and to what extent the actual, empirically discerned brain connectivity can lead to beneficial properties, such as faster learning, better performance or greater robustness.

We explicitly addressed that gap here by building recurrent Echo State Networks (ESN) that are *bio-instantiated*, thus *BioESNs*. We ask if and to what extent the topology of BioESNs affects its performance on concrete memory tasks. This is a necessary step exploring the possible links between biological and artificial neural systems, not by means of abstract network models but exploiting the wealth of empirical data being generated.

Concretely, in order to test the potential effect of the topology of real connectomes on the computation capacities of recurrent networks, we devised a hybrid Echo State Network (ESN) integrating real brain connectivity, thus *BioESN*. Classical ESNs have an internal reservoir of neurons sparsely connected at random between them. The reservoir works as an internal non-linear projection of the input(s), generating a rich variety features, such that the readout layer can linearly separate the patterns more easily. Thus, the performance of an ESN is related to the richness of the representation generated by the reservoir neurons, in turn related to the connectivity pattern between the reservoir neurons.

We investigate here if the non-random topology of biological neural networks could affect the performance of ESN by integrating real connectomes as reservoir and letting the BioESN solve concrete cognitive tasks (see Fig. 3.19). Importantly, we constructed the BioESN reservoirs based on the wiring diagrams (i.e., who connects to whom) of connectomes, but using the weights initialization typically

used in classical ESNs (see Fig. 3.20) and Methods for details).
We tested connectomes of three different primate species (Human, Macaque and Marmoset) in two different memory tasks.

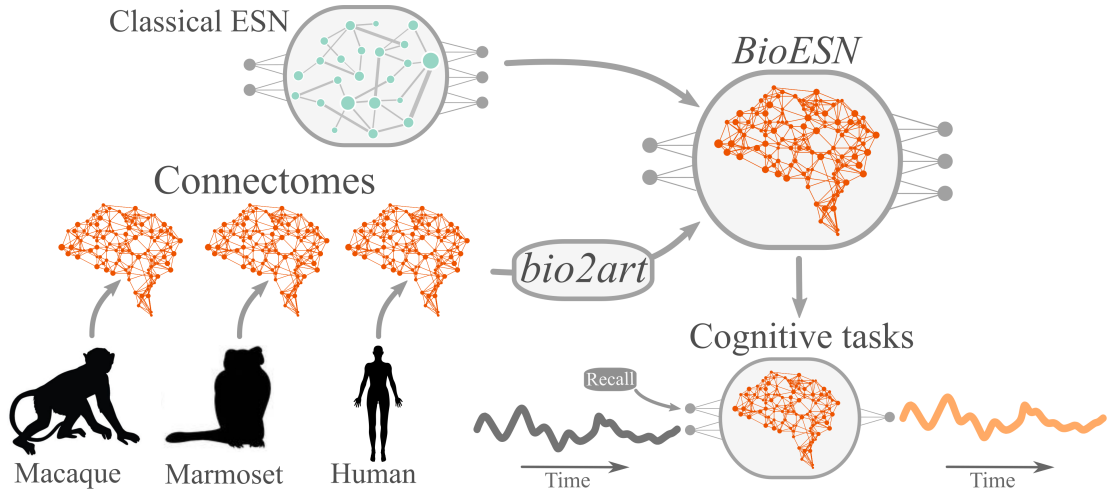

*Figure 3.19: General approach scheme. For each of the three species we generated a Bio-Echo State Network (*BioESN*) by integrating the real connectivity pattern as reservoir of an Echo State Network (ESN). Thus, in contrast to the classical ESN with randomly connected reservoir, BioESNs have connectomes based on connectivity coming from the empirical connectomes. We also propose a framework for mapping biological to artificial networks,* bio2art*, which allows to optionally scale up the empirical connectomes to augment the model capacity. The resulting BioESNs are then tested on cognitive tasks (Methods for details on the tasks).*

Since we aimed at testing if the connectivity pattern of empirical connectomes could have an effect on the performance of BioESNs, we generated several variations of the connectivity as surrogate network for contrast, where each surrogate preserves (or not) specific connectivity properties, as summarized in Fig. 3.20). The conditions *Bio (rank)* and *Bio (no-rank)* preserved the empirical binary topology mask (i.e., who connects to whom) and thus constitute the conditions that we mainly aimed at testing. The difference between both conditions is that *Bio (rank)* preserved the ranking of the weights. That means, in spite of the weights coming from a random distribution, the links in the network where allocated such that links with high strength in the empirical connectome also corresponded to stronger weights in the BioESN. In contrast to that, such rearrangement of links

was not performed for the *Bio (no-rank)* condition, thus only keeping the binary mask of empirical connectivity but respecting no ranking order of links. The rest of the surrogate conditions (*Random (density), Random (k), Random (full)*) have totally random wiring diagram and their density of connections is the only factor varying across conditions. For the condition *Random (density)*, the density of connections is the same as the empirical connectome. For the condition *Random (k)*, the network forming the reservoir has a fixed number of links per node $k = 10$, as in classical ESNs approaches (Lukoševičius 2012). For the condition *Random (full)*, there are no restrictions in terms of links, thus generating a fully connected network, i.e., density equal to 1 (Fig. 3.20) or a summary on all the tested conditions). Larger reservoirs are *per se* expected to have better performance than otherwise equivalent networks. Thus, given that the different sizes of the empirical connectomes, the results are not comparable across connectomes, but only across connectivity conditions for one connectome.

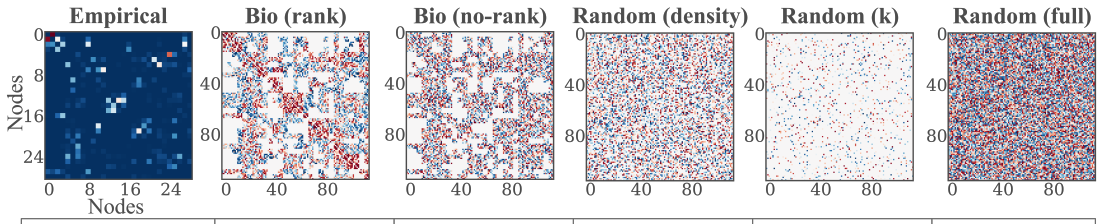

Wiring (topology)	Empirical	Empirical	Random	Random	All-to-all
Weights rank order	Empirical	Random	Random	Random	Random
Density of connections	Empirical	Empirical	Empirical	Mean degree k = 10	1

Figure 3.20: bio2art, *scaling up connectivity and surrogates. The connectivity of the networks derived from the empirical connectivity and used as reservoirs in the BioESNs can be represented as an adjacency matrix. This figure shows examples of adjacency matrices representing a scaled up version (4x) of the Macaque monkey empirical brain connectivity then integrated into the BioESN as reservoir. We also build surrogate connectivities for comparison with the empirical case that preserves real connectivity patterns. Each surrogate network controls for different aspects of the connectivity, as shown in the summary table in the figure. The figure depicts an example of the empirical (Macaque) connectivity and the different derived connectivities tested. Notice the nodes indices, explicitly showing the upscaling of the connectivity. This was repeated for all the other connectomes tested. See for more details on connectivity generation and surrogates.*

3.4.2 Memory Capacity Task

In this classical paradigm, the network is presented with a random sequence of numbers through a unique input neuron. Each output neuron is trained independently to learn a lagged version of the input, thus there are as many output neurons as lags to be tested (Jaeger 2001). The performance, the so called *Memory Capacity (MC)*, is calculated as the cumulative score across all outputs (i.e., all time lags, see Methods for details).
Our results show a comparable performance across all reservoir types except for the *Bio (rank)* condition (Fig. 3.21). Networks from all the tested conditions were able to learn the task, at least for the lowest difficulty (time lag $\tau = 5$), but the *Bio (rank)* condition showed significantly worse memory capacity. This pattern was consistent for all the empirical connectomes tested (Macaque, Marmoset and Human). On the other hand, we did not find differences in the performance for all the rest of tested conditions. This indicates that a certain level of randomization is actually necessary to reach a better performance and that biological wiring diagrams can achieve the same performance as the purely random networks, provided an adequate level of randomness is allowed, as in the *Bio (no-rank)* condition.

3.4.3 Sequence Memory Task

In this task, the network is presented with two inputs, a sequence of random numbers to memorize and a cue input, thus having two input neurons. The cue input indicates whether to fixate (output equal to zero) or to recall the presented pattern. When the recall cue is presented, the network is supposed to output the memorized sequence in the previous L steps, where L is the *pattern length*, a parameter regulating the task difficulty (see Methods for details). One trial of the task consists of a fixation period followed by a recall period. In order to avoid inflation of the score, the performance was evaluated exclusively during the recall steps, which are more difficult to get right than the fixation phase.

In agreement with the results for the Memory Capacity task, we found that all tested ESNs were able to learn the task, at least in its easier variations (pattern length $L = 5$). Along the same lines, the *Bio (rank)* condition was the only one

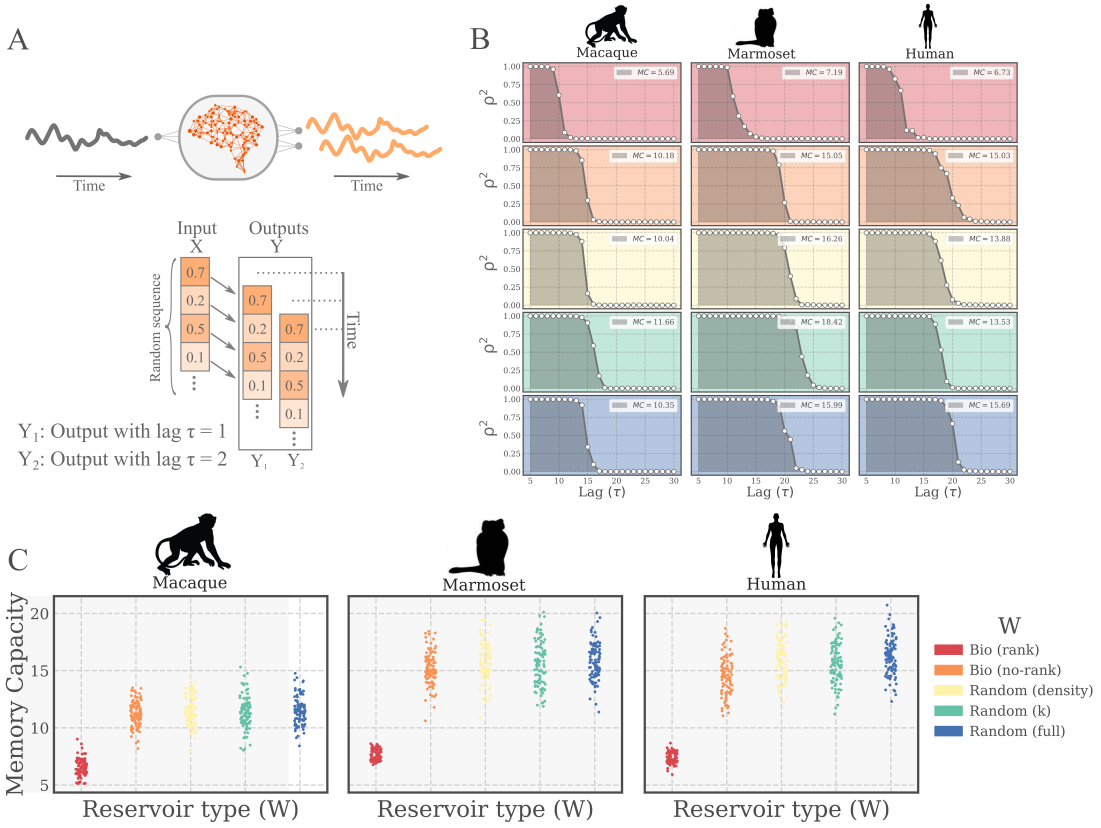

Figure 3.21: Memory Capacity Task. ***(A)*** *(Upper) Schematic representation of the task. An input signal (X) is feed as a time series into the network through an input neuron. Each output neuron independently learns a lagged version of the input (Y_τ) (Lower) Alternative representation of the task in terms of the input/output structure of the data.* ***(B)*** *Examples of network evaluation on the task. A forgetting curve (grey line) is shown for each tested species (columns) and connectivity W condition (color coded). For each time lag (τ) the score is plotted (squared Pearson correlation coefficient, ρ^2). The memory capacity (MC, see legends) is defined as the sum of performances over all values of τ and represents the shaded areas in the plotted examples.* ***(C)*** *Performance of the bio-instantiated echo state networks (*BioESNs*) for the three different species tested. For each pattern length, 100 different networks with newly instantiated weights were trained (4000 time steps) and tested (1000 time steps). The test performance of each networks is represented by a point in the plots.*

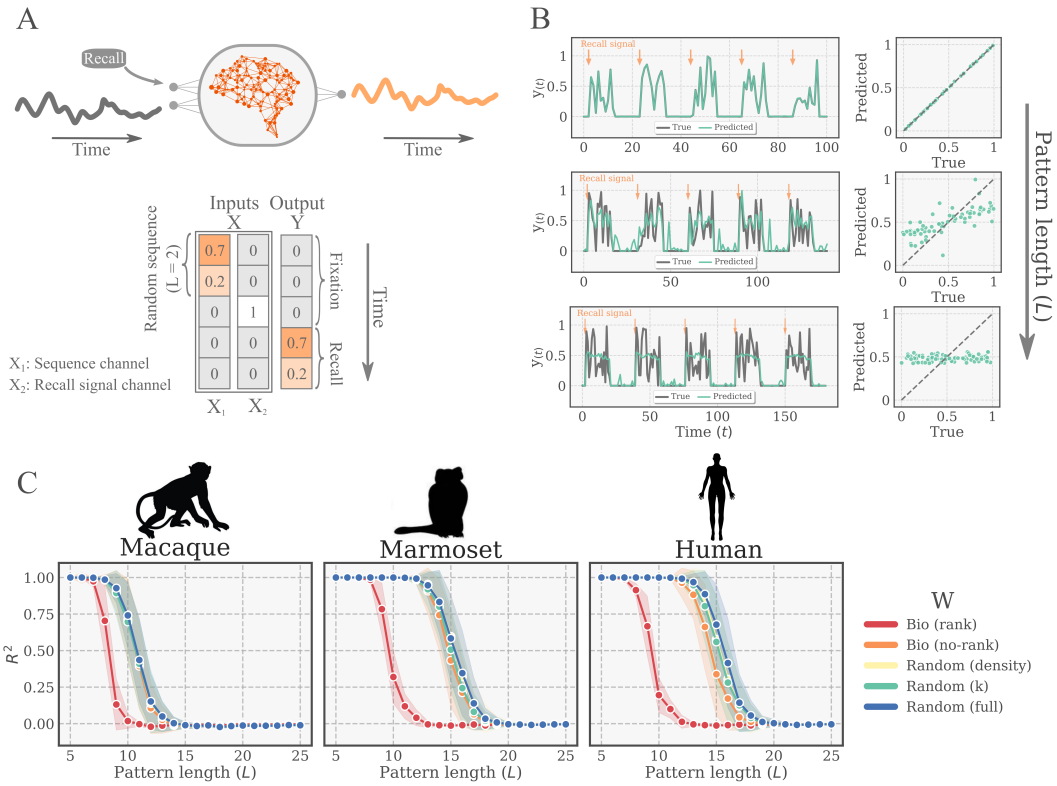

Figure 3.22: Sequence Memory Task. ***(A)*** *(Upper) Schematic representation of one trial of the task. The input signal (X_1) and the recall signal (X_2) are feed as a time series into the network through two input neurons. When the recall signal comes ($X_2 = 1$), the output neuron is supposed to output the memorized input of the last L steps. (Lower) Alternative representation of the task in terms of the input/output structure of the data.* ***(B)*** *Examples of actual and predicted times series for 5 trials at three different difficulty levels (pattern length, from top to bottom: $L = 10/14/18$). The scatter plots on the right show the predicted* vs. *the true output (as explained in main text). The BioESN in the example was built from human connectome with the* Bio (no-rank) *variation.* ***(C)*** *Performance of the bio-instantiated echo state networks (BioESNs) for different task difficulties (pattern length) for the three different species. The bio-instantiated reservoirs,* Bio (rank/no-rank), *are compared to surrogates with random connectivity patterns. For each pattern length, 100 different networks with newly instantiated weights were trained (800 trials) and tested (200 trials). The curves depict the mean test performance and standard deviation across networks.*

with a significantly different performance, showing worse performance than the rest of the conditions. The *Bio (rank)* networks had a different performance decay profile, only being able to memorize shorter sequences than the rest of the network types (Fig. 3.22). These findings were again consistent across all the different connetomes tested.

3.4.4 *bio2art*: Mapping and up-scaling connectomes

The performance of an echo state network is intimately related to the reservoir size, as a larger network can potentially generate a richer repertoire of features and has more trainable parameters. Our next goal was to investigate the scaling behaviour of our model, i.e., how the performance changes as the reservoir size is increased. For that, we applied our *bio2art* approach (Goulas 2020), which allows us to map the connectivity of real connectomes onto artificial recurrent networks and scale up the number of neurons by an arbitrary scaling factor while preserving the wiring diagram of the original connectome (see Methods for details). Although not totally conclusive because of the different experimental methodologies, that brings us closer to a comparison across species connectomes (see Discussion). At the same time, this allows us to explore the extent to which the pattern observed for the different weights mappings (*Bio (rank), Bio (no-rank)*, etc.) holds for larger networks and how it plays out with the model capacity driven by reservoir size.

When upscaling the connectomes with *bio2art*, one important parameter is whether to have homogeneous or heterogeneous distribution of weights between scaled-up areas, as shown in Fig. 3.23 A. With the homogeneous variation all connections between two upscaled areas have exactly the same weight. In other words, after scaling up the number of neurons per area, the total original weight between every two areas is equally partitioned amongst all the area-to-area connections. In contrast to that, the heterogeneous variation allows the area-to-area connections between scaled up regions to be different. More specifically, the total original weight between every two upscaled areas is partitioned and distributed at random amongst the area-to-area connections.
We evaluated a wide range of scaling factors (i.e., neurons per area) for the BioESNs

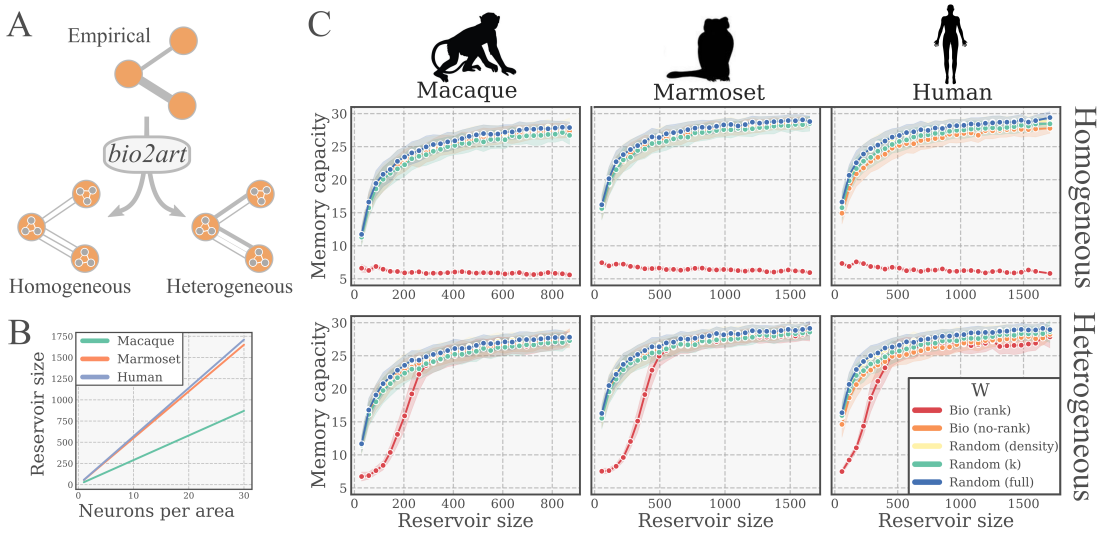

Figure 3.23: Scaling of performance with reservoir size. ***(A)*** *Scaling up empirical connectome with* bio2art. *Scaling allows to specify a number of neurons per area (brain region as defined in the connectome). The interareal weights might be mapped either homogeneously or heterogeneously. Homogeneous mapping partitions total weights in equal parts amongst interareal connections. Heterogeneous mapping partitions total weights at random amongst interareal connections.* ***(B)*** *Relationship between the neurons per area and the total reservoir size for all the studied scaling factors.* ***(C)*** *Performance of BioESNs with scaled up connectomes on the memory capacity task, for heterogeneous and homogeneous interareal connectivity patterns (upper and lower row, respectively). For each single condition (size, interareal connectivity), 100 different networks with newly instantiated weights were trained (4000 time steps) and tested (1000 time steps). The curves depict the test performance mean and standard deviation across runs.*

generation with *bio2art*, considering both homogeneous and heterogeneous interareal connectivity pattern as explained above. We found a clear pattern of raising performance, reaching an asympthotic value roughly comparable across all connectomes when looking at reservoirs of same size. Interestingly, the otherwise consistently lower performance of the *Bio (rank)* condition could be reverted with large enough reservoirs. Importantly, this was only the case for scaled up connectomes with heterogeneous interareal connectivity pattern but not with homogeneous (see Fig. 3.23). This indicates that the randomness and diversity of connections in interareal connectivity plays a crucial role determining the memory capacity of the network. For this series of experiments we also found the pattern to be consistent across all studied connectomes.

Chapter 4

Discussion

In this chapter, I will first briefly discuss a few general aspects relevant to all the presented studies and our approach in general. After that, I will discuss our specific findings in more detail, their implications and important aspects to take into account in their interpretation.

4.1 Our modeling approach

The first general point to be made is about our modeling approach. The kinds of models that we adopted for the presented work, especially for the modeling of emergence of topological features, is definitely a minimalistic take on modeling with rule-based models. The importance of minimal models to understand biological, social and economic phenomena has been summarized in (Sneppen 2014). We recognized that this approach is opinionated and assumes things, but at the same time understand that modeling is *"horses for courses"*. That means, as long as they capture essential aspects of the phenomena to be modelled, this class of models can be informative insofar they allow to test ideas that are less dependant on the specific parameter constellations as for more detailed models. If nothing else, the outcomes of simple models like these can serve as a baseline to be then compared to the outcome of more complicated models, should that be the appropriate way to go. Which is the ultimate potential application of these minimalistic kind

of models has inspired lifetime research programs (Wolfram & Gad-el-Hak 2003), but that is beyond the scope of this discussion. Here, I will rather focus on the concrete advantages and disadvantages of the very models that we implemented in the context of modeling brain networks. One important aspect of our perspective with focus on the topological structure of brain networks is that it does not take into account the spatial embedding of the networks, which is known to play a role in constraining the architecture of brain networks (Stiso & Bassett 2018). This choice affects all the models that I presented here and responds to the attempt to isolate the topological effects from other potential factors that could then override the effects of the pure topological changes. Thus, there is potential for future work on models that incorporate the interplay between geometrical constraints and topological remodeling.

4.2 Representing neural activity

Regarding the modeling of neural activity for plasticity models, previous studies have used a large variety of neural activity models ranging from abstract representations, such as chaotic maps (Berg & Leeuwen 2004) and phase oscillators (Gleiser & Zanette 2006), to more physiologically realistic models, such as neural masses (Stam et al. 2010) and spiking neuron (Kwok et al. 2006) models. We opted for the classical SER model, which is a cellular automaton model with discrete time and space evolution (Greenberg & Hastings 1978). In spite of its simplicity, this minimalistic excitable network model has a rich history across disciplines and in particular in neuroscience (Bak et al. 1990; Anderson & May 1992; Drossel & Schwabl 1992; Kinouchi & Copelli 2006; Furtado & Copelli 2006), where it can capture non-trivial statistical features of brain activity patterns (Haimovici et al. 2013; Messé et al. 2015). This model has also been used to study the impact of network topology, such as modules, hubs and cycles, on network activity patterns (Müller-Linow et al. 2008; Garcia et al. 2014; Messé et al. 2015). A relative-threshold variant (requiring a certain percentage of a node's neighbors to be active, in order to activate the node) was explored in (Hütt et al. 2012) and (Fretter et al. 2017). The deterministic limit of the model ($p \to 1$, $f \to 0$) has been

analysed in (Garcia et al. 2012) and in much detail in (Messé et al. 2018). The SER model, offers the advantage of capturing essential characteristics of stylized neuronal activity while being more tractable than detailed typical models.

4.3 Modules from plasticity model with deterministic dynamics

4.3.1 Emergence of modular network topology

The importance of coherent neural activity and the consequences of such firing patterns in the development of neural circuits are widely recognized (Feller 1999). In this study, we investigated the influence of a simple Hebbian plasticity rule that embodies the principle of "what fires together, wires together." Neuronal activity was represented via a minimalistic model of excitable units and coactivations between units determined the retention probability of each link. This rule captures the essence of recent experimental findings, which support the notion that activity-dependent cellular phenomena, such as Long Term Potentiation/Depression, influence the maintenance probability of individual synapses (Wiegert & Oertner 2013). Moreover, the pruned links were reintroduced into the network in a uniformly random fashion. Therefore, the model also loosely reflected the biological process of intrinsic fluctuations of dendritic spines that expand and retract in a stochastic exploration of the surrounding space before establishing synaptic contacts (Kasai et al. 2010). The mechanisms behind the emergence of modularity across species and spatial scales remain poorly understood. Several potential factors have been hypothesised to be involved including developmental pressure (Gómez-Robles et al. 2014), the geometrical embedding of the brain in physical space (Henderson & Robinson 2013), and plastic rules aiming at maximizing functional repertoires (Ellefsen et al. 2015).

4.3.2 Final modules composition

Our framework led in a systematic way to the emergence of a modular structure both starting from random graphs and well-structured networks (i.e., multi-modular and scale- free graphs). By means of a relatively small but constant proportion of connections changing over time, three modules were generated in all the studied cases. Interestingly, when a non-random network was used as initial condition, the original structure was disassembled in the first rewiring steps and a new global structure emerged. Similar results were obtained by Rubinov et al. (2009), where coupled chaotic maps on a lattice or a spatially constrained network were used as initial condition and the final outcome of their plasticity model held the same that for random initial graphs. Taking this finding into account together with the fact that in all the studied cases we found three modules as outcome, it leads us to think that in this stylized model of excitable dynamics (and with this particular form of a local Hebbian plasticity rule), the emergent network topology is predominantly governed by the dynamics, which is an effect that has been observed in other related studies, where the number of modules depended on properties of the dynamical model (Yuan & Zhou 2011). While this is an extreme scenario, it emphasizes that the relative influences of the two main factors – original network architecture and dynamical model – can vary widely, according to the specific scenario at hand. However the precise mechanisms remain elusive. Previous theoretical work by Ravid Tannenbaum & Burak (2016) showed that the contribution of specific motifs induces correlations between nodes that, in presence of a STDP rule, promote the formation of self-connected assemblies. The particular motif in question (nodes co-activated by common input) is precisely the one that is reinforced by our plasticity rule and therefore suggests that the emergence of modules could be a generic property of networks evolving under selection for co-activation. Due to its deterministic nature, one important property of the simple dynamical model is that (without plasticity and for not too sparse graphs) the dynamics rapidly settle into a stable period-three oscillation. The initial conditions, together with the initial network architecture, thus partition the nodes of the graph in three "cohorts": those jointly active at time t, $t+1$ and $t+2$, respectively. It seems intuitive that these cohorts can rather directly be associated

with the emerging modules. However, in our investigation no simple relationship between initial conditions and the modules could be found.

4.3.3 Nodes turnover in the modules and final degree distribution

Another interesting finding in our study was a kind of topological 'dynamic equilibrium.' Namely, once established, the global modular organization of the network persisted, but the specific composition of the modules varied in time, such that after a number of rewiring steps, the module elements where completely different. This finding is similar to the results in (Rubinov et al. 2009), where even in the defined asymptotic phase structural fluctuations were present; and also in (Stone & Tesche 2013), where a "dynamic local topology" was reported, as the authors tracked the triads across the simulation in a network model with spike-timing dependant plasticity (STDP), and found a constant number of triads but a varying composition. However some relevant differences in the model set-up do not allow further interpretation. The degree distribution in all the cases studied in the present project converged to a Gaussian-like distribution, practically identical to that of a random graph of the same density. Thus, this shaping of the distribution appears to be an emergent property of the model. This finding is consistent with (Rubinov et al. 2009) and (Gong & Leeuwen 2003), where such degree distribution was found in spite of small-world properties of the network. In any case, this fact should be carefully considered, since it has been reported that different degree distributions may emerge as consequence of identical plasticity rules when much larger networks were studied (600 and 100 nodes) (Berg & Leeuwen 2004).

4.3.4 Evolution of SC-FC correlation

An important emergent feature of our model was the increase in the correlation between structural and functional connectivity (SC-FC). This result was also reported in (Rubinov et al. 2009) and constitutes a relevant outcome since the plasticity rule not only contributes to shaping the network organization, but also to the coupling between structure and function of the network. This result

is also in line with previous investigations (Garcia et al. 2012; Messé et al. 2015; Hütt et al. 2014), where such correlations have been investigated across a broad range of network topologies, and found that the emergence of modular structure goes along with the emergence of high SC-FC correlations, suggesting modular organization as one important topological ingredient underlying such correlations. Modelling studies focused on the on-going topological changes of brain networks as a result of biologically relevant plasticity rules are scarce. Our minimalistic model was able to produce, based on a local plasticity rule and without external input, a global reorganization of the structural and functional connectivity patterns of the network. In particular, relevant patterns in the context of brain networks emerged and they were robust to variations of the model parameters. In addition, different from other studies, our model did not require complicated activity patterns (e.g. chaotic dynamics in (Rubinov et al. 2009; Gong & Leeuwen 2003; Berg & Leeuwen 2004)) for the global structured topology to emerge.

4.3.5 Limitations and future work

We see several opportunities for further investigations. Due to the simplicity of the model, it should be possible to understand some aspects of the emergent properties (modules, SC-FC correlations) also analytically and understand in more detail, how initial conditions and the initial network architecture give rise to the striking turnover in module compositions. Future work could also address limitations of our assumptions and set-up; for instance, considering not only excitatory but also inhibitory neurons, adding noise to the dynamical units, or considering different ways of growing connections rather than in a uniformly random fashion. Also, an important aspect (and topic of next study) is to develop a model where the dynamics are not decoupled from the structure as we have shown for this simple model.

4.4 Topological Reinforcement model

The importance of segregation in the brain is supported by numerous studies (Sporns & Betzel 2016; Wig 2017). However, there is a lack of general mechanisms explaining the emergence of brain modularity. In the presented study, we proposed an explicit mechanism of reshaping local neighbourhoods through Topological Reinforcement (TR) that might act as a fundamental principle contributing to the emergence of modules in brain networks. The Topological Reinforcement model is different from previous generative modeling work (Betzel et al. 2016) because it can be instantiated in a biologically more realistic fashion, since those model rather describe the end result of the network configuration and do not focus in the actual mechanistic explanation.

Our Topological Reinforcement model focuses on the contributions of pure topological changes, being more general than previous models with regard to the dynamical regime representing neuronal activity. Given accumulated evidence that global network properties can systematically affect the composition of local network structure such as motifs (Vazquez et al. 2004; Reichardt et al. 2011; Fretter et al. 2012), we propose a complementary bottom-up approach that is acting locally in order to shape global features. Our proposed mechanism is in line with empirical data where "homophily" appears as an essential feature of brain connectivity. At the micro scale, it has been shown that the probability to find a connection between a pair of neurons is proportional to the number of their shared neighbours (Perin et al. 2011); while, at the macro scale, the strength of connections between brain regions tends to be the higher the more similar their connectivity profiles are (Goulas et al. 2015).

4.4.1 Random networks evolve towards modular organization

Our results showed that local reinforcement reliably and robustly produces modular network architectures over time, accompanied by the small-world property. Additionally, the final modular organization of the networks seemed to correspond to groups of nodes in the initial networks that have higher than average

connection density. As such, our rewiring mechanism acts as an amplification of these "proto-modules," similarly to a previously reported effect in weak modular weighted networks evolving under a Hebbian rule based on chaotic maps synchronization (Yuan & Zhou 2011). We extended the framework of topological reinforcement by introducing a plausible biological implementation. In the biological implementation, the topological reinforcement rule was reformulated by using functional connectivity (FC) as a surrogate of TO. These results were consistent with TR, indicating that the biological implementation appears to act indirectly at the topological level. In other words, the FC served as a proxy of TO, and therefore Hebbian reinforcement led indirectly and ultimately to the topological reinforcement of a modular network organization. The explanation for this finding is based on the fact that, for suitable dynamical regimes and structural architectures, FC is positively correlated with TO in excitable networks (Messé et al. 2018), which is intuitive if one considers that common inputs may promote correlations. Thus, we propose the topological reinforcement principle as an underlying common ground, a gap bridging alternative between this activity-based Hebbian model and a pure topological generative model. Our results are in line with recent theoretical work on the contribution of specific network motifs to higher order network organization, in which the reinforcement of connections between neurons receiving common inputs led to the formation of self-connected assemblies (Ravid Tannenbaum & Burak 2016).

4.4.2 Correspondence between pure topological and dynamics-based model

Our Hebbian plasticity scenario exploited the correspondence between TO and FC as it could be observed with the exploration of different SER parameter constellations. These parameters promoted different relations between TO and FC, and we found that such a dependence systematically predicted the emergence (or not) of modular networks.

Previous modeling studies with Hebbian reinforcement scenarios have also shown that Hebbian reinforcement may lead to the formation of modular architectures,

consistently with our results for the excitable model (Berg & Leeuwen 2004; Gleiser & Zanette 2006; Rubinov et al. 2009; Yuan & Zhou 2011). Interestingly, as a practical biological example beyond the pure theoretical realm, this type of plasticity-guided modular emergence has recently been studied also in real neural activity in zebrafish larvae (Triplett et al. 2018), pointing to the relevance of the current results. The open question for this type of models concerns the specific underlying topological changes that they promote, since these studies focus on the implementation of the phenomenon (based on the activity) and not on the algorithmic level (the topological dimension) and both levels interact in non-trivial ways. In other words, they do not provide insights about a general mechanism specifying which topological changes might be necessary for the emergence of modular structure. Compared to this group of models, our Topological Reinforcement model is different in that reinforcement principle is agnostic with respect to the specific dynamical regime and it explicitly addresses the topological changes that take place in the network.

Previous work on generative models of brain connectivity have provided with a valuable basis for confirming the importance of TO as an essential feature and reducing the dimensionality of brain connectivity by few model parameters (Betzel & Bassett 2017), disentangling the mechanistic nature of the phenomena (e.g., modularity emergence) turns out to be non-trivial, since information about the final state might be explicitly built-in in the generative model already. But even more crucially, how the generative function is actually implemented in real systems is out of the scope of this kind of modeling approach. As a complement to this group of models, our contribution offers a concrete scenario where a generative mechanism can actually be implemented in a biologically more realistic fashion.

In summary, as expected for any modeling approach, a trade-off exists between generative and activity-based models. Phenomenological descriptions and mechanistic explanations complement each other and a gap remains for explaining on how they link to each other. Our contribution represents an attempt to address this gap; first, by providing an explicit topological mechanism of module formation (generative mechanism); second, by trying to reconcile such an abstract level of analysis with the biological implementation, by means of an activity-based formulation of

the model.

4.4.3 Limitations and future work

The presented results are subject to several methodological considerations. For example, our study did not take into account a geometrical embedding and rather focused on the pure topological contribution of the topological reinforcement. Although we certainly recognize the brain as a spatially embedded system and that physical constraints, such as wiring-cost, play a fundamental role shaping brain connectivity (Henderson & Robinson 2013), previous studies have shown that, in addition to them, topological aspects are essential to describe real connectomes (Kaiser & Hilgetag 2006; Betzel et al. 2016). Thus, we aimed at isolating the pure topological effect and avoiding the situation in which geometric constraints, such as the distance-dependent probability of connection used in previous studies (Jarman et al. 2014), introduce already by themselves a clustered connectivity, thus potentially overriding the changes based on the topology itself. Specifically for the case of our model, an initial spatially constrained, distance-dependant connectivity could also create 'proto-modules' upon which the connectivity would develop.
Due to their relative simplicity, the rules tended to disconnect the evolving networks. This consequence can also be found in previous studies with this type of models, where other modeling choices were made, such as discarding runs with disconnections or explicitly using network size and density that avoid such scenario (Berg & Leeuwen 2004; Rubinov et al. 2009). From a practical point of view, we chose a number of rewiring steps that avoids such scenario. We recognize an interesting line for future work taking into account possible counteracting mechanisms that might balance out disconnections and add realism to the model.
Regarding the plausible biological implementation, we chose a simple abstract model for computational tractability. It would be also interesting to compare our framework with more biologically realistic dynamical models, such as networks of spiking neurons.

4.5 Sequential Reinforcement model

Heterogeneous degree distributions are ubiquitous in biological networks in general and brain networks in particular (Newman 2006; Sporns 2011). There are a number of open questions when it comes to the best way to mathematically describe them (Stumpf & Porter 2012; Broido & Clauset 2019), but such a discussion is beyond the scope of this discussion and thus we adopted a relatively flexible notion of heterogeneous degree distribution, namely a distribution that extends well over the expectations for counterpart Erdos Renyi graphs, accurately described by a binomial distribution. In this section I will present a study with a minimalistic plasticity model, the Sequential Reinforcement, that promotes the creation of links between from a node i to a not yet connected node j for which the sequential activation $i \rightarrow j$ was the maximum, while preserving the network density by removing a randomly picked link.

4.5.1 Emergence of heterogeneous degree distribution

We found that this simple mechanism is enough to remodel the degree distribution of an initially random graph into a heterogeneous degree distribution. This results are in line with previous work with a similar plasticity rule, but where the dynamics of the network was represented by a diffusion process, being the diffusion rate a crucial parameter to be tuned (Jarman et al. 2017). Our model is a simpler one, e.g., does not have such a global order parameter, but still has some essential dynamical properties of neural systems, such as the non-linear activations and a refractory period. Modeling work with more biologically detailed models has also shown emergence of long tail distribution of link weights with an STDP-like model (Effenberger et al. 2015). An important difference is though, that their network activity is driven by a permanent input to the nodes, while our model is only based on the ongoing self-sustained activity of the network under the SER model, thus being a scenario with less assumptions. This is important, as previous modeling work has also shown that the input itself can shape the network structural connectivity of a network and promote by itself the emergence of certain topological features (Hartley 2020).

Another interesting finding from the Sequential Reinforcement model was the presence of a long-term stationary state of the degree distribution. After an initial strong remodeling of the connectivity pattern, the skewness of the degree distribution stabilized at a consistently similar value for all the runs simulated. That is, in spite of the ongoing application of the plasticity rule the system showed a form of attractor state where a balance was achieved without any extra explicit control mechanism imposed on top of the plasticity rule. This type of self-regulated interplay between topology and dynamics has been demonstrated to be important in the emergence and maintainance of dynamical regimes thought to be important for the dynamics of biological neural networks, such as self-organized criticality (Landmann et al. 2020). The core idea behind the self-regulatory phenomenon is that patterns of node activity could reflect underlying topological structural features of the network, thus making activity-based plasticity to indirectly affect the topology in specific ways that could promote the right balance. We observed in our model a correlation between sequential activations and degrees of nodes, so we can hypothesize that a similar interplay could have taken place and, at least partially, contributed to the long-term stationary behavior that we reported.

4.5.2 Predictability of the final degree distribution

The next interesting finding from our experiments with the Sequential Reinforcement rule was that the final degree distribution was to some extent related to the initial one. That is, even after all the rewiring events the final state of the network still preserved information about the initial degree distribution. This is interesting not only because it allows for certain predictability, but also because it points to the importance of contingencies in the evolution of complex systems such as brain networks. Previous modeling studies have shown that the initial graph used as seed can lead to radically dissimilar outcomes in terms of the final topology to which the network converges. For example, a model of preferential attachment based on the activity of random walkers on the network had to be necessarily initialized with a very special graph, i.e., a ring graph, in order to find power-law degree distributions as typically expected from common preferential at-

tachment, which constitutes a rather strong assumption (Herrera & Zufiria 2011). We opted for a more conservative approach in our modeling and only started with random graph our simulations, as an attempt to assume as little as possible about the initial state. In the realm of models more closely related to brain networks, previous work on neural networks and STDP-like plasticity has also demonstrate that small asymmetries in the initial structure can be amplified by the synaptic plasticity (Effenberger et al. 2015). This findings also align with our work presented in previous sections, where the Topological Reinforcement rule exploited subtle initial asymmetries in random networks to carve a modular network structure by amplifying the asymmetries.

This sensitivity to initial conditions is a generally important fact for brain networks if we take into account that initial structure in the connectivity can emerge from developmental processes, thus providing with an initial state that could heavily influence later shaping of the network topology. Recent modeling studies have shown how simple developmental models of brain development informed by general spatio-temporal developmental principles can account for the formation of a scaffold of topological features that could later be refined by activity-dependant mechanisms (Goulas et al. 2019). Our model results complement such studies, as we showed that even just tonic activity of the network could lead to shaping its degree distribution into a heterogeneous one.

4.5.3 Stability of the node degree ranking structure

In order to better understand the long-term behavior of the Sequential Reinforcement model, we analyzed the stability of the degree distribution along the run. The goal was to gain a more detailed insight into the organization of such distribution that goes beyond the mere global shape of the distribution and we found that the overall degree ranking of nodes evolved into a relatively well organized and stable structure. The largest hubs established themselves as the group with the largest overlap across time. Previous modeling work has denominated this hubs dynamics as “frozen hubs” (Rosvall & Sneppen 2003). In our model we do not have a complete extreme situation and there is a small turnover of hubs,

most likely because of the randomizations that our model implies as part of the rewiring rule. Importantly, the emergent hub group in our model also showed the lowest variance along the simulation across runs. A similar feature has been reported for other real world biological networks with clear hub structures (Jeong et al. 2000), which is interesting if we think about these properties as signatures of hub networks that the behavior of the model could reproduce.

4.5.4 Limitations and future work

The presented results should be interpreted in the light of several limitations of our approach. The simplicity of the Sequential Reinforcement model should be also acknowledged, both in terms of the minimalistic nature of the model as one with very few parameters and the limited extrapolation capacity to real-world neuronal networks that comes with such a model formulation. As a consequence, further refinement would be appropriate to render the model more comparable to more sophisticated plasticity mechanisms, such as spike-timing dependent plasticity.

Another fruitful future work direction would be to explore initial graphs other than random ones. As previously mentioned, that was a modeling decision responding to the necessity of making as few assumptions as possible. For example, when experimental techniques allow it, early brain anatomical data could be incorporated in the model as a prior basis upon which the plasticity rule takes place. Lastly, compared to the Topological Reinforcement model that led to the emergence of modules, we unfortunately could not identify a clear topological gradient (such as reinforcement of common neighborhoods) for the Sequential Reinforcement model. Despite of a number of attempts to relate the topological changes promoted by the activity-based plasticity rule to a mechanistic explanation at the pure topological level, we could not come to a conclusive result along those lines. Some of the fundamental problems found along that exploration were the following: A strong tendency of pure topological rules to fall into "winner-takes-all" regimes, which led to an artefactual dominance of one or two nodes connecting to almost all the rest of the nodes; generation of unrealistic network properties, such as a large number of

disconnections which then force additional modeling assumptions, such as explicit reconnections events; difficult balance of the different sources of noise that affect the information accesible for the nodes, for example, at the moment of forming new connections, that can lead to the effects of the plasticity rule to be completely overriden by the random reinsertion of links. Therefore, this also remains as an interesting research direction that would allow to better understand the interplay between topology and dynamics in shaping the connectivity of brain networks.

4.6 Bio Echo State Networks

We addressed two fundamental questions aiming at bridging the gap between artificial and biological neural networks: Can actual brain connectivity guide the design of better ANNs architectures? Can we better understand what network features support the performance of brains in specific tasks by experimenting with ANNs? Concretely, we investigate the potential effect of connectivity built based on real connectomes on the performance of artificial neural networks. To the best of our knowledge, this is the first cross-species study of this kind, comparing results from empirical connectomes of three primate species.

The gap that we aimed at emerges from two under-explored aspects in artificial and biological neural networks. First, connectivity patterns (i.e., architectures) of ANNs are very different from actual brain connectivity. For example, echo state networks use a sparse, randomly connected reservoir, which is incongruent with the highly non-random connectivity empirically found in the brain (Sporns et al. 2004; Sporns 2011). Thus it is not clear, how more realistic architectures would impact the performance of such ANNs. Second, computational neuroscience studies have characterized the relation between structural and functional connectivity patterns (Breakspear 2017; L. Suárez et al. 2020) and attempted to relate brain connectivity to behavioural differences (Mišić & Sporns 2016; Seguin et al. 2020). Nevertheless, it remains unclear how those patterns of neural activity translate into brain computational capabilities, i.e., how they support performance of brain networks on concrete tasks. We set out to evaluate real whole brain connectomes on specific tasks, in order to identify a potential role of such wiring patterns, in a

similar vein to previous studies on feedforward networks (Gaier & Ha 2019).

4.6.1 Bio ESNs match performance of classical ESNs

We found that constraining reservoir connectivity of ESNs with real connectomes led to performances as good as for the random conditions, classically used for ESNs, as long as a certain degree of randomness is allowed. In general, we observed a degeneracy of structure and function, in which different topologies lead to the same performance, so no unique connectivity pattern appears necessary to support optimal performance in this modeling context.
Our results were similar across tasks. This is to a certain extent logical considering that both tested tasks are memory tasks, but the consistency also speaks for the robustness of the networks to different recall mechanisms.
Importantly, all our results were consistent across the three evaluated species. This supports the generality of our findings, at least for the evaluated tasks. This observation is especially relevant considering that the connectomes were obtained with very different experimental methodologies (Markov et al. 2012; Majka et al. 2016; Betzel & Bassett 2018). Moreover, our experiments with scaled up connectomes showed similar performance scores across species when the reservoir size was matched. Nevertheless, the different experimental methodologies to infer the connectivity prevent us from drawing specific comparative conclusions across connectomes, such as whether the wiring diagram of any of the tested connectomes is intrinsically better suited for the task regardless of the size.

4.6.2 The importance heterogeneity of connections

Our surrogate networks also showed that, in general terms, the more heterogeneity and randomness allowed in the connectivity, the better performance the BioESNs achieved. Interestingly, that effect was also observable by augmenting the computational capacity of the models by means of larger reservoirs. Using the *bio2art* framework, we scaled up connectomes with either homogeneous or heterogeneous interareal distributions of connectivity weights and found that only the larger reservoirs with heterogeneous wiring could overcome the lower performance

inherent to the underlying connectivity. This points out once again to the importance of random wiring diagrams for ESNs' performance. This fact is as well in line with a recent study using human connectivity as reservoir of ESNs, which showed that random connectivity indeed achieved globally maximal performances across almost all tested hyperparameters, provided the wiring cost is not considered (L. E. Suárez et al. 2020). The functional importance of randomness is also consistent with the fact that stochastic processes play a fundamental role in brain connectivity formation, both at a micro and meso/macro-scale, as supported by empirical (Kasai et al. 2010), and computational modeling studies (Beul et al. 2018; Goulas et al. 2019).

4.6.3 Generalizability of the framework

While here we tested the performance of the ANNs in two memory tasks, our approach is versatile and extendable, since it allows an open ended examination of the consequences of network topology found in nature for artificial systems. Specifically, the following contributions hold: First, we offer an approach for creating ANNs with network topology dictated directly from empirical observations in BNNs. Second, creating and upscaling BioESNs from real connectomes is in itself a highly non-trivial problem and here we offer, although not exhaustively, insights into the consequences of each strategy. Third, our method allows building ANNs with network topologies based on empirical data from diverse biological species (mammalian brain networks).

4.6.4 Limitations and future work

We are aware of a number of limitations of our study as well as interesting research avenues for future work.

We evaluated our BioESNs models on two different memory tasks framed as regression problems; so future work could, for example, include classification tasks as well as more ecologically realistic tasks.

Connections in the adult brain change constantly as a consequence of stochastic fluctuations and activity-driven plasticity, e.g., learning and memory (Abbott &

Nelson 2000). In our study, we assumed connectivity within the reservoir to be constant during the tasks. Previous studies have shown some effects of plasticity rules on ESNs (Barrios Morales 2019), so we foresee interesting future work along those lines as well.

As we aimed at testing the potential impact of the global wiring diagram of connectomes, we consider the entire connectomes as one unique network to create the reservoirs. This is different from a previous study where the connectivity was divided into subnetworks corresponding to brain systems that were separately trained (L. E. Suárez et al. 2020). We decided to avoid here the strong assumptions that such an approach implies, but we recognize a potential for future studies in the direction, for example, exploring the division of networks as different input/output subsystems.

4.7 Concluding remarks

I presented the results of a series of studies in which the topology of brain networks was the common denominator, the underlying thread. In particular, our studies aimed at two goals: First, understanding how certain characteristic topological features of brain networks could emerge. Second, evaluating the performance of networks which embodied real brain connectivity on concrete tasks.

We approached the first goal from a modeling perspective of rule-based plasticity models. The focus of the approach was to explore simple rules that could lead to the emergence of two fundamental properties of brain networks: modular organization and a heterogeneous degree distribution.

The models we explored were certainly minimal in several ways, but they nevertheless allowed us to gain instructive insight into how simple mechanisms lead to a reorganization of a complex network such that characteristic topological features of brain networks emerge.

In general, we found that simple rules, such as topological reinforcement and sequential reinforcement, can lead to network topology remodeling even in the absence of inputs and just driven by the tonic activity of the network. Interestingly, some of the plasticity rules that we explored were able to amplify relatively sub-

tle asymmetries of the initial random graphs that we started the simulations with, which means that an initial connectivity scaffold resulting from developmental processes could then further be refined by simple plasticity rules acting purely under the sustained activity of the network. Despite of the simplicity of our framework, we trust it to carry a conceptual value that contributes to understanding the fundamental principles of brain organization. Our second goal was to evaluate the performance on concrete tasks of networks which embody real brain connectivity. This was a cross-species study with a hybrid approach integrating real brain connectomes into Echo State Networks, which we used to solve concrete memory tasks, allowing us to probe the potential computational implications of real brain connectivity patterns on task solving. We found results consistent across species and tasks, showing that biologically inspired networks can perform as well as classical echo state networks. An important prerequisite for that was a minimum level of randomness and diversity of connections, which showed a crucial importance of the diversity of interareal connectivity patterns, potentially stressing the relevance of stochastic processes determining neural networks connectivity in general. Our work represents a new interface between network neuroscience and artificial neural networks, precisely at the level of the network topology. We contributed an original approach to blend real brain connectivity and artificial networks, paving the way to future hybrid research, a promising exploration path leading to potential better performance and robustness of artificial networks and understanding of brain computation.

Chapter 5

Summary

5.1 English Summary

The networks of connections between neurons and brain regions are the physical substrate of brain function. The topology of these brain networks, i.e. the wiring diagram, exhibits characteristic features across species and spatial scales. We addressed two questions about brain networks topology. First: Which plasticity mechanisms could lead to the emergence of the characteristic topological features of brain networks? Second: Which effect does the connectivity of brain networks have on their performance on concrete tasks?

Two topological features of brain networks are crucially important for information processing: Modular organization and a heterogeneous distribution of links leading to nodes with many connections, known as hubs. However, the mechanisms underlying the generation and maintenance of such characteristic topological features of brain networks are still unclear. We carried out an exploration of plasticity mechanisms that could lead to formation of modules and heterogeneous degree distributions in brain networks.

We first formulated a network model with excitable nodes and discrete deterministic dynamics, where we studied the effects of a Hebbian plasticity rule on global network topology. This simple rule reorganized the network topology into a modular structure and enhanced the correlation between structural and functional

connectivity, regardless of the initial structure. Nevertheless, the final modules were dominated by the deterministic formulation of the used dynamical model.
As a next step, we went beyond those limitations with another model – the Topological Reinforcement (TR). The TR model was derived from a purely topological perspective, which even allowed for an implementation without neural activity. The TR rule acted iteratively enhancing the topological overlap between nodes and evolved initially random networks towards a modular architecture by amplifying initial "proto-modules." We also showed this topological selection principle acting in a biologically more realistic fashion with an activity-based rule, obtaining consistent results with the pure topological rule, suggesting the reinforcement of topological overlap as a fundamental mechanism contributing to modularity emergence.
Subsequently, we studied a model aiming at explaining the emergence of a heterogeneous degree distribution - the Sequential Reinforcement model. This activity-based plasticity model promoted the creation of links between nodes with high correlations delayed in time, which led to a remodelling of the degree distribution into a heterogeneous degree distribution. The final degree distribution was related to the initial one and reached a stable organization across time, showing that the model could lead to a self-organized stable connectivity pattern.
Our last study dealt with the implications of real brain networks topologies on machine learning tasks. We carried out a cross-species study with a hybrid approach integrating real brain connectomes and Echo State Networks (ESNs) that allowed us to probe real brain connectivity on concrete tasks. We found that biologically inspired networks performed as well as classical ESNs, provided a minimum level of randomness and diversity of connections was present. Our results also highlighted the relevance of the diversity of interareal connectivity patterns.

5.2 Deutsche Zusammenfassung

Die Netzwerke von Verbindungen zwischen Neuronen und Gehirnarealen sind die physikalische Grundlage von Hirnfunktionen. Die Topologie solcher Hirnnetzwerke, d.h. der Schaltplan, zeigt charakteristische Eigenschaften, die sowohl bei verschiedenen Tierarten als auch über verschiedene räumliche Skalen hinweg zu finden sind. Wir sind zwei Fragen über Hirnnetzwerke nachgegangen. Erstens: Welche Plastizitätsmechanismen könnten zur Entstehung der charakteristischen topologischen Eigenschaften führen? Zweitens: Welchen Effekt hat die Topologie von Hirnnetzwerken auf die Performance dieser Netzwerke beim Lösen von konkreten Aufgaben.

Zwei topologische Eigenschaften von Hirnnetzwerken sind besonders wichtig für die Informationsverarbeitung: Modulare Organisation und heterogene Verteilung von Verbindungen (Kanten), welche Knoten mit vielen Verbindungen impliziert - so genannte Hubs. Trotzdem sind die Mechanismen, die zur Entstehung und Erhaltung von solch charakteristisch topologischen Eigenschaften von Hirnnetzwerken führen, unbekannt. Wir haben eine Exploration von Plastizitätsmechanismen durchgeführt, die zur Entstehung von Modulen und heterogener Verteilung von Verbindungen führen könnten. Zuerst haben wir ein Modell von exzitablen Knoten und diskreter Aktivität formuliert. Dabei haben wir die Effekte einer Hebbian-Plastizitätsregel auf die globale Netzwerktopologie untersucht. Diese einfache Regel rief eine Reorganisation der Netzwerktopologie mit modularer Struktur hervor. Dieser Effekt trat unabhängig von den Ausgangsbedingungen der Simulation auf und hat zu einer erhöhten Korrelation zwischen struktureller und funktioneller Konnektivität geführt. Dennoch waren die entstandenen Module durch das deterministische Aktivitätsmuster des Modells limitiert. Im nächsten Schritt haben wir anhand eines neuen Modells - dem Topological Reinforcement (TR) Modell - diese Limitationen überwunden. Das TR Modell wurde aus einer rein topologischen Perspektive konzipiert, die sogar eine Implementierung ohne jegliche neuronale Aktivität ermöglichte. Die TR-Regel hat iterativ für eine stärkere topologische Überlappung zwischen den Knoten gesorgt, die wiederum zu einer Umwandlung von Zufalls- auf Modularenetzwerken geführt hat, indem

"Proto-Module" von der TR-Regel amplifiziert wurden. Wir waren außerdem in der Lage eine biologisch realistischere, auf Aktivität basierende Variation des TR-Modells zu formulieren, die nach dem gleichen Prinzip von topologischer Selektion funktioniert. Die damit erhobenen Ergebnisse waren konsistent mit denen der rein topologischen Regel, was für das Topological-Reinforcement-Prinzip als fundamentalen Mechanismus spricht, der Entstehung von Modulen in Hirnnetzwerken beiträgt. Des Weiteren untersuchten wir ein Modell, dessen Ziel die Erklärung der Entstehung heterogener Knotengradsverteilung war - das Sequential Reinforcement Modell. Diese aktivitätsbasierte Plastizitätsregel begünstigte die Entstehung von Kanten zwischen Knoten mit zeitlich stark versetzter Korrelation, was wiederum eine heterogene Knotengradsverteilung verursachte. Die Knotengradsverteilung am Ende der Simulationen war denen vom Simulationsanfang ähnlich und zeigte einen stabilen Zeitverlauf. Dies spricht für ein selbstorganisiertes Konnektivitätsmuster.

Zuletzt untersuchten wir die Rolle der Topologie echter Hirnnetzwerke beim Lösen von Machine-Learning-Aufgaben. Anhand einer hybriden Herangehensweise haben wir echte Hirnnetzwerke von verschiedenen Spezies mit Echo State Networks (ESNs) integriert, was die Testung dieser Hirnnetzwerke ermöglichte. Wir haben gezeigt, dass die biologisch inspirierten ESNs eine so gute Leistung wie klassische ESNs haben konnten, solange genügend zufällige und diverse Verbindungen vorhanden waren. Unsere Ergebnisse betonen somit die Relevanz der Diversität der interarealen Verbindungsmuster.

Chapter 6

Bibliography

Abbott, L.F. & Nelson, S.B., 2000. Synaptic plasticity: Taming the beast. *Nature Neuroscience*, 3, pp.1178 EP–. Available at: http://dx.doi.org/10.1038/81453.

Albert, R., Jeong, H. & Barabási, A.-L., 2000. Error and attack tolerance of complex networks. *Nature*, 406(6794), pp.378–382. Available at: https://doi.org/10.1038/35019019.

Anderson, R. & May, R.M., 1992. *Infectious diseases of humans: Dynamics and control*, Oxford: Oxford University Press.

Arenas, A., Díaz-Guilera, A. & Pérez-Vicente, C.J., 2006. Synchronization reveals topological scales in complex networks. *Phys. Rev. Lett.*, 96, p.114102. Available at: https://link.aps.org/doi/10.1103/PhysRevLett.96.114102.

Aslak, U. & Maier, B.F., 2019. Netwulf: Interactive visualization of networks in python. *Journal of Open Source Software*, 4(42), p.1425.

Avena-Koenigsberger, A. et al., 2015. Network morphospace. *Journal of The Royal Society Interface*, 12(103), p.20140881. Available at: https://royalsocietypublishing.org/doi/abs/10.1098/rsif.2014.0881.

Avena-Koenigsberger, A., Misic, B. & Sporns, O., 2018. Communication dynamics in complex brain networks. *Nature Reviews Neuroscience*, 19(1), pp.17–33. Available at: https://doi.org/10.1038/nrn.2017.149.

Bak, P., Chen, K. & Tang, C., 1990. A forest-fire model and some thoughts on turbulence. *Physics Letters A*, 147(5), pp.297–300. Available at: http://www.sciencedirect.com/science/article/pii/037596019090451S.

Barabási, A.-L. & Albert, R., 1999. Emergence of scaling in random networks. *Science*, 286(5439), pp.509–512. Available at: https://science.sciencemag.org/content/286/5439/509.

Barrios Morales, G.G., 2019. *Constructive role of plasticity rules in reservoir computing*. PhD thesis. Universitat de les Illes Balears.

Bass, J.I.F. et al., 2013. Using networks to measure similarity between genes: Association index selection. *Nature methods*, 10(12), p.1169.

Bassett, D.S. & Bullmore, E.T., 2017. Small-world brain networks revisited. *The Neuroscientist*, 23(5), pp.499–516. Available at: https://doi.org/10.1177/1073858416667720.

Bassett, D.S. & Sporns, O., 2017. Network neuroscience. *Nature Neuroscience*, 20(3), pp.353–364. Available at: https://doi.org/10.1038/nn.4502.

Bassett, D.S., Xia, C.H. & Satterthwaite, T.D., 2018. Understanding the emergence of neuropsychiatric disorders with network neuroscience. *Biological Psychiatry: Cognitive Neuroscience and Neuroimaging*, 3(9), pp.742–753. Available at: http://www.sciencedirect.com/science/article/pii/S245190221830079X.

Bauer, R. & Kaiser, M., 2017. Nonlinear growth: An origin of hub organization in complex networks. *Open Science*, 4(3). Available at: http://rsos.royalsocietypublishing.org/content/4/3/160691.

Baum, G.L. et al., 2017. Modular segregation of structural brain networks supports the development of executive function in youth. *Current Biology*, 27(11), pp.1561–1572.e8. Available at: http://www.sciencedirect.com/science/article/pii/S0960982217304967.

Berg, D. van den & Leeuwen, C. van, 2004. Adaptive rewiring in chaotic networks renders small-world connectivity with consistent clusters. *EPL (Europhysics Letters)*, 65(4), p.459. Available at: http://stacks.iop.org/0295-5075/65/i=4/a=459.

Bettencourt, L.M.A. et al., 2007. Functional structure of cortical neuronal networks grown in vitro. *Phys. Rev. E*, 75, p.021915. Available at: https://link.aps.org/doi/10.1103/PhysRevE.75.021915.

Betzel, R., 2020. Network neuroscience and the connectomics revolution. Available at: https://arxiv.org/abs/2010.01591.

Betzel, R.F., 2020. Community detection in network neuroscience. Available at: https://arxiv.org/abs/2011.06723.

Betzel, R.F. et al., 2016. Generative models of the human connectome. *NeuroImage*, 124, pp.1054–1064. Available at: http://www.sciencedirect.com/science/article/pii/S1053811915008563.

Betzel, R.F. & Bassett, D.S., 2017. Generative models for network neuroscience: Prospects and promise. *Journal of The Royal Society Interface*, 14(136). Available at: http://rsif.royalsocietypublishing.org/content/14/136/20170623.

Betzel, R.F. & Bassett, D.S., 2018. Specificity and robustness of long-distance connections in weighted, interareal connectomes. *Proceedings of the National Academy of Sciences*, 115(21), pp.E4880–E4889. Available at: https://www.pnas.org/content/115/21/E4880.

Beul, S.F., Goulas, A. & Hilgetag, C.C., 2018. Comprehensive computational modelling of the development of mammalian cortical connectivity underlying an architectonic type principle. *PLOS Computational Biology*, 14(11), pp.1–45. Available at: https://doi.org/10.1371/journal.pcbi.1006550.

Bi, G. & Poo, M., 1998. Synaptic modifications in cultured hippocampal neurons: Dependence on spike timing, synaptic strength, and postsynaptic cell type. *Journal of Neuroscience*, 18(24), pp.10464–10472. Available at: https://www.jneurosci.org/content/18/24/10464.

Blondel, V.D. et al., 2008. Fast unfolding of communities in large networks. *Journal of Statistical Mechanics: Theory and Experiment*, 2008(10), p.P10008. Available at: http://stacks.iop.org/1742-5468/2008/i=10/a=P10008.

Bounova, G. & Weck, O. de, 2012. Overview of metrics and their correlation patterns for multiple-metric topology analysis on heterogeneous graph ensembles. *Phys. Rev. E*, 85, p.016117. Available at: https://link.aps.org/doi/10.1103/PhysRevE.85.016117.

Breakspear, M., 2017. Dynamic models of large-scale brain activity. *Nature neuroscience*, 20(3), pp.340–352.

Broido, A.D. & Clauset, A., 2019. Scale-free networks are rare. *Nature Communications*, 10(1), p.1017. Available at: https://doi.org/10.1038/s41467-019-08746-5.

Bullmore, E. & Sporns, O., 2012. The economy of brain network organization. *Nature Reviews Neuroscience*, 13(5), pp.336–349.

Bullmore, E.T. & Bassett, D.S., 2011. Brain graphs: Graphical models of the human brain connectome. *Annual Review of Clinical Psychology*, 7(1), pp.113–140. Available at:%20%0A%20%20%20%20%20%20%20%20https://doi.org/10.1146/annurev-clinpsy-040510-143934%0A%20%20%20%20%0A.

Cajal, S.R. & others, 1995. Histology of the nervous system of man and vertebrates. *History of Neuroscience (Oxford Univ Press, New York)*, (6).

Caporale, N. & Dan, Y., 2008. Spike timing–dependent plasticity: A hebbian learning rule. *Annual Review of Neuroscience*, 31(1), pp.25–46. Available at:%20%0A%20%20%20%20%20%20%20%20https://doi.org/10.1146/annurev.neuro.31.060407.125639%0A%20%20%20%20%0A.

Chialvo, D.R., 2010. Emergent complex neural dynamics. *Nature Physics*, 6(10), pp.744–750. Available at: https://doi.org/10.1038/nphys1803.

Csardi, G., Nepusz, T. & others, 2006. The igraph software package for complex network research. *InterJournal, complex systems*, 1695(5), pp.1–9.

Damicelli, F., 2019. Echoes: Echo state networks with python. *GitHub repository*.

Damicelli, F. et al., 2017. Modular topology emerges from plasticity in a minimalistic excitable network model. *Chaos: An Interdisciplinary Journal of Nonlinear Science*, 27(4), p.047406.

Damicelli, F. et al., 2019. Topological reinforcement as a principle of modularity emergence in brain networks. *Network Neuroscience*, 3(2), pp.589–605. Available at:%20%0A%20%20%20%20%20%20%20%20https://doi.org/10.1162/netn_a_00085%0A%20%20%20%20%0A.

De Carlos, J.A. & Borrell, J., 2007. A historical reflection of the contributions of cajal and golgi to the foundations of neuroscience. *Brain Research Reviews*, 55(1), pp.8–16. Available at: http://www.sciencedirect.com/science/article/pii/S0165017307000574.

Drossel, B. & Schwabl, F., 1992. Self-organized critical forest-fire model. *Phys. Rev. Lett.*, 69, pp.1629–1632. Available at: https://link.aps.org/doi/10.1103/PhysRevLett.69.1629.

Effenberger, F., Jost, J. & Levina, A., 2015. Self-organization in balanced state networks by STDP and homeostatic plasticity. *PLOS Computational Biology*, 11(9), pp.1–30. Available at: https://doi.org/10.1371/journal.pcbi.1004420.

Ellefsen, K.O., Mouret, J.-B. & Clune, J., 2015. Neural modularity helps organisms evolve to learn new skills without forgetting old skills. *PLOS Computational Biology*, 11(4), pp.1–24. Available at: https://doi.org/10.1371/journal.pcbi.1004128.

Erdős, P. & Rényi, A., 1959. On random graphs i. *Publicationes Mathematicae (Debrecen)*, 6, pp.290–297.

Feller, M.B., 1999. Spontaneous correlated activity in developing neural circuits. *Neuron*, 22(4), pp.653–656. Available at: http://www.sciencedirect.com/science/article/pii/S0896627300807242.

Filan, D. et al., 2020. Neural networks are surprisingly modular. *arXiv preprint arXiv:2003.04881*.

Fretter, C. et al., 2017. Topological determinants of self-sustained activity in a simple model of excitable dynamics on graphs. *Scientific Reports*, 7, pp.42340 EP–. Available at: http://dx.doi.org/10.1038/srep42340.

Fretter, C., Müller-Hannemann, M. & Hütt, M.-T., 2012. Subgraph fluctuations in random graphs. *Physical Review E*, 85(5), p.056119.

Furtado, L.S. & Copelli, M., 2006. Response of electrically coupled spiking neurons: A cellular automaton approach. *Phys. Rev. E*, 73, p.011907. Available at: https://link.aps.org/doi/10.1103/PhysRevE.73.011907.

Gaier, A. & Ha, D., 2019. Weight agnostic neural networks. In H. Wallach et al., eds. *Advances in neural information processing systems*. Curran Associates, Inc., pp. 5364–5378. Available at: https://proceedings.neurips.cc/paper/2019/file/e98741479a7b998f88b8f8c9f0b6b6f1-Paper.pdf.

Garcia, G.C. et al., 2012. Building Blocks of Self-Sustained Activity in a Simple Deterministic Model of Excitable Neural Networks. *Frontiers in Computational Neuroscience*, 6(August), p.50.

Garcia, G.C. et al., 2014. Role of long cycles in excitable dynamics on graphs. *Phys. Rev. E*, 90, p.052805. Available at: https://link.aps.org/doi/10.1103/PhysRevE.90.052805.

Gleiser, P.M. & Zanette, D.H., 2006. Synchronization and structure in an adaptive oscillator network. *The European Physical Journal B - Condensed Matter and Complex Systems*, 53(2), pp.233–238. Available at: https://doi.org/10.1140/epjb/e2006-00362-y.

Golosovsky, M., 2018. Mechanisms of complex network growth: Synthesis of the preferential attachment and fitness models. *Phys. Rev. E*, 97, p.062310. Available at: https://link.aps.org/doi/10.1103/PhysRevE.97.062310.

Gong, P. & Leeuwen, C. van, 2003. Emergence of scale-free network with chaotic units. *Physica A: Statistical Mechanics and its Applications*, 321(3), pp.679–688. Available at: http://www.sciencedirect.com/science/article/pii/S0378437102017351.

Goulas, A., 2020. bio2art: Convert biological neural networks to recurrent neural networks. *GitHub repository*.

Goulas, A., Betzel, R.F. & Hilgetag, C.C., 2019. Spatiotemporal ontogeny of brain wiring. *Science Advances*, 5(6). Available at: https://advances.sciencemag.org/content/5/6/eaav9694.

Goulas, A., Schaefer, A. & Margulies, D.S., 2015. The strength of weak connections in the macaque cortico-cortical network. *Brain Structure and Function*, 220(5), pp.2939–2951. Available at: https://doi.org/10.1007/s00429-014-0836-3.

Gould, S.J. et al., 1979. The spandrels of san marco and the panglossian paradigm: A critique of the adaptationist programme. *Proceedings of the Royal Society of London. Series B. Biological Sciences*, 205(1161), pp.581–598. Available at: https://royalsocietypublishing.org/doi/abs/10.1098/rspb.1979.0086.

Gómez-Robles, A., Hopkins, W.D. & Sherwood, C.C., 2014. Modular structure facilitates mosaic evolution of the brain in chimpanzees and humans. *Nature communications*, 5, p.4469. Available at: http://www.ncbi.nlm.nih.gov/pubmed/25047085%7B/%%7D5Cnhttp://www.ncbi.nlm.nih.gov/pubmed/25047085.

Greenberg, J.M. & Hastings, S.P., 1978. Spatial patterns for discrete models of diffusion in excitable media. *SIAM Journal on Applied Mathematics*, 34(3), pp.515–523. Available at: https://doi.org/10.1137/0134040.

Hagberg, A.A., Schult, D.A. & Swart, P.J., 2008. Exploring network structure, dynamics, and function using NetworkX. In G. Varoquaux, T. Vaught, & J. Millman, eds. *Proceedings of the 7th python in science conference*. Pasadena, CA USA, pp. 11–15.

Hagmann, P. et al., 2008. Mapping the structural core of human cerebral cortex. *PLOS Biology*, 6(7), pp.1–15. Available at: https://doi.org/10.1371/journal.pbio.0060159.

Haimovici, A. et al., 2013. Brain organization into resting state networks emerges at criticality on a model of the human connectome. *Phys. Rev. Lett.*, 110, p.178101. Available at: https://link.aps.org/doi/10.1103/PhysRevLett.110.178101.

Hartley, S.A.B., Caroline AND Farmer, 2020. Temporal ordering of input modulates connectivity formation in a developmental neuronal network model of the cortex. *PLOS ONE*, 15(1), pp.1–20. Available at: https://doi.org/10.1371/journal.pone.0226772.

Hassabis, D. et al., 2017. Neuroscience-inspired artificial intelligence. *Neuron*, 95(2), pp.245–258.

Henderson, J.A. & Robinson, P.A., 2013. Using geometry to uncover relationships between isotropy, homogeneity, and modularity in cortical connectivity. *Brain connectivity*, 3(4), p.423—437. Available at: https://doi.org/10.1089/brain.2013.0151.

Herrera, C. & Zufiria, P.J., 2011. Generating scale-free networks with adjustable clustering coefficient via random walks. In *2011 IEEE network science workshop*. pp. 167–172.

Heuvel, M.P. van den & Sporns, O., 2019. A cross-disorder connectome landscape of brain dysconnectivity. *Nature Reviews Neuroscience*, 20(7), pp.435–446. Available at: https://doi.org/10.1038/s41583-019-0177-6.

Hilgetag, C.C. et al., 2000. Anatomical connectivity defines the organization of clusters of cortical areas in the macaque and the cat. *Philosophical Transactions of the Royal Society of London B: Biological Sciences*, 355(1393), pp.91–110. Available at: http://rstb.royalsocietypublishing.org/content/355/1393/91.

Hilgetag, C.C. et al., 2002. Computational methods for the analysis of brain connectivity. In *Computational neuroanatomy*. Springer, pp. 295–335.

Hilgetag, C.C., 1999. *Mathematical approaches to the analysis of neural connectivity in the mammalian brain*. PhD thesis. University of Newcastle upon Tyne.

Humphries, K., Mark D. AND Gurney, 2008. Network 'small-world-ness': A quantitative method for determining canonical network equivalence. *PLOS ONE*, 3(4), pp.1–10. Available at: https://doi.org/10.1371/journal.pone.0002051.

Hütt, M.-T. et al., 2012. Stochastic resonance in discrete excitable dynamics on graphs. *Chaos, Solitons & Fractals*, 45(5), pp.611–618. Available at: http://www.sciencedirect.com/science/article/pii/S096007791100244X.

Hütt, M.-T., Kaiser, M. & Hilgetag, C.C., 2014. Perspective: Network-guided pattern formation of neural dynamics. *Philosophical Transactions of the Royal Society B: Biological Sciences*, 369(1653), p.20130522. Available at: https://royalsocietypublishing.org/doi/abs/10.1098/rstb.2013.0522.

Jaeger, H., 2001. *Short term memory in echo state networks*, GMD-Forschungszentrum Informationstechnik.

Jarman, N. et al., 2017. Self-organisation of small-world networks by adaptive rewiring in response to graph diffusion. *Scientific Reports*, 7(1), p.13158. Available at: https://doi.org/10.1038/s41598-017-12589-9.

Jarman, N. et al., 2014. Spatially constrained adaptive rewiring in cortical networks creates spatially modular small world architectures. *Cognitive Neurodynamics*, 8(6), pp.479–497. Available at: https://doi.org/10.1007/s11571-014-9288-y.

Jeong, H. et al., 2000. The large-scale organization of metabolic networks. *Nature*, 407(6804), pp.651–654.

Kaiser, M. & Hilgetag, C.C., 2007. Development of multi-cluster cortical networks by time windows for spatial growth. *Neurocomputing*, 70(10), pp.1829–1832. Available at: http://www.sciencedirect.com/science/article/pii/S0925231206003821.

Kaiser, M. & Hilgetag, C.C., 2006. Nonoptimal component placement, but short processing paths, due to long-distance projections in neural systems. *PLOS Computational Biology*, 2(7), pp.1–11. Available at: https://doi.org/10.1371/journal.pcbi.0020095.

Kaiser, M. & Hilgetag, C.C., 2010. Optimal hierarchical modular topologies for producing limited sustained activation of neural networks. *Frontiers in Neuroinformatics*, 4, p.8. Available at: https://www.frontiersin.org/article/10.3389/fninf.2010.00008.

Kandel, E.R. et al., 2000. *Principles of neural science*, McGraw-hill New York.

Kasai, H. et al., 2010. Structural dynamics of dendritic spines in memory and cognition. *Trends in Neurosciences*, 33(3), pp.121–129. Available at: http://www.sciencedirect.com/science/article/pii/S0166223610000020.

Kinouchi, O. & Copelli, M., 2006. Optimal dynamical range of excitable networks at criticality. *Nature Physics*, 2, pp.348 EP–. Available at: http://dx.doi.org/10.1038/nphys289.

Kwok, H.F. et al., 2006. Robust emergence of small-world structure in networks of spiking neurons. *Cognitive Neurodynamics*, 1(1), p.39. Available at: https://doi.org/10.1007/s11571-006-9006-5.

Landmann, S., Baumgarten, L. & Bornholdt, S., 2020. Self-organized criticality in neural networks from activity-based rewiring. Available at: https://arxiv.org/abs/2009.11781.

Li, A. & Horvath, S., 2006. Network neighborhood analysis with the multi-node topological overlap measure. *Bioinformatics*, 23(2), pp.222–231.

Lukoševičius, M., 2012. A practical guide to applying echo state networks. In G. Montavon, G. B. Orr, & K.-R. Müller, eds. *Neural networks: Tricks of the trade: Second edition*. Berlin, Heidelberg: Springer Berlin Heidelberg, pp. 659–686. Available at: https://doi.org/10.1007/978-3-642-35289-8_36.

Lukoševičius, M. & Jaeger, H., 2009. Reservoir computing approaches to recurrent neural network training. *Computer Science Review*, 3(3), pp.127–149.

Majka, P. et al., 2016. Towards a comprehensive atlas of cortical connections in a primate brain: Mapping tracer injection studies of the common marmoset into a reference digital template. *Journal of Comparative Neurology*, 524(11), pp.2161–2181. Available at: https://onlinelibrary.wiley.com/doi/abs/10.1002/cne.24023.

Marcus, G., 2020. The next decade in ai: Four steps towards robust artificial intelligence. *arXiv preprint arXiv:2002.06177*.

Markov, N.T. et al., 2012. A Weighted and Directed Interareal Connectivity Matrix for Macaque Cerebral Cortex. *Cerebral Cortex*, 24(1), pp.17–36. Available at: https://doi.org/10.1093/cercor/bhs270.

Markram, H., Gerstner, W. & Sjöström, P.J., 2012. Spike-timing-dependent plasticity: A comprehensive overview. *Frontiers in Synaptic Neuroscience*, 4, p.2. Available at: https://www.frontiersin.org/article/10.3389/fnsyn.2012.00002.

Maslov, S. & Sneppen, K., 2002. Specificity and stability in topology of protein networks. *Science*, 296(5569), pp.910–913. Available at: http://science.sciencemag.org/content/296/5569/910.

Meilă, M., 2007. Comparing clusterings—an information based distance. *Journal of Multivariate Analysis*, 98(5), pp.873–895. Available at: http://www.sciencedirect.com/science/article/pii/S0047259X06002016.

Messé, A. et al., 2015. A closer look at the apparent correlation of structural and functional connectivity in excitable neural networks. *Scientific reports*, 5, p.7870. Available at: http://www.pubmedcentral.nih.gov/articlerender.fcgi?artid=4297952%7B/&%7Dtool=pmcentrez%7B/&%7Drendertype=abstract.

Messé, A., Hütt, M.-T. & Hilgetag, C.C., 2018. Toward a theory of coactivation patterns in excitable neural networks. *PLOS Computational Biology*, 14(4), pp.1–19. Available at: https://doi.org/10.1371/journal.pcbi.1006084.

Meunier, D., Lambiotte, R. & Bullmore, E., 2010. Modular and hierarchically modular organization of brain networks. *Frontiers in Neuroscience*, 4, p.200. Available at: https://www.frontiersin.org/article/10.3389/fnins.2010.00200.

Milo, R. et al., 2002. Network motifs: Simple building blocks of complex networks. *Science*, 298(5594), pp.824–827.

Milo, R. et al., 2004. Superfamilies of evolved and designed networks. *Science*, 303(5663), pp.1538–1542.

Mišić, B. & Sporns, O., 2016. From regions to connections and networks: New bridges between brain and behavior. *Current opinion in neurobiology*, 40, pp.1–7.

Moretti, P. & Hütt, M.-T., 2020. Link-usage asymmetry and collective patterns emerging from rich-club organization of complex networks. *Proceedings of the National Academy of Sciences*, 117(31), pp.18332–18340. Available at: https://www.pnas.org/content/117/31/18332.

Müller-Linow, M., Hilgetag, C.C. & Hütt, M.-T., 2008. Organization of excitable dynamics in hierarchical biological networks. *PLOS Computational Biology*, 4(9), pp.1–15. Available at: https://doi.org/10.1371/journal.pcbi.1000190.

Newman, M.E.J., 2006. Modularity and community structure in networks. *Proceedings of the National Academy of Sciences*, 103(23), pp.8577–8582. Available at: https://www.pnas.org/content/103/23/8577.

Oh, S.W. et al., 2014. A mesoscale connectome of the mouse brain. *Nature*, 508(7495), pp.207–214. Available at: https://doi.org/10.1038/nature13186.

Oldham, S. & Fornito, A., 2019. The development of brain network hubs. *Developmental Cognitive Neuroscience*, 36, p.100607. Available at: http://www.sciencedirect.com/science/article/pii/S1878929318301397.

Perin, R., Berger, T.K. & Markram, H., 2011. A synaptic organizing principle for cortical neuronal groups. *Proceedings of the National Academy of Sciences*, 108(13), pp.5419–5424. Available at: http://www.pnas.org/content/108/13/5419.

Ravasz, E. et al., 2002. Hierarchical organization of modularity in metabolic networks. *Science*, 297(5586), pp.1551–1555. Available at: http://science.sciencemag.org/content/297/5586/1551.

Ravid Tannenbaum, N. & Burak, Y., 2016. Shaping neural circuits by high order synaptic interactions. *PLOS Computational Biology*, 12(8), pp.1–27. Available at: https://doi.org/10.1371/journal.pcbi.1005056.

Reichardt, J., Alamino, R. & Saad, D., 2011. The interplay between microscopic and mesoscopic structures in complex networks. *PloS one*, 6(8), p.e21282.

Rosvall, M. & Bergstrom, C.T., 2008. Maps of random walks on complex networks reveal community structure. *Proceedings of the National Academy of Sciences*, 105(4), pp.1118–1123. Available at: http://www.pnas.org/content/105/4/1118.

Rosvall, M. & Sneppen, K., 2003. Modeling dynamics of information networks. *Phys. Rev. Lett.*, 91, p.178701. Available at: https://link.aps.org/doi/10.1103/PhysRevLett.91.178701.

Roth, G. & Dicke, U., 2005. Evolution of the brain and intelligence. *Trends in Cognitive Sciences*, 9(5), pp.250–257. Available at: http://www.sciencedirect.com/science/article/pii/S1364661305000823.

Rubinov, M., 2016. Constraints and spandrels of interareal connectomes. *Nature communications*, 7(1), pp.1–11.

Rubinov, M. et al., 2009. Symbiotic relationship between brain structure and dynamics. *BMC Neuroscience*, 10(1), p.55. Available at: https://doi.org/10.1186/1471-2202-10-55.

Rubinov, M. et al., 2015. Wiring cost and topological participation of the mouse brain connectome. *Proceedings of the National Academy of Sciences*, 112(32), pp.10032–10037.

Rubinov, M. & Sporns, O., 2010. Complex network measures of brain connectivity: Uses and interpretations. *NeuroImage*, 52(3), pp.1059–1069. Available at: http://www.sciencedirect.

com/science/article/pii/S105381190901074X.

Schroeter, M.S. et al., 2015. Emergence of rich-club topology and coordinated dynamics in development of hippocampal functional networks in vitro. *Journal of Neuroscience*, 35(14), pp.5459–5470. Available at: https://www.jneurosci.org/content/35/14/5459.

Seguin, C., Tian, Y. & Zalesky, A., 2020. Network communication models improve the behavioral and functional predictive utility of the human structural connectome. *bioRxiv*.

Semon, R., 1921. Chapter II. Engraphic action of stimuli on the individual. *The Mneme*.

Shi Zhou & Mondragon, R.J., 2004. The rich-club phenomenon in the internet topology. *IEEE Communications Letters*, 8(3), pp.180–182.

Sneppen, K., 2014. *Models of life*, Cambridge University Press.

Sporns, O., 2003. Graph theory methods for the analysis of neural connectivity patterns. In *Neuroscience databases*. Springer, pp. 171–185.

Sporns, O., 2013. Network attributes for segregation and integration in the human brain. *Current Opinion in Neurobiology*, 23(2), pp.162–171. Available at: http://www.sciencedirect.com/science/article/pii/S0959438812001894.

Sporns, O., 2010. *Networks of the brain*, MIT press.

Sporns, O. et al., 2004. Organization, development and function of complex brain networks. *Trends in Cognitive Sciences*, 8(9), pp.418–425. Available at: http://www.sciencedirect.com/science/article/pii/S1364661304001901.

Sporns, O., 2011. The Non-Random Brain: Efficiency, Economy, and Complex Dynamics. *Frontiers in Computational Neuroscience*, 5(February), p.5. Available at: http://journal.frontiersin.org/article/10.3389/fncom.2011.00005/abstract.

Sporns, O. & Betzel, R.F., 2016. Modular Brain Networks. *Annual review of psychology*, 67(1), pp.613–40. Available at: https://arxiv.org/abs/15334406.

Sporns, O., Tononi, G. & Edelman, G.M., 2000. Connectivity and complexity: The relationship between neuroanatomy and brain dynamics. *Neural Networks*, 13(8), pp.909–922. Available at: http://www.sciencedirect.com/science/article/pii/S0893608000000538.

Sporns, O., Tononi, G. & Kötter, R., 2005. The human connectome: A structural description of the human brain. *PLOS Computational Biology*, 1(4). Available at: https://doi.org/10.1371/journal.pcbi.0010042.

Stam, C.J. et al., 2010. Emergence of modular structure in a large-scale brain network with interactions between dynamics and connectivity. *Frontiers in Computational Neuroscience*, 4, p.133. Available at: https://www.frontiersin.org/article/10.3389/fncom.2010.00133.

Stiso, J. & Bassett, D.S., 2018. Spatial embedding imposes constraints on neuronal network architectures. *Trends in Cognitive Sciences*, 22(12), pp.1127–1142. Available at: https://www.sciencedirect.com/science/article/pii/S1364661318302250.

Stone, D. & Tesche, C., 2013. Topological dynamics in spike-timing dependent plastic model neural networks. *Frontiers in Neural Circuits*, 7, p.70. Available at: https://www.frontiersin.org/article/10.3389/fncir.2013.00070.

Stumpf, M.P.H. & Porter, M.A., 2012. Critical truths about power laws. *Science*, 335(6069), pp.665–666. Available at: https://science.sciencemag.org/content/335/6069/665.

Suárez, L. et al., 2020. Linking structure and function in macroscale brain networks. *Trends in Cognitive Sciences*.

Suárez, L.E. et al., 2020. Learning function from structure in neuromorphic networks. *bioRxiv*. Available at: https://www.biorxiv.org/content/early/2020/11/11/2020.11.10.350876.

Triplett, M.A., Avitan, L. & Goodhill, G.J., 2018. Emergence of spontaneous assembly activity in developing neural networks without afferent input. *PLOS Computational Biology*, 14(9), pp.1–22. Available at: https://doi.org/10.1371/journal.pcbi.1006421.

Vazquez, A. et al., 2004. The topological relationship between the large-scale attributes and local interaction patterns of complex networks. *Proceedings of the National Academy of Sciences*, 101(52), pp.17940–17945.

Wang, S.-J. & Zhou, C., 2012. Hierarchical modular structure enhances the robustness of self-organized criticality in neural networks. *New Journal of Physics*, 14(2), p.023005. Available at: http://stacks.iop.org/1367-2630/14/i=2/a=023005.

Wheeler, A.L. et al., 2013. Identification of a functional connectome for long-term fear memory in mice. *PLOS Computational Biology*, 9(1), pp.1–18. Available at: https://doi.org/10.1371/journal.pcbi.1002853.

Wiegert, J.S. & Oertner, T.G., 2013. Long-term depression triggers the selective elimination of weakly integrated synapses. *Proceedings of the National Academy of Sciences of the United States of America*, 110(47), pp.E4510–E4519. Available at: https://doi.org/10.1073/pnas.1315926110.

Wig, G.S., 2017. Segregated systems of human brain networks. *Trends in Cognitive Sciences*, 21(12), pp.981–996. Available at: http://www.sciencedirect.com/science/article/pii/S1364661317301948.

Wildie, M. & Shanahan, M., 2012. Metastability and chimera states in modular delay and pulse-coupled oscillator networks. *Chaos: An Interdisciplinary Journal of Nonlinear Science*, 22(4), p.043131. Available at: https://doi.org/10.1063/1.4766592.

Wolfram, S. & Gad-el-Hak, M., 2003. A new kind of science. *Appl. Mech. Rev.*, 56(2), pp.B18–B19.

Xie, S. et al., 2019. Exploring randomly wired neural networks for image recognition. In *The IEEE international conference on computer vision (ICCV)*.

Yuan, W.-J. & Zhou, C., 2011. Interplay between structure and dynamics in adaptive complex networks: Emergence and amplification of modularity by adaptive dynamics. *Phys. Rev. E*, 84, p.016116. Available at: https://link.aps.org/doi/10.1103/PhysRevE.84.016116.

Zamora-López, G., Zhou, C. & Kurths, J., 2009. Graph analysis of cortical networks reveals complex anatomical communication substrate. *Chaos: An Interdisciplinary Journal of Nonlinear Science*, 19(1), p.015117. Available at: https://doi.org/10.1063/1.3089559.

Zhou, C. et al., 2006. Hierarchical organization unveiled by functional connectivity in complex brain networks. *Phys. Rev. Lett.*, 97, p.238103. Available at: https://link.aps.org/doi/10.1103/PhysRevLett.97.238103.

Chapter 7

Supplementary figures

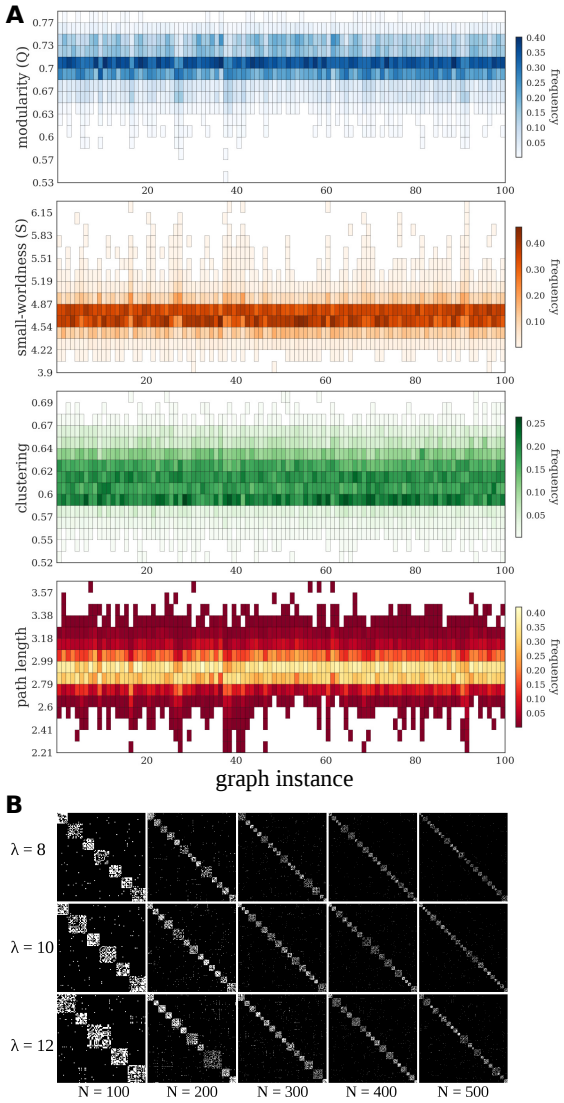

Figure 7.1: Robustness of results for different initial random graph instances, final networks characteristics. (A) The heat maps show a summary of the results for 100 different initial random graph instances used as initial condition. For each one, 500 simulation runs were performed. For each final graph, modularity (Q), characteristic path length, mean clustering coefficient and and small-worldness coefficient (S) were computed. Each column of the heat map represents the distribution of values obtained across 500 simulations carried out with the same initial random graph instance. (B) Examples of final adjacency matrices of individual runs with different network sizes (N) and densities (λ).

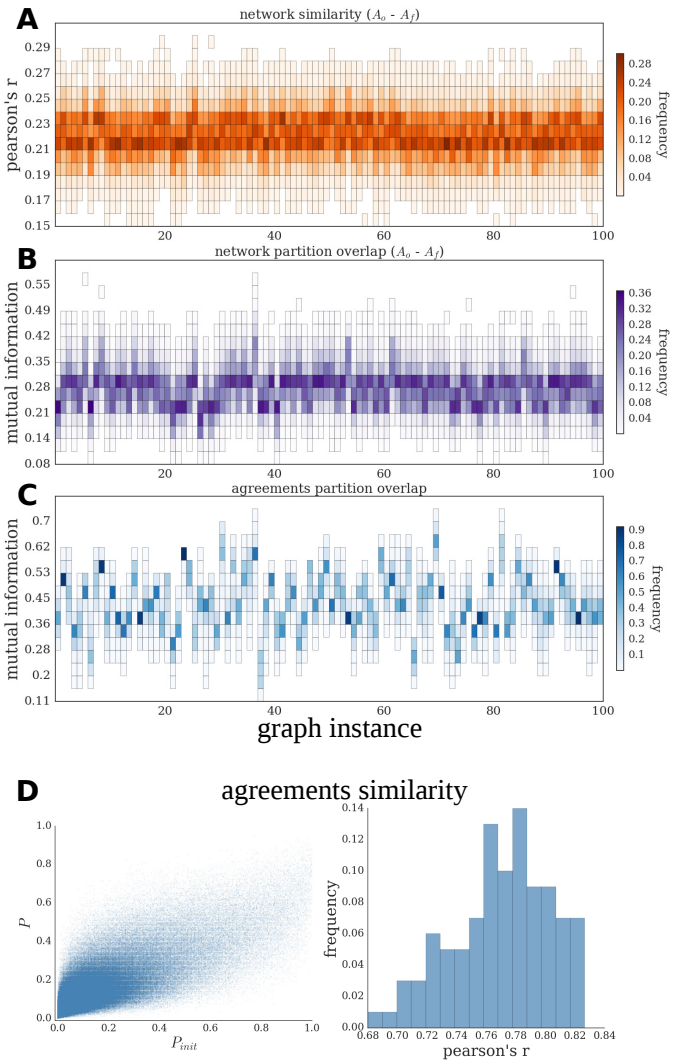

Figure 7.2: Robustness of results for different initial random graph instances, correspondence between initial and final networks. (A-C) The heat maps show a summary of the results for 100 different initial random graph instances used as initial condition. Each column of the heat maps represents the distribution of values obtained across 500 simulations carried out with the same initial random graph instance. (A) Distribution of the correlation values between all pairs of initial and final networks. (B) Partition overlap between all pairs of initial and final networks (quantified as normalized mutual information, NMI). (C) Partition distance between initial (P_{init}) and final (P) agreements. (D) Similarity between P_{init} and P agreements, the scatter plot (left) shows the values over 100 different random graph instances used as initial condition, and the histogram (right) represents the Pearson's correlation coefficient between all pairs of P_{init}-P.

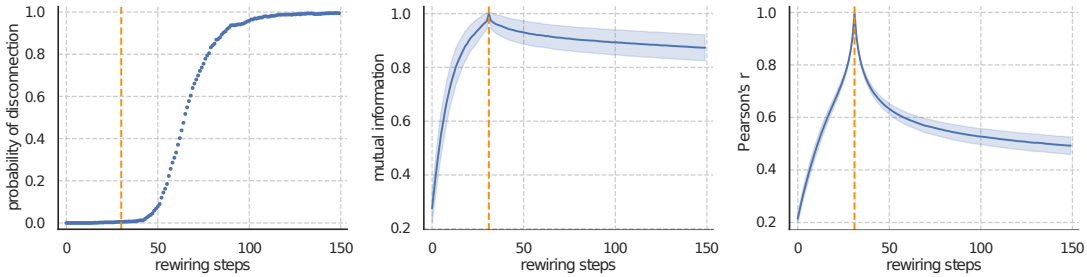

Figure 7.3: Probability of network disconnection and steady state for long runs. (Left) Probability of network disconnection as a function of the number of rewiring steps. (Middle) Module partition overlap and (Right) correlation between the network at the typical final point (orange line) and at all other time points (shown as mean and standard deviation). In all cases, the orange line shows the typical length of our simulations. Results from 1000 runs (aggregated from 10 network instances, 100 runs each) of networks with $N = 100$ nodes and average connectivity $\lambda = 10$ (i.e., density $= 0.1$).

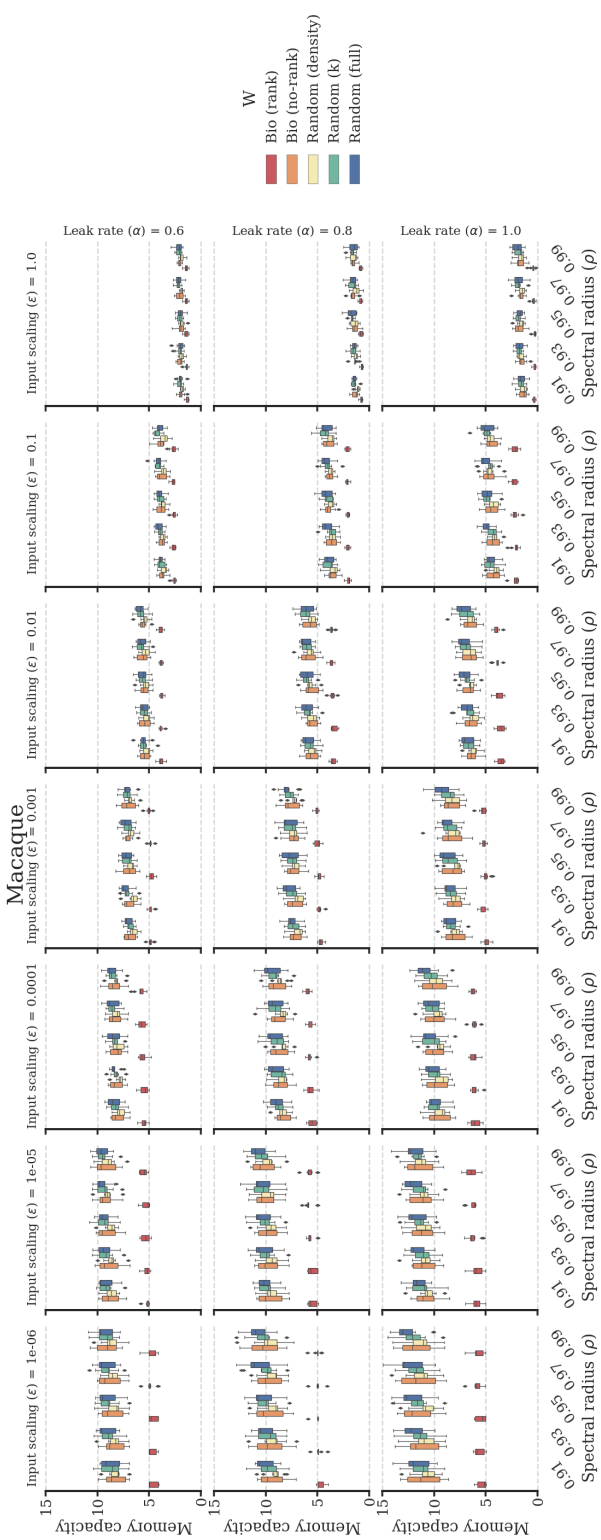

Figure 7.4: Memory Capacity task. Echo state network hyperparameters grid search. Homogeneous interareal connectivity. Macaque connectome. Results of grid search over input scaling, leakage rate and spectral radius hyperparameters. For each parameter constellation, the boxplots show the aggregated validation scores of ten independently generated and trained reservoirs.

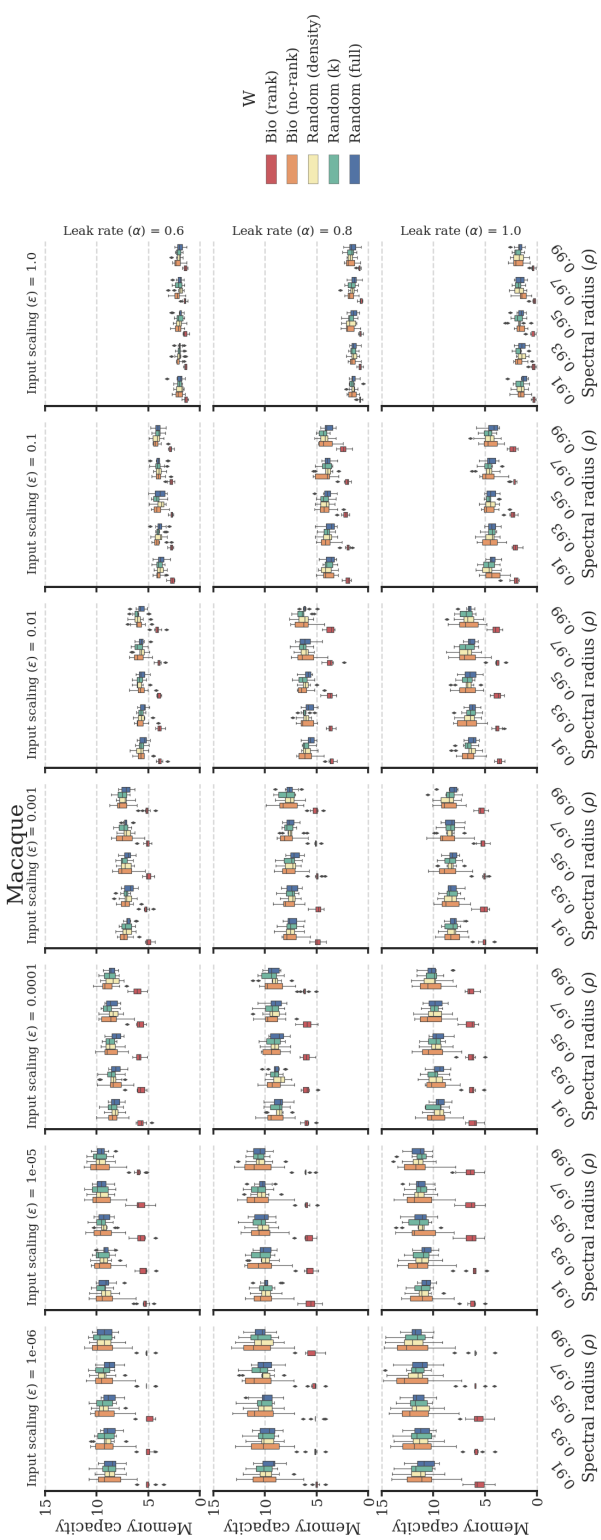

Figure 7.5: Memory Capacity task. Echo state network hyperparameters grid search. Heterogeneous interareal connectivity. Macaque connectome. Results of grid search over input scaling, leakage rate and spectral radius hyperparameters. For each parameter constellation, the boxplots show the aggregated validation scores of ten independently generated and trained reservoirs.

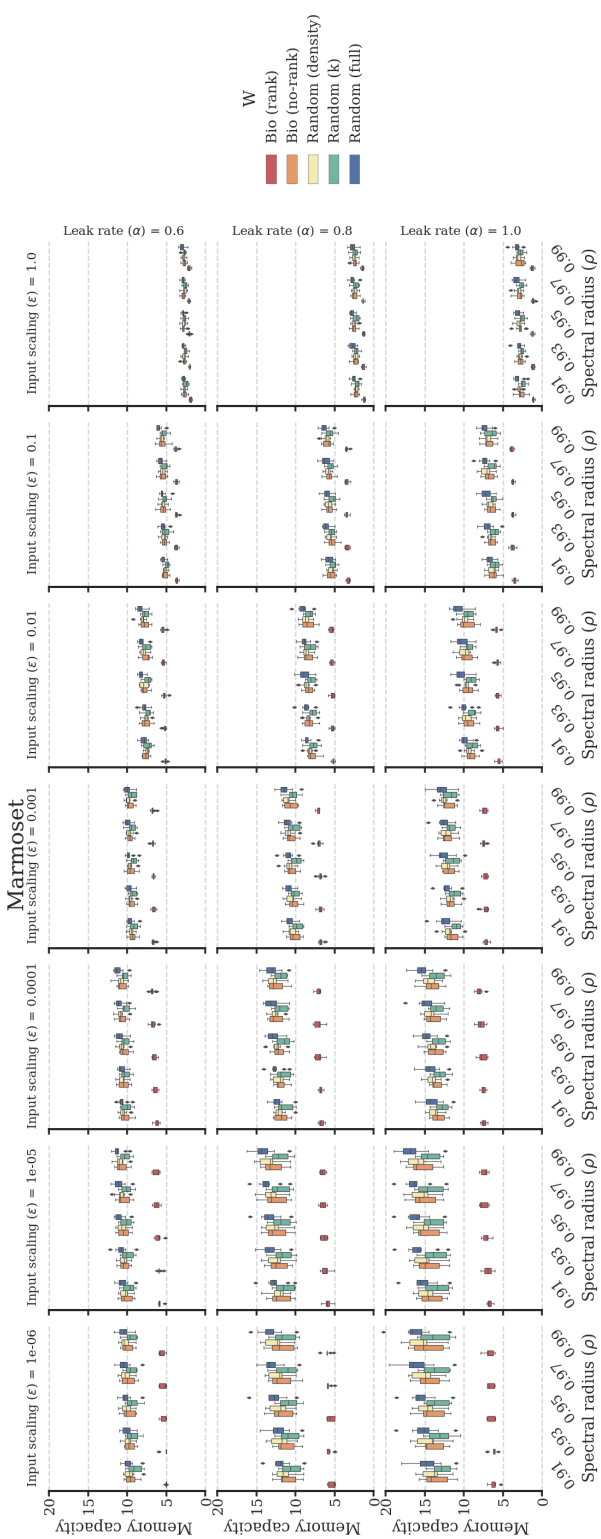

Figure 7.6: Memory Capacity task. Echo state network hyperparameters grid search. Homogeneous interareal connectivity. Marmoset connectome. Results of grid search over input scaling, leakage rate and spectral radius hyperparameters. For each parameter constellation, the boxplots show the aggregated validation scores of ten independently generated and trained reservoirs.

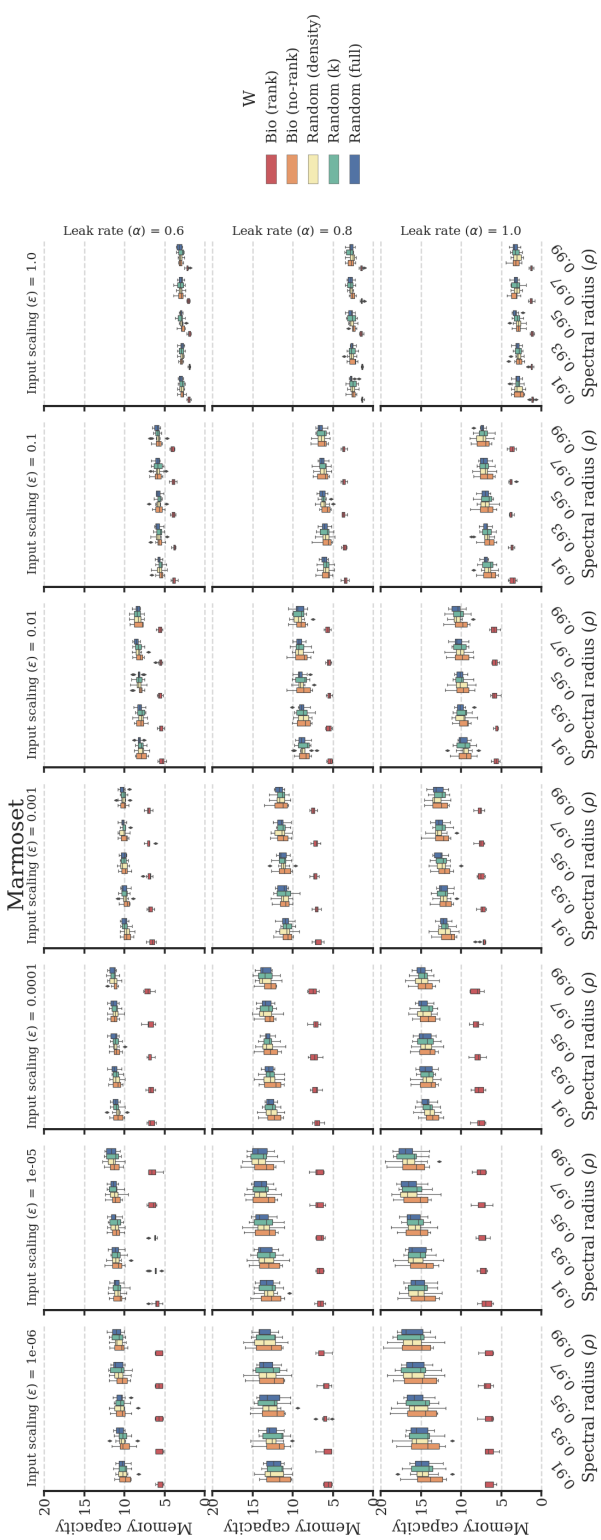

Figure 7.7: Memory Capacity task. Echo state network hyperparameters grid search. Heterogeneous interareal connectivity. Marmoset connectome. Results of grid search over input scaling, leakage rate and spectral radius hyperparameters. For each parameter constellation, the boxplots show the aggregated validation scores of ten independently generated and trained reservoirs.

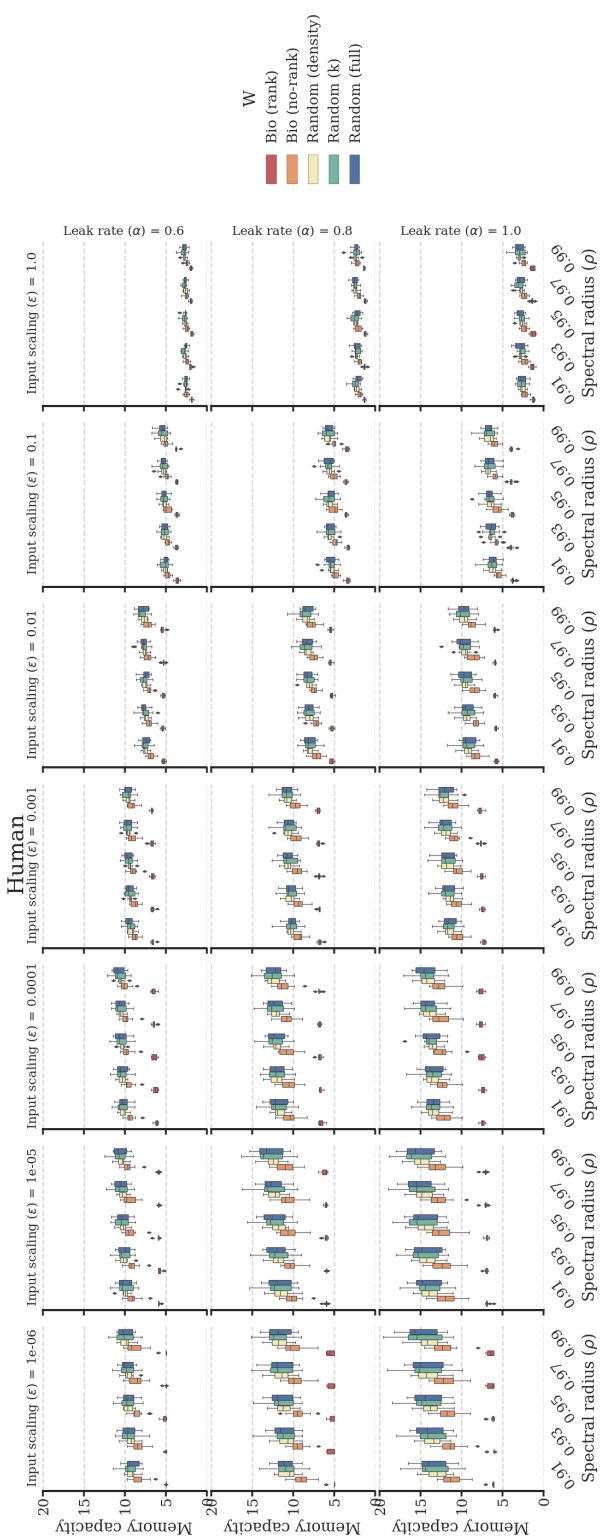

Figure 7.8: Memory Capacity task. Echo state network hyperparameters grid search. Homogeneous interareal connectivity. Human connectome. Results of grid search over input scaling, leakage rate and spectral radius hyperparameters. For each parameter constellation, the boxplots show the aggregated validation scores of ten independently generated and trained reservoirs.

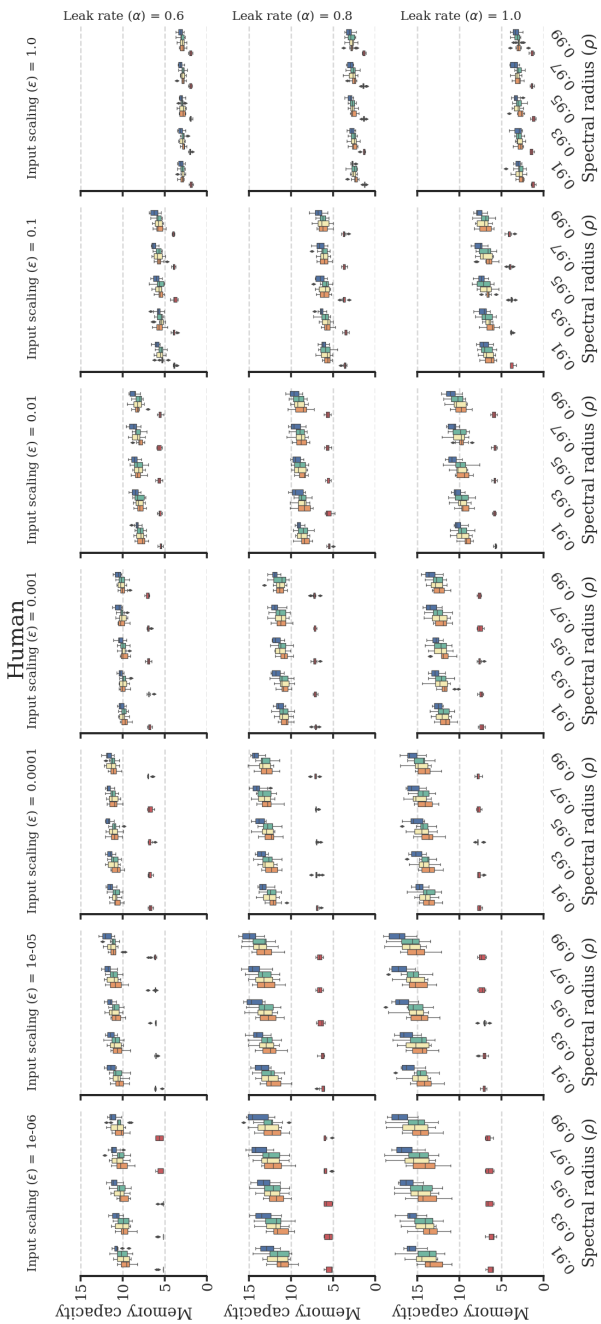

Figure 7.9: Memory Capacity task. Echo state network hyperparameters grid search. Heterogeneous interareal connectivity. Human connectome. Results of grid search over input scaling, leakage rate and spectral radius hyperparameters. For each parameter constellation, the boxplots show the aggregated validation scores of ten independently generated and trained reservoirs.

Publications

The following articles resulted directly from the work on this dissertation:

- **Damicelli, F.**, Hilgetag, C. C., Hütt, M. T., & Messé, A. (2017). Modular topology emerges from plasticity in a minimalistic excitable network model. Chaos: An Interdisciplinary Journal of Nonlinear Science, 27(4), 047406.
- **Damicelli, F.**, Hilgetag, C. C., Hütt, M. T., & Messé, A. (2019). Topological reinforcement as a principle of modularity emergence in brain networks. Network Neuroscience, 3(2), 589-605.
- **Damicelli, F.**, Hilgetag, C. C., & Goulas, A. (2021). Brain Connectivity meets Reservoir Computing. bioRxiv preprint. doi: https://doi.org/10.1101/2021.01.22.427750. (Submitted).
- **Damicelli, F.**, Hilgetag, C. C., Hütt, M. T., & Messé, A. Sequential reinforcement plasticity leads to heterogeneous degree distributions in brain networks. (In preparation)

Additional collaborations resulted in the following publications:

- Goulas, A., **Damicelli, F.**, & Hilgetag, C. C. (2021). Bio-instantiated recurrent neural networks. bioRxiv preprint. doi: https://doi.org/10.1101/2021.01.22.427744. (Submitted).
- Hadaeghi, F., Diercks, BP., Schetelig, D., **Damicelli, F.**, Wolf, I., & Werner, R. Spatio-Temporal Feature Learning with Reservoir Computing for T-Cell Segmentation in Live-Cell Ca2+ Fluorescence Microscopy. (Submitted)

Aknowledgements

I want to thank Claus, for many reasons. Thank you for always being professional and respectful to me. Thank you for supporting me while I developed my eclectic interests, for your patience to accept my pace of work and the freedom you gave me to explore topics that sparked my curiosity.
Arnaud, thank you for being the invisible hand that helped me make progress in the core projects of this thesis. Thanks for sharing with me with few words your vast "know-how," for showing me how to stay humble and to look for simpler solutions.
Marc, I owe you also my gratitude. For many hours of inspiring discussions and for teaching me to appreciate the beauty of simple little things behind complex phenomena.
Alex, I want to thank you for making the workplace a place fun to be at. Thank you for the fun work did together and for so many enjoyable chats and laughs about the most diverse topics in the world. Thanks for showing me a path of honesty and truly inspiring scientific inquiry.
Thanks to the team members, especially Kayson for the coffee and the good humor and Fatemeh for answering my silly questions.
Thanks to the ICNS-Bildverarbeitung crew, for being nice to be around and for so many hours of Kicker and jokes - that was fun.
Last big one goes to my family and friends, especially my Hamburg friends who turned this city into my home and shared with me so many nice moments along these years - Thank you very much!

Fabrizio

Curriculum Vitae

Lebenslauf wurde aus datenschutzrechtlichen Gründen entfernt.

Eidesstattliche Erklärung

Ich versichere ausdrücklich, dass ich die Arbeit selbständig und ohne fremde Hilfe verfasst, andere als die von mir angegebenen Quellen und Hilfsmittel nicht benutzt und die aus den benutzten Werken wörtlich oder inhaltlich entnommenen Stellen einzeln nach Ausgabe (Auflage und Jahr des Erscheinens), Band und Seite des benutzten Werkes kenntlich gemacht habe. Ferner versichere ich, dass ich die Dissertation bisher nicht einem Fachvertreter an einer anderen Hochschule zur Überprüfung vorgelegt oder mich anderweitig um Zulassung zur Promotion beworben habe. Ich erkläre mich einverstanden, dass meine Dissertation vom Dekanat der Medizinischen Fakultät mit einer gängigen Software zur Erkennung von Plagiaten überprüft werden kann.

Unterschrift: ……